THE USE OF GASIFICATION ASH IN CEMENT AND CONCRETE

HANLI DU PLESSIS

A dissertation submitted in partial fulfillment for the degree of

MASTER OF ENGINEERING (STRUCTURAL ENGINEERING)

In the

FACULTY OF ENGINEERING

UNIVERSITY OF PRETORIA

November 2005

SUMMARY

THE USE OF GASIFICATION ASH IN CEMENT AND CONCRETE

H DU PLESSIS

Supervisor: Professor E.P. Kearsley

Department: Civil Engineering

University: University of Pretoria

Degree: Master of Engineering (Structural Engineering)

Cement is an essential material in today's society because, as a major constituent of concrete, it forms a fundamental element of any housing or infrastructure development. The chemical process of making cement clinker produces CO_2, a major greenhouse gas contributing to climate change. This makes it imperative for us to find ways of using this resource more efficiently.

Using waste from other industries, as a raw material is a huge opportunity for the cement industry to reduce its environmental impact. Cement extenders are used as a substitute for some of the Portland cement in concrete. The reasons for the use of extenders, is a growing awareness of the engineering, economical and ecological benefits and the variety of useful enhancements, which they give to the concrete properties.

The aim of the research is to determine whether a gasification ash can be used as a cement extender in concrete. In this study detail of the manufacturing of Portland cement (PC), cement classes and the hydration of cement will be discussed. Consideration will be given to properties like the optimisation of sulphate and fineness of cement. The particle size distribution is discussed with specific reference to the Rosin-Rammler distribution function. The use of coal combustion by-products, specifically fly ash, in concrete will be discussed. Consideration will be given to properties like shape, particle size, mineralogical and chemical composition, durability and the chemical requirements for using fly ash as a cement extender.

The physical properties of gasification ash indicated that the gasification ash, grinded separate and interground had similar particle size distributions. The chemical and mineralogical composition of a gasification ash sample was investigated, and it was found that gasification ash has an angular shape and a similar chemical composition as fly ash.

The chemical requirements of the gasification ash meet the majority of the requirements specified for cement extenders. Where limits are exceeded it is by a very narrow margin.

The effect of a gasification ash on the short and long term properties of concrete of both interblending and intergrinding was investigated. The use of gasification ash as cement extender does not have a negative impact on the strength development of concrete. There was no reduction in the tensile strength of concrete. Gasification ash does not have a detrimental effect on stiffness of concrete, and did not shrink or creep significantly more than concrete containing fly ash.

The porosity and permeability does not increase when gasification ash is used as a cement extender. Gasification ash should therefore not decrease the durability of concrete.

SAMEVATTING VAN

DIE BENUTTING VAN GASIFIKASIE-AS IN SEMENT EN BETON

H DU PLESSIS

Promotor: Professor E.P. Kearsley

Departement: Siviele Ingenieurswese

Universiteit: Universiteit van Pretoria

Graad: Magister van Ingenieurwese (Struktuur Ingenieurswese)

Sement is ‘n belangrike materiaal in die hedendaagse gemeenskap want as ‘n hoof vervangingsmateriaal in beton, vorm dit ‘n belangrike element van enige behuising of infrastruktuur ontwikkeling. Die chemiese proses tydens die vervaardiging van sement stel CO_2, ‘n gas wat lei tot klimaatsverandering, vry. Hierdie aspek maak dit belangrik vir ons om maniere te kry om hierdie bron meer effektief te gebruik.

Benutting van afval materiale van ander industrieë as a rou materiaal is a groot kans vir die sement industrie om hul omgewingsimpak te verminder. Sement-vervangers word gebruik as vervanging vir ‘n deel van die Portland Sement in beton. The redes vir die gebruik van vervangers is ‘n groeiende bewuswording van die ingenieurs

ekonomiese en ekologiese voordeel asook die verskeidenheid verbeterings wat hulle bydra tot die eienskappe van beton.

Die doel van die navorsing is om te bepaal of gasifikasie-as gebruik kan word as ‘n sement-vervanger in beton. In hierdie studie word inligting oor die vervaardiging van Portland sement, sement klasse en die hidrasie van sement bespreek. Konsiderasie word gegee aan eienskappe soos die optimisering van sulfaat en die fynheid van sement. Die partikelgrootte verspreiding word bespreek met spesifieke verwysing na die Rosin-Rammler verspreidingfunksie. Die gebruik van steenkool as afval produkte, spesifiek Vliegas, in beton word bespreek. Konsiderasie word gegee aan eienskappe soos vorm, partikelgrootte, mineralogie en chemiese samestelling, duursaamheid en die chemiese vereistes vir die gebruik van Vliegas as ‘n sement-vervanger.

Die fisiese eienskappe van gasifikasie-as dui daarop dat gasifikasie-as, apart gemaal en saam gemaal dieselfde partikelgrootte verspreidings het. Die chemiese en mineralogiese samestelling van gasifikasie-as is ondersoek en daar is gevind dat gasifikasie-as ‘n hoekige vorm en dieselfde samestelling as vliegas het.

The chemiese vereistes vir gasifikasie as voldoen aan die meerderheid van die vereistes gespesifiseer vir sement-vervangers. Waar die limiete oorskrei word is dit slegs met ‘n klein margin.

Die effek van gasifikasie as op die kort en lang termyn eienskappe van beton vir beide saamgemeng en saamgemaal is ondersoek. Die gebruik van gasifikasie-as as ‘n sement-vervanger het geen negatiewe impak op die sterkte ontwikkeling van beton nie. Daar was geen vermindering in die treksterkte van die beton nie. Gasifikasie-as het nie ‘n nadelige effek op die styfheid van die beton en het nie besonders meer gekrimp of kruip nie as beton met vliegas nie.

Die porositeit en permeabiliteit het nie vermeerder as gasifikasie-as gebruik word as ‘n sement-vervanger nie. Gasifikasie-as sal daarvoor nie die duursaamheid van beton verminder nie.

ACKNOWLEDGEMENT

I wish to express my appreciation to the following organizations and persons who made this dissertation possible.

a) Sasol Technology Research and Development for the donation of gasification ash tested in this investigation.

b) Professor E.P Kearsley, my promoter for her guidance and support.

c) The following persons for their assistance during the course of study:

Mr. D. Mostert
Mr. H. Matjie
Mrs. S. Verryn
Mrs. J. Callanan
Personnel of the concrete laboratory of the Civil Engineering department of the University of Pretoria.

d) My family and friends for their encouragement and support.

TABLE OF CONTENTS

LIST OF FIGURES

LIST OF TABLES

1. INTRODUCTION

1.1 BACKGROUND

In recent years there has been a significant increase in the use of waste materials as both cement extenders and fillers in concrete (Escalante, 2004). The reason for this is a growing awareness of the engineering, economical and ecological benefits, the use of waste materials have in the cement and concrete industries. Waste materials can however only be used in concrete if they are not detrimental to the short- or the long-term properties of the concrete.

The main reason for the use of extenders in concrete is their variety of useful enhancements of or modifications to the concrete properties. Cement extenders have two common features:

- their particle size range is similar to or smaller than that of Portland cement.
- they become involved in the hydration reactions.

In blended cement production, extenders can be introduced to the cement by interblending or intergrinding (Erdogdu, 1999).

The feed to Sasol gasifiers principally consists of coarse coal (>5mm) and extraneous rock fragments (stone). During the gasification of this coarse coal at elevated temperatures and pressure a mixture of carbon monoxide and hydrogen (also referred to as synthesis gas) is produced. The coarse ash is formed at these elevated temperatures and pressure by the interaction of inert minerals present in the coal and stone. The coarse ash is removed from the gasifier and disposed as a by-product (Van Dyk, 2005).

1.2 OBJECTIVES OF THE STUDY

The main aim of this investigation is to determine the suitability of using gasification ash as cement extender in concrete. To meet this aim, the objectives of the investigation are as follows:

- To investigate the properties of cement manufacturing with specific reference to cement classes, hydration of cement, and the optimisation of gypsum, specific surface area and particle size distribution, to evaluate the performance of cement produced in the laboratory.
- Investigate the physical, chemical and mineralogical composition of a gasification ash sample to determine if gasification ash can be used as a cement extender in concrete.
- Determine the compliance of gasification ash with the requirements for use in cement.
- Determine an optimum grinding time for both the interblending and intergrinding of gasification ash and cement.
- Determine the effect of replacement level on the properties of interblended and interground gasification ash and cement.
- Investigate the effect of interblended and interground gasification ash and cement on the short and long term properties of concrete.
- Investigate the effect of the gasification ash on the durability of concrete.

1.3 SCOPE OF THE STUDY

This study will consist of a literature review on the manufacture and properties of cement. Detail of different coal ash by-products is discussed and the use of fly ash as a cement extender in concrete is considered. Consideration is given to properties like mineralogical and chemical composition, shape,

particle size distributions, chemical requirements of using fly ash in concrete, strength development and durability of concrete.

A gasification ash sample is tested to determine how this waste material compares to the extenders currently used in the cement industry. Consideration is given to the chemical and physical properties of gasification ash. All data is analysed to achieve conclusions on the above-mentioned objectives.

Cement is manufactured by grinding clinker. Particle size distributions are investigated and optimum grinding times is investigated. The optimisation of gypsum is also investigated with reference to the hydration of cement. Different replacement levels of gasification ash are investigated to determine restriction on the use of gasification ash in cement.

Gasification ash is used in concrete and the strength development, deformation and durability of these concrete mixes are examined. This will provide adequate understanding of the advantages that waste materials have to both the cement industry and the environment.

To accurately estimate and predict behaviour, it is necessary to repeat tests on as many independent samples as possible. In this study the tests were only conducted once. Therefore it is not statistically correct to draw final conclusions and predict trends based on the results.

This study does not include the following:

- The effect of variability of gasification ash as far as physical and chemical properties is concerned.
- The response of gasification ash to admixtures.
- The effect of gasification ash on the long-term durability of concrete.
- Durability tests performed excludes the damaging effects of ultra violet (UV) light and physical scouring.

1.4 METHODOLOGY

There were seven principal objectives in this research project. The methodology followed in each is selected to objectively evaluate gasification ash for its use in cement and concrete.

- The physical properties of a gasification ash sample will be investigated by examining the particle size distribution and shape. This includes determining an optimum grinding time and gypsum content.
- The chemical and mineralogical composition of a gasification ash sample is investigated and compared to that of extenders commonly used that are known to enhance the properties of concrete.
- The compliance of a gasification ash with the chemical requirements for use in concrete is determined.
- The reactivity of gasification ash is established by considering interblending and intergrinding in mortar, and testing against fly ash in concrete.
- The effect of gasification ash on the short and long term properties of concrete is established by measuring workability, strength development, elasticity, shrinkage and creep, porosity and permeability.
- In conclusion recommendations are made for the use of gasification ash.

1.5 ORGANISATION OF THE REPORT

The dissertation has been divided into the following sections:

- Chapter 1 serves as an introduction to the thesis.
- Portland cement as well as properties of manufacturing of cement is discussed in chapter 2.
- The composition and properties of coal ash are discussed in Chapter 3, with special reference to the properties of fly ash.

- Chapter 4 describes the experimental programme and test procedures for cement.
- Experimental programme and test procedures for concrete are discussed in Chapter 5.
- Chapter 6 contains the results for the properties and utilisation of gasification ash as a replacement of cement in mortar prisms.
- The results of using gasification ash as a cement extender in concrete are evaluated in Chapter 7.
- Chapter 8 contains the conclusions and recommendations of the study.
- A list of references follows in Chapter 9.
- Various results are provided in the appendices. These appendices are referred to in the main body of the dissertation.

2. COMPONENTS AND PROPERTIES OF PORTLAND CEMENT

2.1 INTRODUCTION

Global population is rising, placing increasing pressure on essential natural resources such as land and energy. This makes it imperative for us to find ways of using these resources more efficiently. This need for more environmentally and socially sustainable development has become a key agenda for governments, non-governmental organisations (NGO) and businesses.

Cement is an essential material in today's society because, as a major constituent of concrete, it forms a fundamental element of any housing or infrastructure development. The chemical process of making cement clinker produces CO_2, a major greenhouse gas contributing to climate change.

In this chapter, detail of the manufacturing of Portland cement (PC), cement classes and the hydration of cement will be discussed. Consideration will be given to properties like the optimisation of sulphate and fineness of cement. The particle size distribution is discussed with specific reference to the Rosin-Rammler distribution function. This will provide adequate understanding of the properties of cement and the influence blended cements have on the cement hydration process.

2.2 CEMENT MANUFACTURE

SANS 50197-1/SABS EN 197-1:2000 states that “cement is a hydraulic binder, a finely ground inorganic material which, when mixed with water, forms a paste which sets and hardens by means of hydration reactions and processes and which after hardening, retains its strength and stability even under water.”

Cement is manufactured from four raw material oxides: lime, silica, alumina and ferric oxide. Lime cannot be found in nature and is produced by heating calcium carbonate (Addis, 2001). Cement manufacturing consists of quarrying or excavating raw materials. Cement manufacturers obtain silica, alumina and ferric oxides from clay or shale. The raw materials are crushed, blended, milled and preheated in a kiln. In the kiln, calcium carbonate is converted to calcium oxide at temperatures of 800°C to 1000°C:

$$CaCO_3 \rightarrow CaO + CO_2 \qquad \text{(equation 2.1)}$$

The materials flow to a hotter (1450°C) part of the kiln where, the blend of the four oxides is converted to cement clinker (Addis, 2001). The clinker is then ground with a small amount of gypsum into a powder with a specific surface area (Blaine) of 300 – 350 m²/kg to make 'Ordinary Portland Cement', the most commonly used type of cement (often referred to as OPC). A schematic presentation of the cement manufacturing process can be seen in Figure 2.1.

The CO_2 emissions from Portland cement manufacturing are generated by two mechanisms. These mechanisms are the calcining of limestone (see equation 2.1) and the combustion of fuels to generate energy. Typically, Portland cement contains the equivalent of about 63.5 % CaO. Consequently, about 1.135 units of $CaCO_3$ are required to produce 1 unit of cement, and the amount of CO_2 released in the calcining process is about 500 kilograms (kg) per metric ton of Portland cement produced (1,000 pounds [lb] per ton of cement). Total CO_2 emissions depend on energy consumption and generally fall in the range of 0.85 to 1.35 metric ton of CO_2 per metric ton of clinker (www.wbcsdcement.org, 2005). This means that the cement industry produces 5% of global man-made CO_2 emissions, of which 50% is from the chemical process, and 40% from burning fuel. The remainder is split between electricity and transport uses. Climate protection, and in particular reduction of carbon

dioxide (CO_2) emissions is therefore an issue which very seriously needs to be addressed by the cement industry.

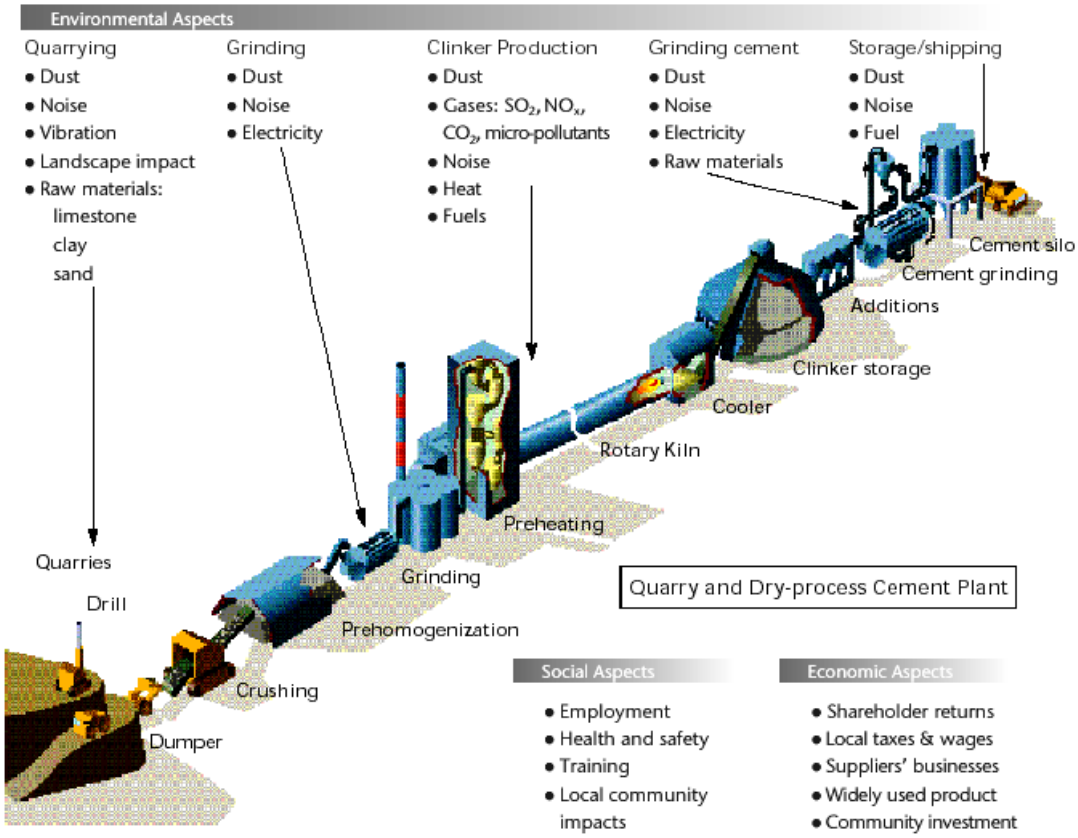

Figure 2.1 Cement manufacture and the influenced aspects (from www.wbcsdcement.org, 2005)

Because climate protection has such a high profile in the industry, effective strategies for managing CO_2 emissions are of crucial importance in the marketplace. The reduction options are likely to include: innovation in improving the energy efficiency of processes and equipment; switching to lower carbon fuels; using alternative raw materials to reduce limestone use; developing CO_2 capture and sequestration techniques; and taking advantage of market mechanisms such as emissions trading and voluntary initiatives.

The use of waste materials decrease the amount of clinker manufactured and thus decreases the amount of CO_2 emissions.

2.3 CEMENT CLASSES

Table 2.1 indicates the most common Portland and Portland fly ash cement used in South Africa. Table 2.2 indicates the mechanical and physical requirements of cement used in South Africa. These tables are used to describe the commercially available cement. The classification of cements in terms of their strength-giving properties has been practised for many years.

Table 2.1 Common Portland and Portland fly ash cements (from SANS 50197-1/SABS EN 197-1:2000)

Main types	Notation of the products		Composition (percentage by mass)					
			Main constituents					Minor additional constituents
			clinker	Pozzolana		Fly ash		
				natural	natural calcined	siliceous	calcerous	
			K	P	Q	V	W	
CEM I	Portland cement	CEM I	95-100	-	-	-	-	0-5
CEM II	Portland fly ash cement	CEM II/A-V	80-94	-	-	6-20	-	0-5
		CEM II/B-V	65-79	-	-	21-35	-	0-5
		CEM II/A-W	80-94	-	-	-	6-20	0-5
		CEM II/B-W	65-79	-	-	-	21-35	0-5

Table 2.2 Mechanical and Physical requirements of cement (from SANS 50197-1/SABS EN 197-1:2000)

Strength Class	Compressive strength MPa				Initial setting time	Soundness (expansion) mm
	Early Strength		Standard Strength			
	2 Days	7 Days	28 Days			
32.5 N	-	≥16.0	≥ 32.5	≤ 52.5	≥ 75	≤ 10
32.5 R	≥ 10.0	-				
42.5 N	≥ 10.0	-	≥ 42.5	≤ 62.5	≥ 60	
42.5 R	≥ 20.0	-				
52.5 N	≥ 20.0	-	≥ 52.5	-	≥ 45	
52.5 R	≥ 30.0	-				

2.4 HYDRATION OF PORTLAND CEMENT

The setting and hardening of Portland cement occur as a result of the reaction between the compounds of cement and water. The major compounds of cement that react with water to produce reaction products are tricalcium silicate (C_3S), dicalcium silicate (C_2S), tricalcium aluminate (C_3A), and tetracalcium aluminoferrite (C_4AF) (Neville, 1995).

The presence of gypsum affects the hydration pattern of PC both kinetically and thermodynamically. Firstly the influence of gypsum on the principal individual constituents is discussed and then the influence of the reactions as a whole which occur with PC hydration.

2.4.1 The hydration of C_3S and C_2S

The hardening of cement paste is due mainly to the formation of Calcium silicate hydrate (CSH), and this formation is affected by the presence of $CaSO_4$ in the paste. The gypsum in cement not only affects the setting time, but also the strength development. The optimum gypsum content is the value at which the optimum combination of quantity and quality occurs.

Locher et al (1995), have discussed factors governing the optimum gypsum content and the effects of varying the source of the sulphate. The situation is complicated by the fact that, contrary to some early conclusions, the amounts needed to optimise different properties, such as strength at various ages and drying shrinkage are not necessarily the same; also, the amount needed to optimise a given property in a concrete may not be the same as that required in a paste or mortar (Tang and Gartner, 1988).

During the early and middle periods of reaction in a cement paste, gypsum dissolve and react at or close to the surfaces of the clinker grains, more specifically the aluminate and ferrite phases. The factor most directly influencing the course of the early reactions is not so much the relative amounts of calcium sulphate, aluminate and ferrite phases, as the rate at which the relevant ionic species are made available at the surface of the cement grains. Other major factors affecting the supply of these ions are the particle size distribution of the calcium sulphate and the distribution in space of the particles (Taylor, 1995). Frigione (1995) has, by measuring the Ca^{2+} concentration of the liquid phase shown that the presence of gypsum increased the C_3S hydration rate, Figure 2.2.

The calcium silicate hydrate reactions are the most important as these are responsible for the majority of strength of the hardened cement paste (hcp). The hydration products of the two calcium silicates are similar and differ only in the terms of the rate at which they occur and in the amount of calcium hydroxide formed as seen in equation 2.3 and 2.4. The reaction of the C_3S with water is the more rapid of the two.

$$\underset{\textit{Alite}}{2C_3S} + 6H \rightarrow C_3S_2H_3 + 3CH \qquad \text{(equation 2.3)}$$

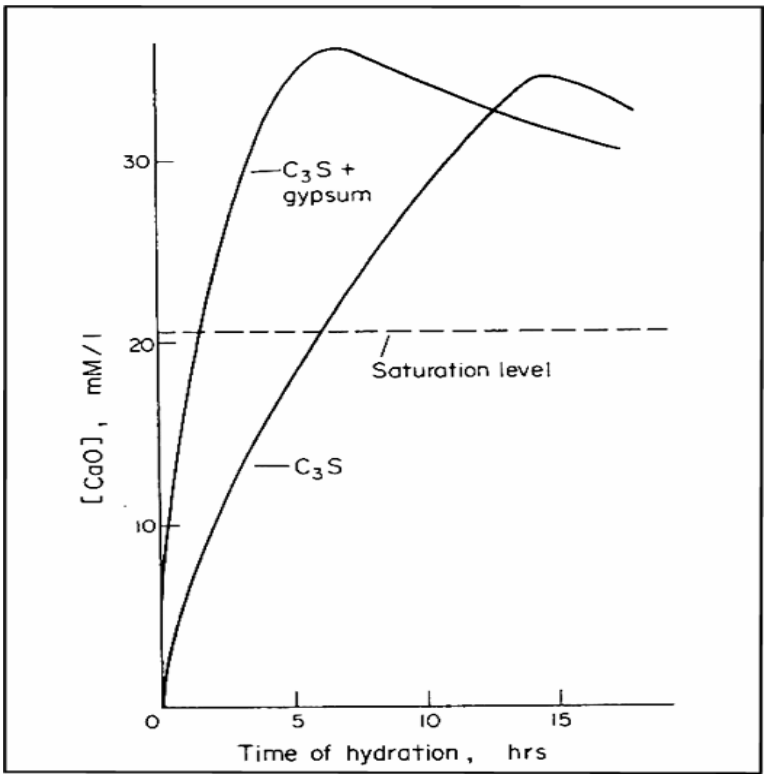

Figure 2.2 Changes in Ca^{2+} in solution curing C_3S hydration vs. time in the absence and presence of gypsum (Frigione, 1995)

The C_2S reaction is similar, but it takes place at a slower rate, contributes less heat than the C_3S and is responsible for the later strength development.

$$2C_2S + 4H \rightarrow C_3S_2H_3 + CH \qquad \text{(equation 2.4)}$$

Belite

When water is added to the reactions above, the calcium hydroxide ions are rapidly released into the solution and the pH of the solution rises rapidly to over 12. During this stage a considerable amount of heat is evolved.

While the concentration of calcium and hydroxide ions are building up, a dormant period occurs which coincides with the ettringite delay from the C_3A reaction and helps to explain why paste can remain workable for so long. Once the critical concentration of the ions is reached the CSH and CH start to

crystallise out from the solution, strength is developed and workability is lost.

2.4.2 Hydration of C_3A

The reaction of C_3A with water is very fast and involves reactions with sulphate ions supplied by the dissolution of gypsum (see Equations 2.5 and 2.6).

$$C_3A + 3CSH_2 + 26H \rightarrow C_3A.3CSH_{32} \quad \text{(equation 2.5)}$$

Where:
H - Water
CSH - Calcium sulphate (Gypsum)
$C_3A.3CSH_{32}$ - Calcium Sulphate Aluminate Hydrate (Ettringite)

The formation of ettringite slows down the hydration of C_3A by creating a barrier around the cement grains. After a certain portion of the sulphate has been consumed, the ettringite becomes unstable and a second reaction begins to take place (Wainwright, 2004).

Ettringite

$$C_3A + CSH + 10H \rightarrow C_3A.CSH_{12} \quad \text{(equation 2.6)}$$

Monosulphate

It is not until this second reaction occurs that the paste begins to stiffen significantly and workability begins to drop. The overall C_3A reaction produces a significant quantity of heat but contribute little to the strength.

An inadequate supply of soluble calcium sulphate can result in a rapid loss of workability known as flash set. This is accompanied by the release of heat and is irreversible. However, if too high a level of gypsum is present; crystals of gypsum crystallize from the solution and cause a plaster or false set (cement). If mixing continues or is resumed, the initial level or workability is restored. The cement manufacturer thus

needs to optimize the level of gypsum in the cement and match this to the reactivity of C_3A present. This concept is illustrated in Figure 2.3.

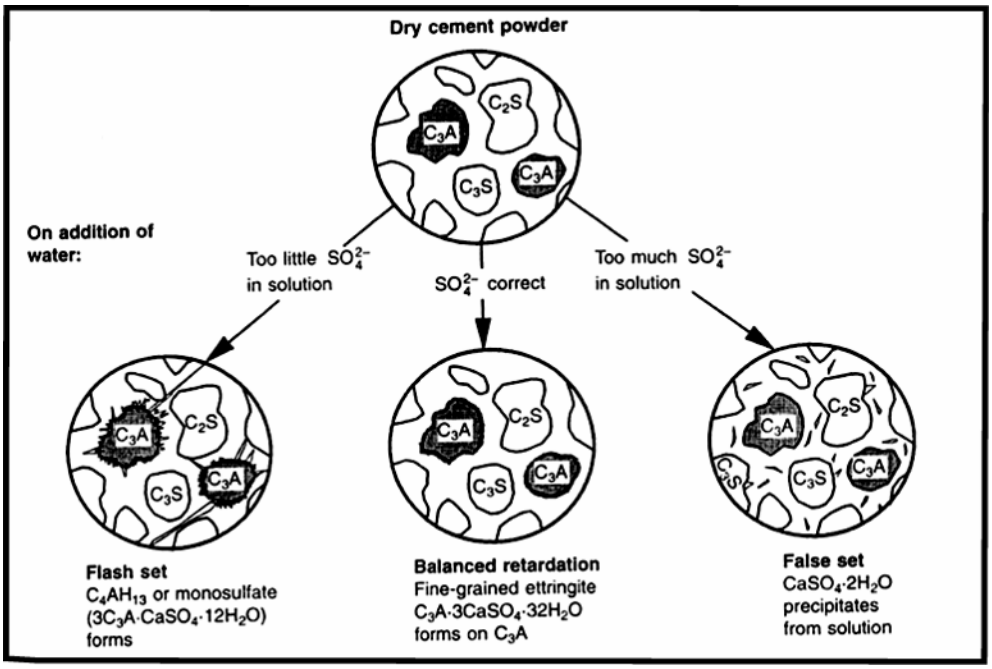

Figure 2.3 Optimization of soluble calcium sulphate (cements) (Newman, 2003)

2.4.3 Hydration of C_4AF

The ferrite phase (C_4AF) is of no great importance compared to the others. It is a slow reaction (see equation 2.7) with little heat evolved and contributes little to the strength.

$$C_4AF + 10H + 2CH \rightarrow C_6AFH_{12} \quad \text{(equation 2.7)}$$

Sulphoferrite

2.5 HEAT OF HYDRATION

The chemical reactions between unhydrated cement and water during setting and hardening release heat which results in a rise in temperature of the fresh concrete. If optimum performance is to be achieved from the cement, it is thought that the peak hydration rate associated with C_3A should be

delayed by SO_3 additions until the silicate hydration rate has passed its peak.

2.5.1 Optimization of Cement Sulphate

Neville, (1995) suggested that the optimum gypsum content be determined by observation of the generation of heat of hydration. Optimum sulphate with respect to strength development and dimensional stability occurred when the depletion of soluble sulphate used up by the aluminate hydration occurred at a time later than the maximum heat evolution from the main silicate hydration peak (Sandberg, 2004). Figure 2.4 shows an example of hydrating PC with slightly higher than optimum sulphate content monitored at room temperature by an isothermal conduction calorimeter.

The initial peak in Figure 2.4 occurs as soon as water is added to the PC, resulting from the ettringite being formed in the C_3A reaction. The calcium hydroxide ions passing into solution in the cement mixed with water initially display strong exothermic behaviour by rapid dissolution and initial hydration of mainly the aluminate phase as seen at A in Figure 2.4. If sufficient sulfate is available in the solution, the hydration rate rapidly decreases as the aluminate reacts with calcium and sulfate to form ettringite (B on the curve). The formation of ettringite prevents flash set and allows the concrete to be transported and placed while it is still fluid. After some time the strength giving Alite hydration takes off, which results in a broad exotherm C. Set usually occurs at the initial part of the Alite exotherm. The Alite and aluminate hydration continue in parallel until the mixture runs out of soluble sulphate (at D), which initiates the formation of aluminates with less sulfate than ettringite (Sandberg, 2004).

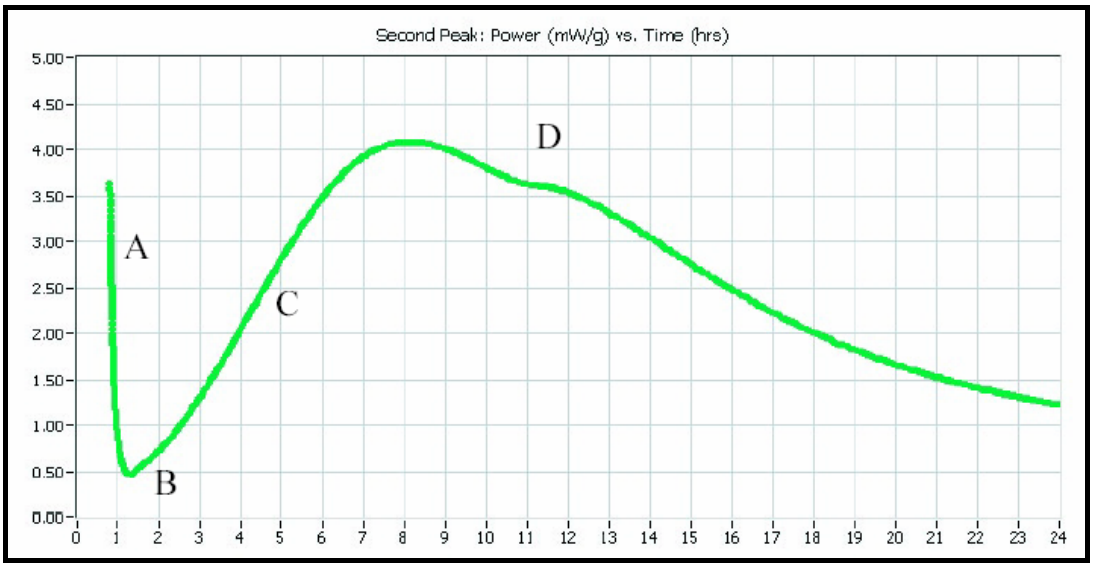

Figure 2.4 Example of normal hydration of Portland cement (Sandberg, 2004)

After the water has been added to the cement the first peak in the rate of heat evolution is followed by a second peak some 4 to 10 hours later. With the correct amount of gypsum there should be little C_3A available for reaction after all the gypsum has combined and no further peak in the heat liberation should occur. Thus optimum gypsum content leads to a desirable rate of early reaction and prevents local high concentration of products of hydration (Neville, 1995). In consequence the size of pores in hydrated cement paste is reduced and strength is increased. The amount of gypsum required increases with the C_3A content and also with the alkali content of the cement. Increasing the fineness of cement has the effect of increasing the quantity of C_3A available at early stages, and this raises the gypsum requirement.

The amount of gypsum added to cement clinker is expressed as the mass of SO_3 present; this is limited by the SANS 50197-1/SABS EN 197-1:2000 to a maximum of 3.5%. There is usually found to be an optimum SO_3 content (2-3% for binders), beyond which (> 4%), compressive strength begins to decline (Lea, 1998). Frigione confirmed this statement using ISO-RILEM mortar prisms, for cements with a wide range of particle size

distributions, gypsum was added to preground clinker, and found that the maximum in strength was not sensitive to particle size grading (Frigione and Mara, 1976). Lerch's, (1946) test results indicate that 2.5% added SO_3 may be sufficient to bring the resulting PC to optimum SO_3 level.

2.6 SPECIFIC SURFACE AREA

At most manufacturing plants a ball mill is used to grind the cement clinker. The principal test carried out at a cement mill is the fineness test in which the specific surface area is determined. The specific gravity and fineness of cement increase with an increase in the grinding time. Bouzoubaâ et al (1997) found that this increase in fineness was less significant beyond 2 hours. An optimum of 4 hours grinding time was established by Bouzoubaâ, beyond which the water requirement increased and the strength either decreased or did not increase significantly.

The fineness of cement is a major factor influencing its rate of hydration, since the hydration reaction occurs at the interface with water (Lea, 1988). Greater cement fineness increases the rate at which cement hydrates and thus accelerates strength development. The effects of greater fineness on paste strength are manifested principally during the first seven days.

Portland cement is usually ground to a surface area in the range 300 – 350 m^2/kg and rapid hardening Portland cement to 400 – 550 m^2/kg.

2.7 PARTICLE SIZE DISTRIBUTION

The particle size distribution curve of a material describes two properties of the material namely mean particle size as well as the distribution of other sizes about the mean. The curve is usually drawn as the cumulative percentage-values on the y-axis of particles smaller than the corresponding sizes on the x-

axis. The x-axis is drawn to a log scale to accommodate large ranges of particle sizes. The shape of the curve gives an indication of the continuity in size distribution and the slope describes the wideness or range of the size distribution.

Particle size distributions of interground blended cements are different than that of separately ground cements (Erdogdu, 1999). The particle size distribution produced when a material is ground becomes wider as the material becomes easier to grind. During the intergrinding of cement constituents of differing grindability, the particle size distribution of the material which is harder to grind becomes narrower, the easier the other component is to grind. Conversely, the particle size distribution of the material which is easier to grind becomes wider the harder the other component is to grind (Lea, 1988).

Approximately 95% of cement particles are smaller than 45µm, with the average particle around 15µm. Bye, (1999) supported the generally held view that the 3-30µm fraction makes a major contribution to the 28-day strength. The range <3µm is important for achieving high 1-day strengths.

2.7.1 Rosin-Rammler distribution function

In searching for a parameter, which will provide a more representative description of the particle size distribution, the Rosin-Rammler function was investigated.

From a probability point of view Rosin and Rammler investigated the particle size distribution of crushed coal and developed a function that describes the distribution as (Rosin, 1933):

$$f(x) = exp(-bx^n) \qquad \text{(equation 2.8)}$$

Where:

b - Fineness characteristic measure of the material being analysed.
n - A measure of the range of particle sizes.

Rosin and Rammler also found that the function does not only apply to crushed coal but also to various other powered materials.

The function was modified as follows:

$$RR = \exp -(x/X_o)^n \qquad \text{(equation 2.9)}$$

Where:
The weighting function *f(x) is denoted as RR.*
X_o – the absolute size constant or position parameter (it represents the particle size for which 36.8% of the particles are coarser).

Taking the double logarithm of equation 2.9 we obtain:

$$lnln(1/RR) = n(lnx - lnX_o) \qquad \text{(equation 2.10)}$$

Equation 2.10 describes a straight line plot with a coordinate system made up of a log scale abscissa for the particle size *x*, and an ordinate with a double logarithm of the reciprocal of the residue RR. The slope of the straight line is *n* and the line intercept the horizontal axis at a value describing the particle size *x* (Olorunsogo, 1990). A hypothetical example of the diagrammatic representation of the particle size distribution by the Rosin-Rammler distribution function is shown in Figure 2.5.

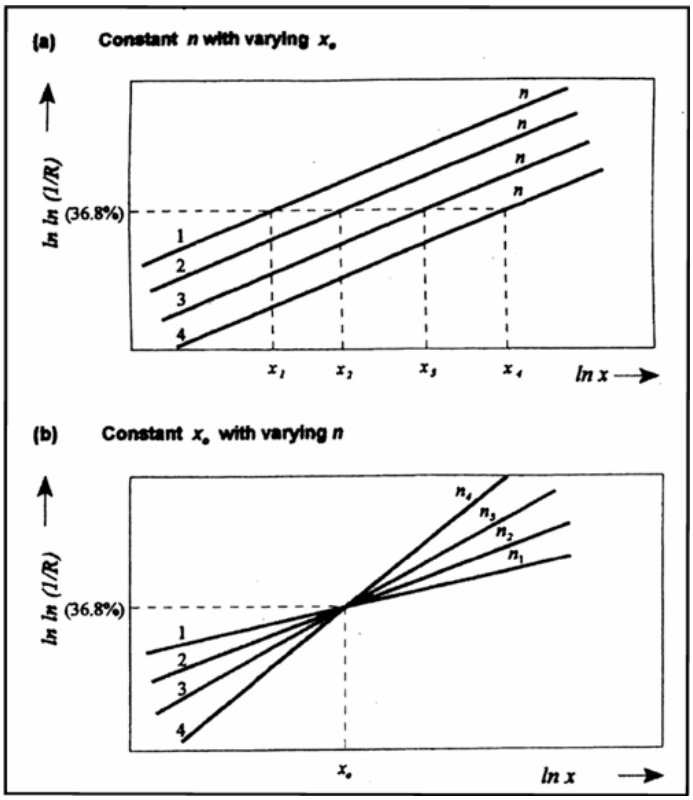

Figure 2.5 Diagrammatic representation of Rosin-Ramler distribution function (Wainwright and Olorunsogo, 1999)

Figure 2.5 (a) shows the typical particle size distribution of four different samples having the same n and different *Xo*. This illustration shows that the sample represented by the four plots might have similar ranges of size distribution (denoted by equal *n*) but with possible varying degrees of fineness (indicated by the various X_o). The sample represented by plot 1 being the finest and the one by plot 4 the coarsest of the four. Similarly, Figure 2.5 (b) illustrates a situation whereby the four samples might be of the same fineness (because of the same X_o) but possibly with different size ranges (Wainwright and Olorunsogo, 1999).

2.8 CONCLUSION

- Test results indicate that 2.5% added SO_3 may be sufficient to bring the resulting PC to optimum SO_3 level.
- The specific gravity and fineness of cement increase with an increase in the grinding time.

- An optimum of 4 hours grinding time was established beyond which the water requirement increase and the strength either decrease or did not increase significantly.
- Greater cement fineness increases the rate at which cement hydrates and thus accelerates strength development.
- The particle size distribution produced when a material is ground becomes wider as the material becomes easier to grind.
- Approximately 95% of cement particles are smaller than 45μm, with the average particle around 15μm.
- The 3-30μm fraction makes a major contribution to the 28-day strength. The range <3μm is important for achieving high 1-day strengths.
- The Rosin-Rammler distribution function can be evaluated as a method providing an easy means of describing the particle size distribution quantitatively.

3. COMPOSITION AND PROPERTIES OF COAL ASH

3.1 INTRODUCTION

Sustainable development can be defined, as development, which meets the needs of people living today without compromising the ability of future generations to meet their own needs. It requires a long-term vision of industrial progress, preserving the foundations upon which human quality of life depends: respect for basic human need and local and global ecosystems.

Using by-products from other industries as raw material is a huge opportunity for the cement industry to reduce its environmental impact, because it allows companies to access materials for use in the kiln and the mill without extracting them directly from the ground. There are a number of mineral by-products that contain useful materials that can be extracted for use in cement production, or in making concrete. Typical additives include slag, coal ash like fly ash and bottom ash, by-products from blast furnaces and power generation.

Cement, a fine grey powder, sets after a few hours when mixed with water, and then hardens in a few days into a solid, strong material. Virtually all the cement produced globally is mixed with sand, aggregates and water and used to make concrete and mortars.

Cement extenders are used as a substitute for some of the PC in concrete. The main reason for the use of extenders is the variety of useful enhancements, which they give to the concrete properties. Fly ash is one of the cement extenders commonly used in South Africa. Fly ash consists of finely divided ashes produced by burning pulverised coal in power stations. Gasification ash is a produced as a by-product during the gasification of coarse coal. The properties of fly ash can be used as a guideline to investigate other ashes for use as cement extenders in concrete.

In this chapter, the use of coal combustion by-products, specifically fly ash, in concrete will be discussed. Consideration will be given to properties like shape, particle size, mineralogical and chemical composition, durability and the chemical requirements for using fly ash as a cement extender. This will provide adequate understanding of the advantages that by-products have to both the cement industry and the environment.

3.2 COAL ASH

Currently, close to a billion tons of coal is burned annually in the world to generate electricity and as a result, nearly 130 million tons of coal combustion by-products (CCBs) are produced. One-third of these CCBs are utilized, while the rest are disposed of mainly in landfills (Schwartz, 2003). Increasing costs and heightened regulations are making the disposal of CCBs an undesirable option. Utilization of CCBs as raw materials results in numerous benefits, including:

- A decrease in the demand for landfill space
- Conservation of natural resources
- A cleaner safer environment
- Reduced carbon dioxide emissions
- Significant economic savings for end users
- A boost in economic development
- Reduced overall cost of generating electricity

Electricity is the fuel of the “Information age” and power plants that burn coal account for more than half of the electricity produced. These power plants also produce coal combustion by-products like fly ash (which is capture from the exhaust of the boiler) and bottom ash (which is heavier and falls to the bottom of the boiler). CCBs are considered to be four distinct and

extremely different materials, as seen in Figure 3.1 (American Coal Ash Association, 1997).

Coal bottom ash and boiler slag are the coarse, granular, incombustible by-products that are collected from the bottom of furnaces that burn coal for the generation of steam and the production of electricity. Bottom ash is a dark gray, granular, porous, predominantly sand size (-12.7mm) material (Babcock, 1978). Material drops into a water filled hopper at the bottom of the furnace. The material is removed by means of high-pressure water jets and conveyed by sluiceways either to a disposal pond or to a decant basin. From here the material is dewatered, crushed and stockpiled for disposal or use (Hect, 1975).

Bottom ash applications are snow and ice control, as aggregate in lightweight concrete masonry units, and raw feed material for the production of PC. Bottom ash has also been used as a road base and subbase aggregate, structural fill material (ASTM E1861-97), and as fine aggregate in asphalt paving.

Flue gas desulphurisation (FGD) gypsum is also known as scrubber gypsum. FGD gypsum is the by-product of an air pollution control system that removes sulphur from the flue gas in calcium-based scrubbing systems. It is produced by employing forced oxidation in the scrubber and is composed mostly of calcium sulphate.

The majority of FDG-produced gypsum used in the United States (American Coal Ash Association, 1997) is employed for wallboard, which reduced the need for mining natural gypsum. As an additive in PC, FDG gypsum is used to retard setting. This enables wet cement in ready-mix trucks to be transported greater distances while remaining workable. Gypsum's high permeability (10-3cm/sec) makes it an excellent soil conditioner. Steffan (1991) indicates that FGD gypsum offers several major benefits as a soil amendment. These include

adjustment of soil pH and means of keeping peanuts and other crops disease-free.

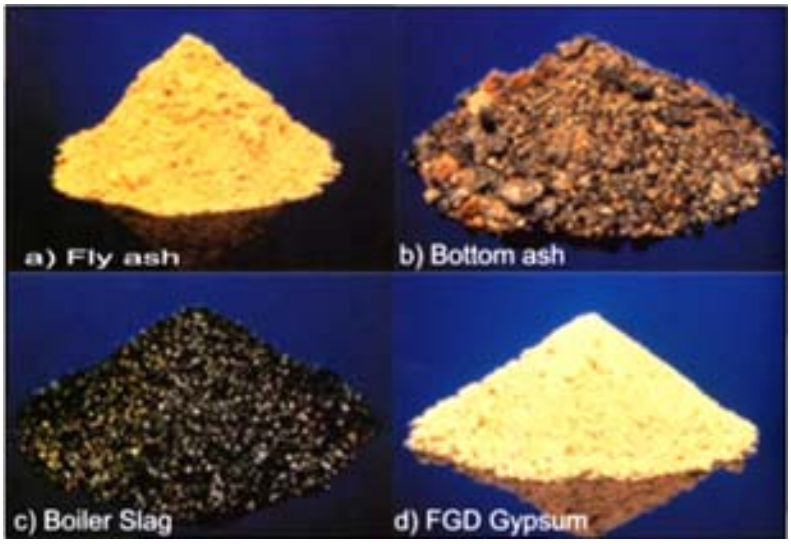

Figure 3.1 Coal combustion by-products

The fourth CCB is fly ash which is most often used in concrete as a replacement for part of the PC in the mix design. The use of fly ash as an extender in concrete will be discussed later in this chapter.

3.3 POZZOLANIC REACTION

The American Society for Testing Materials (ASTM) defines a pozzolan as 'a siliceous or siliceous and aluminous material, which in itself possesses little or no cementitious property but which will, in finely divided form and in the presence of moisture, chemically react with calcium hydroxide at ordinary temperature to form compounds possessing cementing properties'.

As a pozzolanic material fly ash contains active silica (SiO_2), and is not cementitious in itself but will chemically react with calcium hydroxide in the presence of moisture to form cementitious compounds (Illston, 2001). When a pozzolanic material is used in conjunction with a PC, the calcium hydroxide that takes part in the pozzolanic reaction is that produced from

the cement hydration. More quantities of calcium silicate hydrate are produced (see equation 3.1).

$$2S + 3CH \rightarrow C_3S_2H_3 \qquad \text{(equation 3.1)}$$

It is clear that the pozzolanic reaction is secondary to the hydration of PC. The degree of hydration of fly ash is increased in the presence of gypsum because the surface is activated by the destruction of the structure of the glass and crystalline phases caused by the dissociation of Al_2O_3 reacting with SO_4^- (Uchikawa, 1986). The products of the pozzolanic reaction make their own contribution to the strength and other properties of the cement and concrete.

3.4 FLY ASH

Fly ashes (FA) consist of finely divided ashes produced by burning pulverised coal in power stations as seen in Figure 3.2. They are removed from the combustion gases and collected by special mechanical devices and electrostatic precipitators. Owing to the high temperatures reached during the instantaneous burning of coal, most of the mineral component contained in the coal melts and forms small fused drops. The subsequent sudden cooling transforms them partly or entirely into spherical glass particles. The recognition that fly ash exhibits pozzolanic properties has led to its use as a constituent of concrete. Fly ashes contain metastable aluminosilicates that will react with calcium ions in the presence of moisture to form calcium silicate hydrates (Massazza, 1998). Fly ash produced in South Africa is a fine powder, the particles of which are round hollow spheres (see Figure 3.3).

Figure 3.2 A modern pulverised coal-fired thermal power station (Krüger, 1999).

Fly ash is used in concrete either as part of blended cement or as a separate component added at the stage when the concrete mix is prepared. The inclusion of fly ash in concrete affects all aspects of concrete. As part of the composite concrete mass, fly ash acts both as a fine aggregate and as a cementitious component. It influences the rheological properties of the fresh concrete and the strength, finish, porosity, and durability of the hardened mass as well as the cost and energy consumed in manufacturing the final product (Massazza, 1998).

3.4.1 Physical Properties

Fly ash particles are mostly spherical in shape (see Figure 3.3) with sizes ranging from approximately 1 to 100μm in diameter, with an average size of 20μm (Carette, 1986). The surface area of fly ash particles vary from 2000 cm^2/g to 10 000 cm^2/g depending on the proportion of fine particles in the fly ash.

Erdogdu (1998) found that concrete containing a finer fraction of fly ash gave a better compressive strength than that without fly ash or concrete containing coarser fly ash. The particle size distribution, shape and surface characteristics of fly ash have a

considerable influence on the water requirement and workability of freshly made concrete and on the rate of strength development in hardened concrete.

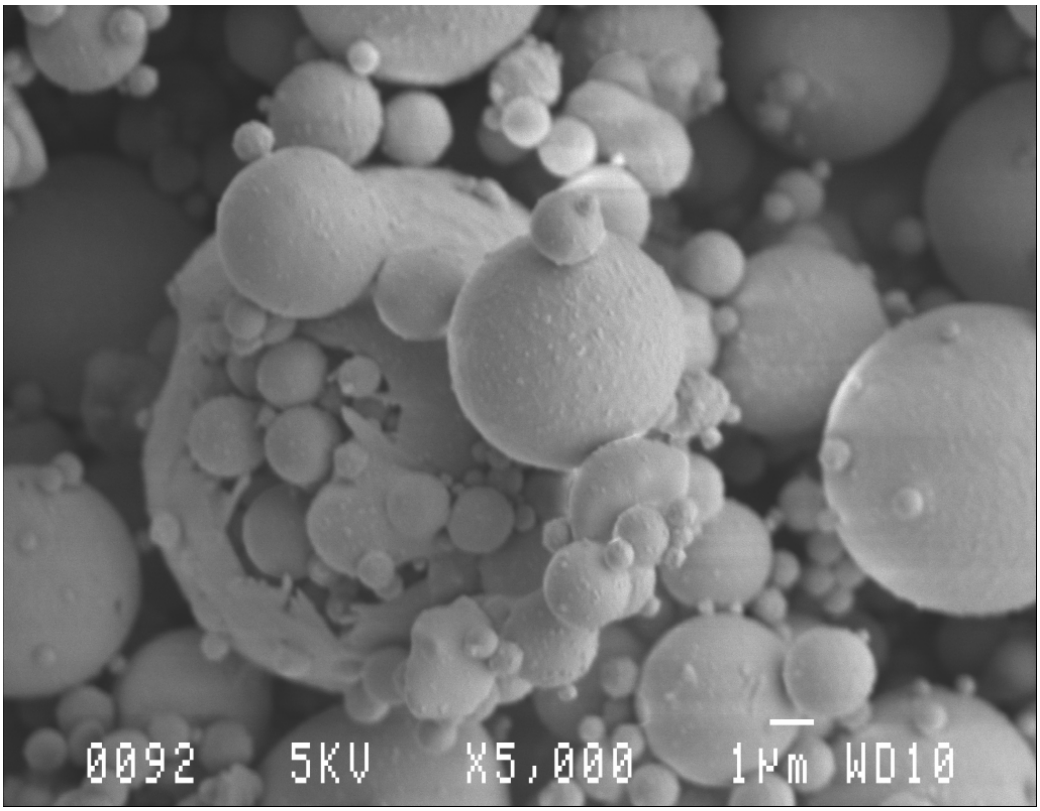

Figure 3.3 Electron microscope photograph of fly ash.

3.4.2 Chemical Composition

The chemical composition of fly ash depends on the characteristics and composition of the coal burned in power stations. The chemical analysis of fly ashes by means of X-ray fluorescence (XRF) and spectrometry techniques shows that SiO_2, Al_2O_3, Fe_2O_3, and CaO are the major constituents of most fly ashes. Table 3.1 shows the typical chemical composition of fly ash.

Table 3.1 Typical chemical composition of fly ash (Addis, 2001)

Oxide	% By mass
SiO_2	45-50
Al_2O_3	25-30
CaO	4-8
FeO	9-11
MgO	2-4
$Na_2O + 0.658K_2O$	1-3

3.4.3 Mineralogical Composition

Both the type and source of fly ash influence its mineralogical composition. Due to the rapid cooling of burned coal in the power plant, fly ash consists of noncrystalline particles (≤ 90%), or glass and a small amount of crystalline material.

In addition to a substantial amount of glassy material, each fly ash may contain one or more of the four major crystalline phases: quartz, mullite, magnetite, and hematite. In subbituminous fly ashes, the crystalline phases may include C_3A, C_3A_3S, calcium sulphate, and alkali sulphates (Metha, 1989).

The reactivity of fly ashes is related to the noncrystalline phase or glass. Diamond (1981) pointed out that the composition of glass in low-calcium fly ashes is different from that in high-calcium fly ashes. X-ray diffraction (XRD) indicates that South African fly ash consists mineralogically mainly of glass and some low-quartz (SiO_2), mullite ($Al_6Si_2O_{13}$) and some quicklime (CaO).

3.4.4 Chemical Specifications

In South Africa fly ash should comply with the requirements of the South African standard specification for Portland cement extenders (SANS 1491-2:2005 / SABS 1941-2:2005). Fly ash complying with SANS 149-2 may be used as a cement extender

with Portland cement for use in concrete when it conforms to Table 3.2.

Loss on ignition, the weight loss of fly ashes burned at temperatures ≤ 1000°C, is related to the presence of carbonates, combined water in residual clay minerals, and combustion of free carbon. The water required for workability of mortars and concretes depends on the carbon content of fly ashes: the higher the carbon content of a fly ash, the more water is needed to produce a paste of normal consistency.

Table 3.2 Chemical specifications for cement extenders. (SANS 1491-2:2005 / SABS 1941-2:2005)

Test	Fly ash max allowed
Sulphur trioxide content, % (m/m)	2.5
Loss on ignition, % (m/m)	5.0
Free water content, % (m/m)	1.0
Fineness, residue retained on a sieve with square apertures of nominal size 45µm, % (m/m)	12.5
Water requirement, % of control	95
Strength factor, %	6
Soundness, expansion, mm	5

3.5 INFLUENCE OF FLY ASH ON THE PROPERTIES OF CONCRETE

3.5.1 Fresh Concrete

Although concrete is in the fresh state for only a few hours, the properties of fresh concrete are important because they influence the handling of the concrete, the degree to which it can be compacted and the uniformity of distribution of constituents within the concrete.

3.5.1.1 Water Demand

Davis (1937) noted, fly ash differs from other pozzolans, which increase the water requirement of concrete mixes. The improved workability allows a reduction in the amount of water used in concrete. Partial replacement of OPC by fly ash, in concrete reduces the water requirement to obtain a given consistency (Malhotra, 1996). This is generally attributed to the spherical shape and smooth texture of the fly ash particles.

According to Owens (1979) the major factor influencing the effects of ash on the workability of concrete is the proportion of coarse material (>45μm) in the ash. Very fine particles of fly ash get absorbed on the oppositely charged surface of cement particles and prevent them from flocculation. The cement particles are thus effectively dispersed and will not trap large amounts of water, which means that the system will have a reduced water requirement for flow. In addition, Portland cement particles are mostly in the size range of 1 to 50μm, which cause the micro fine particles of fly ash to reduce the void space and correspondingly the water requirement.

The relationship between the amount of water and the percentage of fly ash replacement for the same workability with 21, 28 and 34 MPa nominal-strength concrete can be seen in Figure 3.4. As the amount of fly ash increased in the mixture, the water requirement decreased (Naik, 1990).

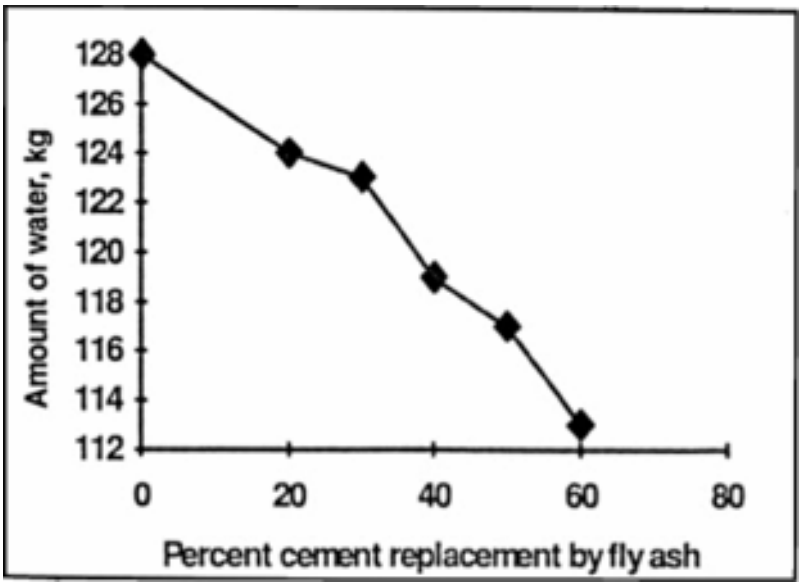

Figure 3.4 Relationship between water requirement and cement replacement with fly ash (Naik, 1990)

3.5.1.2 Workability

The ACI Committee 116R-00:2000 has provided the most suitable definition of workability, which reads as follows:

"that property of freshly mixed concrete or mortar which determines the ease and homogeneity with which it can be mixed, placed, consolidated and finished."

The workability (fluidity) of a Portland concrete can be improved when part of the OPC is replaced with fly ash. Brown (1982) found that both slump and V-B workability improved with increased ash substitutions. The extent of the improvements depends on the fineness and carbon content of the fly ash.

Rheological properties and fluidity has been found to depend on the particle size distribution of cement (Gosh, 1983). Lee (2002) found that the fluidity of a fly ash-cement system increase as the particle size distribution becomes wider. When workability is kept constant the water content of a fly ash mix decreases with an increase in the fineness of the fly ash.

3.5.2 Hardened Concrete

The strength of hardened concrete is of fundamental importance to structural designers. It is also extensively used as an index of other properties and of concrete quality.

3.5.2.1 Compressive Strength Development

The measured compressive strength of concrete depends on the intrinsic properties of the concrete. Many variables influence the strength development of fly ash concrete, these being:

- properties of fly ash
- chemical composition
- particle size
- reactivity
- temperature and curing conditions

At early ages the compressive strengths (up to 28 days) of all concretes containing fly ash are lower than that of the corresponding concrete containing normal Portland cement. After 28 days, if wet curing is continued, the compressive strength of fly ash concrete will be higher than the Portland concrete (Krüger, 1999). This is demonstrated in Figure 3.5.

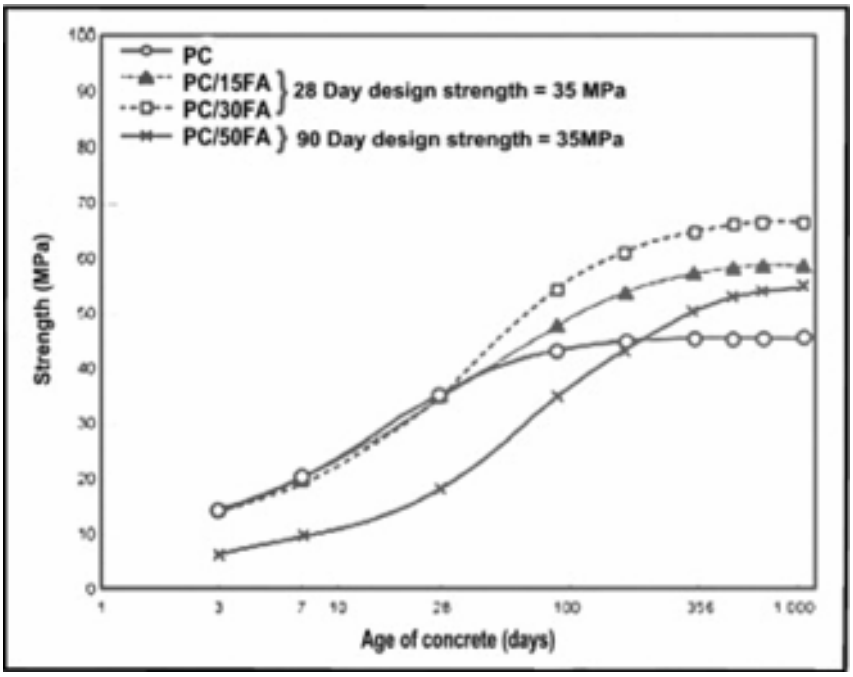

Figure 3.5 Development of compressive strengths of Portland cement and fly ash concretes (from Krüger, 1999)

Particle size can influence the strength development in two ways. Particles larger than 45μm influence water requirements adversely. They counteract to the needs of the methods used to compensate for the slow rate of reaction of fly ash at early ages. Cementing activity occurs on the surface of the solid phases, through processes involving the diffusion of materials in concentrated pastes. Figure 3.6 shows that finer fly ashes imparted greater compressive strengths (Joshi, 1982).

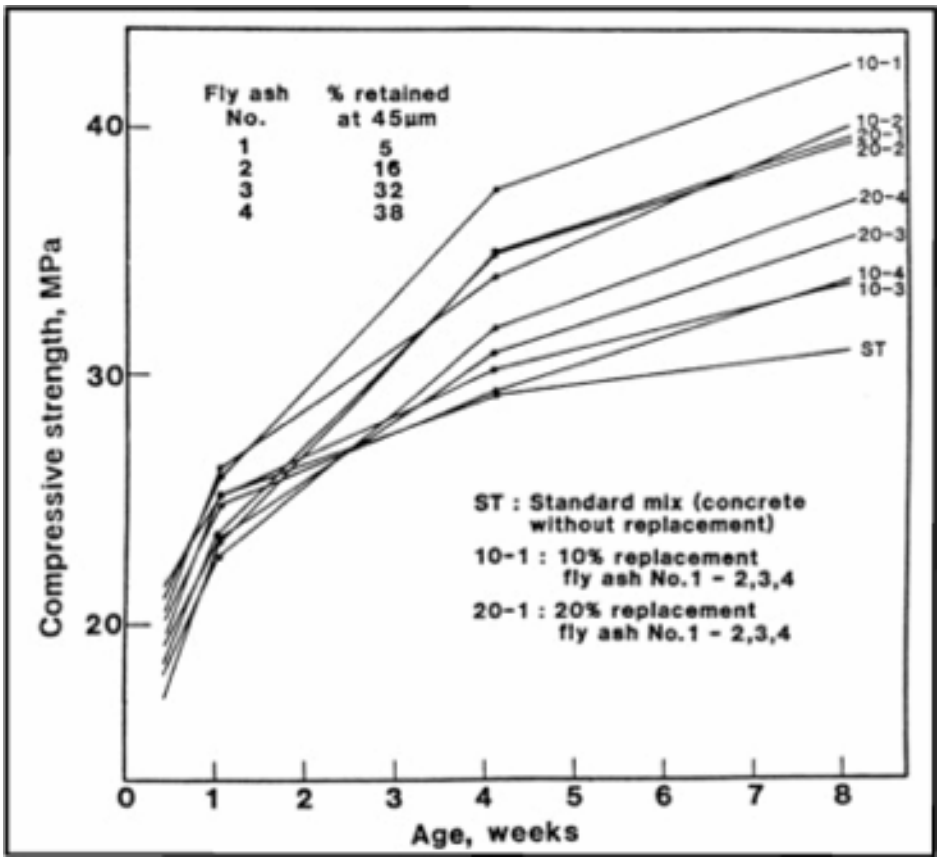

Figure 3.6 Effect of coarse fractions of fly ash on compressive strength development of concretes (Joshi, 1982)

Concrete containing fly ash shows strength gain as a consequence of heating in contrast to the loss of strength that occurs with normal Portland cement (Malhotra, 1996). This property of fly ash is of great value in the construction of mass concrete or in concrete construction at elevated temperatures. The effect of curing temperature on the strength development of concrete containing fly ash can be seen in Figure 3.7.

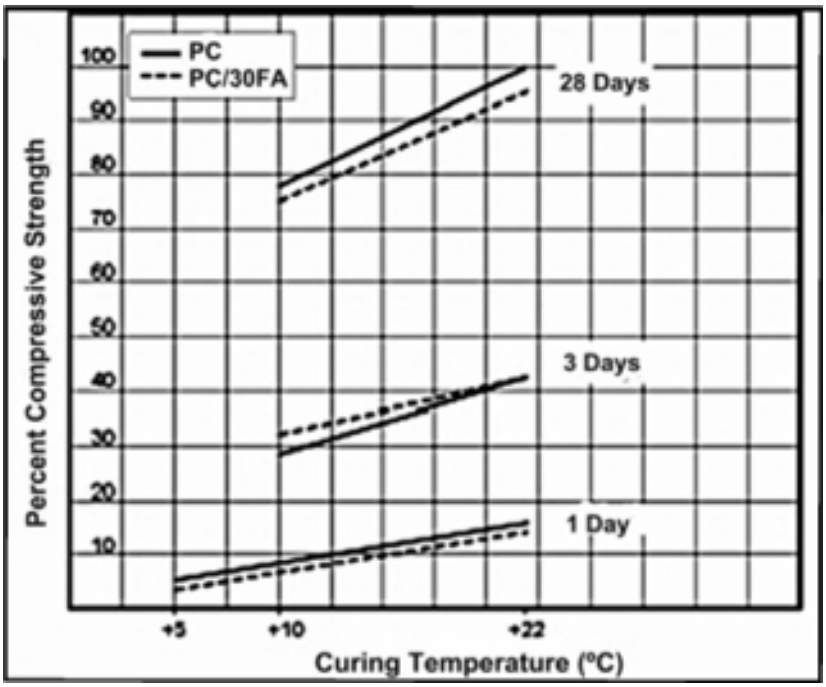

Figure 3.7 Compressive strengths of PC and PC/30FA at different temperatures (Krüger, 1999).

3.5.2.2 Flexural Strength

There is a general trend for the flexural to compressive strength ratio to increase with an increase in fly ash content. The results presented in Figure 3.8, points out that the increase is slight for water cement (w/c) ratios around 0.5. The flexural to compressive strength ratio of Portland cement concrete is similar to that of PC/FA concrete of similar strength. Comparing the flexural to compressive strength ratios of the PC and PC/FA mortar at similar compressive strength, although not reached at the same age, the results indicate that the ratio for the PC/FA mortar is somewhat higher than that for the PC mortar.

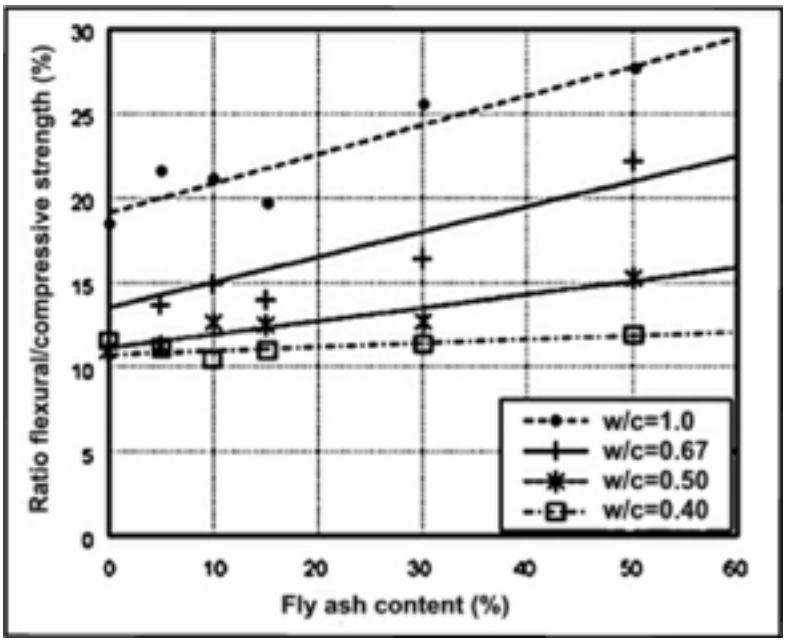

Figure 3.8 The influence of FA content of the cementitious material on the flexural/compressive strength ratio of concrete (Krüger, 1999)

3.5.2.3 Modulus of Elasticity

The modulus of elasticity of a material is defined by the stress: strain curve. The higher the elastic modulus, the more resistant the material is to deformation.

There appears to be no significant difference between the modulus of elasticity of concrete with or without fly ash at 28 days. However, like compressive strength, concrete with fly ash has a lower modulus at early age strength and higher modulus at ultimate strength compared with concrete without fly ash (Lane, 1982). The effect of fly ash content on the relationship between compressive strength and elasticity can be seen in Figure 3.9.

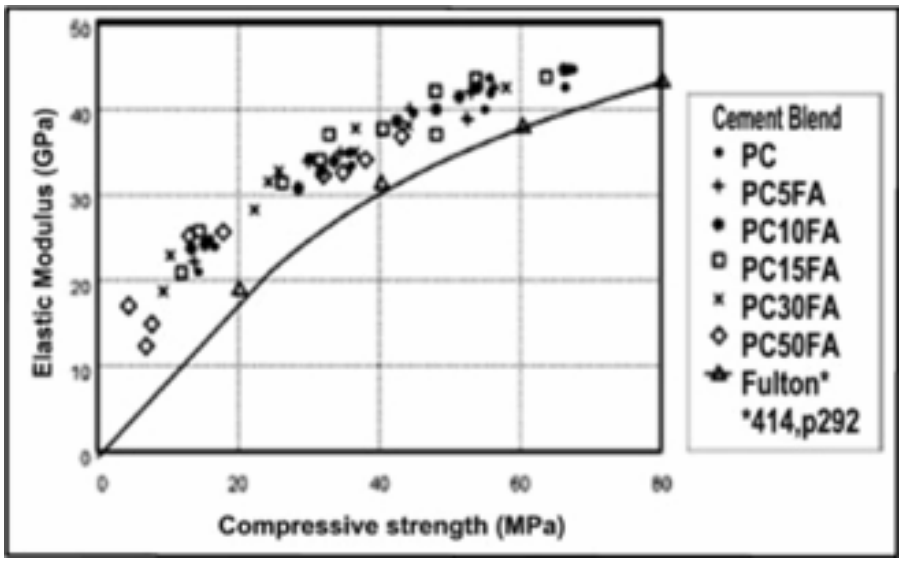

Figure 3.9 The influence of FA on the elastic modulus/ compressive strength of concrete (Krüger, 1999)

3.5.2.4 Drying Shrinkage

When a hydraulic cement-bonded product such as concrete looses its free moisture, it shrinks (drying shrinkage) and when it gains in moisture content, it expands (wetting expansion). The dimensional change with variation in moisture content of concrete is and important property, because if differential dimensional movement in the concrete due to such a change is excessive, cracking may occur. If a dimensionally stable aggregate is used, drying shrinkage and wetting expansion can almost exclusively be attributed to the binder and is affected by factors such as binder content, water/cement ratio, curing and the strength of the concrete (Addis, 2001).

Work by Grieve (1991) on concrete made with a South African fly ash, showed that for similar exposure conditions, the drying shrinkage of such concretes is very similar to plain PC, over a range of fly ash contents up to 30%. This is confirmed by studies of Yuan (1983) which concluded that the replacement of cement with fly ash has little influence on drying shrinkage (see figure 3.10). Chindaprasirt (2003) found that the incorporation of fly ashes reduce the drying shrinkage in comparison with that

of PC. The early shrinkage of mortar with finer fly ash was found to be a little larger than that of the coarser fly ash mortar.

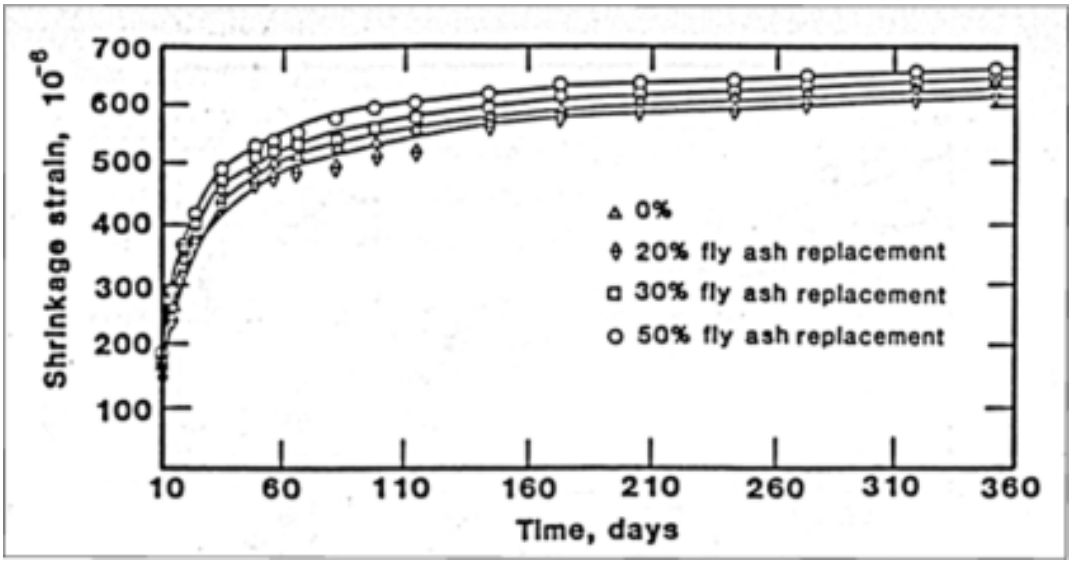

Figure 3.10 Drying shrinkage of concrete incorporating fly ash (Yuan, 1983)

3.5.2.5 Creep

Creep is defined as the increase in strain (deformation) under a sustained stress (load) (Holcim, 2005). Creep imparts to concrete a degree of ductility, which is desirable from the point of view of structural behaviour. However, creep also has detrimental effects on structures, such as increase deflections which can result in cracking, loss of pre-stress and buckling of long columns (Addis, 2001).

Grieve's (1991) work on concrete incorporating fly ash found that specific creep was reduced in fly ash mixes relative to plain mixes with similar 28-day strengths. This confirms the work done by Pandey (1983) which found that fly ash concrete's showed less creep in the majority of specimens than the reference concrete's showed.

3.6 DURABILITY OF CONCRETE

Durability may be defined as the ability of concrete to remain fully functional over an extended period under prevailing service conditions for the purpose for which it was designed. Concrete will remain durable if movement of aggressive chemicals within its structure is minimised.

Degradation of concrete can be a result of the environment to which the concrete is exposed, or from internal causes within the concrete. The rate of degradation is controlled by the rate at which moisture, air or other aggressive agents can penetrate the concrete. Thus considering the various transport mechanisms like porosity and permeability through concrete will indicate the influence on the durability of concrete.

3.6.1 Porosity

Hardened cement pastes and concrete contain pores of varying types and sizes, and therefore the transport of materials through concrete can be considered as the phenomenon of flow through a porous medium. The rate of flow will not only depend on the porosity, but on the degree of continuity of the pores and their size. A low porosity results in high strengths and low permeability in concrete.

The pozzolanic reaction in fly ash produces more calcium silicate hydrate, which tends to fill pore spaces. Fly ash have a lower water content than PC for the same workability and as a result of these factors the porosity of fly ash concrete is lower then PC.

3.6.2 Permeability

Permeability can be defined as the ease with which a liquid or a gas flows into (through) concrete under a pressure differential across the concrete. It is measured by the volume of liquid or

gas transmitted per unit area per time per unit pressure difference.

The major effect on the permeability of concrete is the curing regime. Air exposure under dry conditions is the most disadvantageous. Water curing gives the most impermeable concrete. Another effect on the permeability of concrete is the stronger the concrete and the lower the water/cement ratio; the more impermeable the concrete.

Fly ash has the effect of reducing the permeability and volume of large capillary pores in concrete when compared with a plain CEM I concrete of similar strength (Balim, 1993). This effect drives form the fineness of the material, the pozzolanic reaction and the reduced water requirement of the fly ash mixes. The fluid transport properties of concrete made with fly ash are therefore considerably reduced, thus enhancing the durability.

3.7 ADVATAGES OF USING FLY ASH IN CONCRETE

The use of fly ash in concrete has the following advantages:

- Reduction in material cost and the saving of energy by saving on cement.
- Reduction in building cost because of improved workability of concrete
- Better workability and cohesiveness
- Reduced water requirement for a given slump
- Improved impermeability
- Reduced water penetration of concrete
- Reduction in shrinkage
- Improves the durability of concrete in aggressive environments

3.8 CONCLUSION

- Fly ash is a waste material of the combustion of pulverised coal in thermal power plants. Fly ash is used in concrete for economic, environmental and durability considerations as a cement extender.
- The products of the pozzolanic reaction make their own contribution to the strength and other properties of the cement and concrete.
- The pozzolanic, chemical, physical and durability properties of fly ash have led to its use as a cement extender in concrete. The properties of fly ash can be used to indicate whether a gasification ash is suitable for use as a cement extender in concrete.
- Portland cement particles are mostly in the size range of 1 to 50µm, which cause the micro fine particles of fly ash to reduce the void space and correspondingly the water requirement.
- When workability is kept constant the water content of a fly ash mix decreases with an increase in the fineness of the fly ash.
- Concrete containing fly ash shows strength gain as a consequence of heating in contras to the loss of strength that occurs with normal Portland cement.
- There is a general trend for the flexural to compressive strength ratio to increase with an increase in fly ash content.
- There appears to be no significant difference between the modulus of elasticity of concrete with or without fly ash at 28 days.
- The replacement of cement with fly ash has little influence on drying shrinkage.

- Fly ash concrete's showed less creep in the majority of specimens than the reference concrete's showed.
- Fly ash have a lower water content than PC for the same workability and as a result of these factors the porosity of fly ash concrete is lower then PC.
- The fluid transport properties of concrete made with fly ash are therefore considerably reduced, thus enhancing the durability.
- Consideration of properties like shape, particle size, mineralogical and chemical composition, strength, elasticity, shrinkage and the chemical requirements for using fly ash as a cement extender should be investigated when using gasification ash as a cement extender.

4. EXPERIMENTAL PROGRAMME AND TEST PROCEDURES FOR CEMENT

4.1 INTRODUCTION

The aim of this study is to determine whether gasification ash can be used as a cement extender in concrete. Currently pulverised fuel ash (also called fly ash) is widely used as a cement extender in concrete and the effect of this type of ash is well established. In this study the properties of cement and gasification ash is examined to establish parameters for cement blended with gasification ash.

The aim of this chapter is to discuss the testing methods used in the practical analysis of the reactivity of a gasification ash. Parameters like grinding time and optimum gypsum content was established from the physical and chemical properties of the gasification ash by performing tests for particle size distributions; scanning electron microscopy photo's and x-ray analysis. Standard test performed for cementitious materials will be discussed. Test methods include the casting and testing of mortar prisms and calorimetry testing.

4.2 PREPARATION OF MATERIALS

In an effort to reduce the environmental impact of cement production, cement manufacturers are increasing the use of waste materials to replace a fraction of the cement clinker.

In this project cement is manufactured in the laboratory using cement clinker obtained from a cement factory. The clinker was ground in a ball mill (see figure 4.1) with 25kg of round steel balls. The steel balls (see figure 4.2) were individually measured and weighed to determine their size distribution as indicated in Figure 4.3.

Figure 4.1 Laboratory ball mill used in experiment

Figure 4.2 Steel balls used for grinding

All the samples ground were sieved through a 1.18µm sieve and stored in air-tight containers.

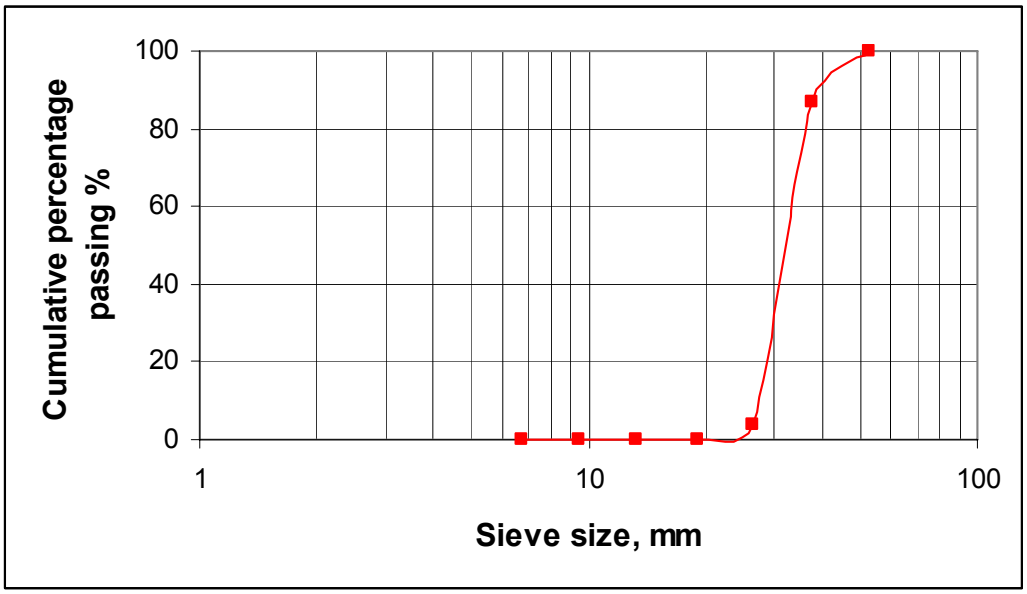

Figure 4.3 Cumulative particle size of steel balls

Cement and gasification ash is ground for different time intervals to establish an optimum grinding time. The grinding time intervals were; 30 minutes, 1hour, 1hour 30 minutes, 2 hours, 2hour 30 minutes and 4hours. The experiment included interblending cement and gasification ash after grinding each material separately, and intergrinding of cement and gasification ash by interblending the two materials in the ball mill and grinding it together. No gypsum was added to the cement clinker in the ball mill.

An optimum grinding time was established by considering the particle size and the flexural and compressive results of mortar prisms.

The effect of gypsum on cement and gasification ash was examined. As gypsum has a direct influence on the setting time and heat of hydration an optimum gypsum content was established. To determine the optimum gypsum content, heat of hydration curves were established and isothermal calorimetry tests were performed on samples with different gypsum replacement levels.

4.3 PHYSICAL AND CHEMICAL PROPERTIES OF GASIFICATION ASH

The feed to Sasol gasifiers principally consists of coarse coal (>5mm) and extraneous rock fragments (stone). During the gasification of this coarse coal at elevated temperatures and pressure a mixture of carbon monoxide and hydrogen (also referred to as synthesis gas) is produced. The coarse (see figure 4.4) ash is formed at these elevated temperatures and pressure by the interaction of inert minerals present in the coal and stone. The coarse ash is removed from the gasifier and disposed as a by-product (Van Dyk, 2005).

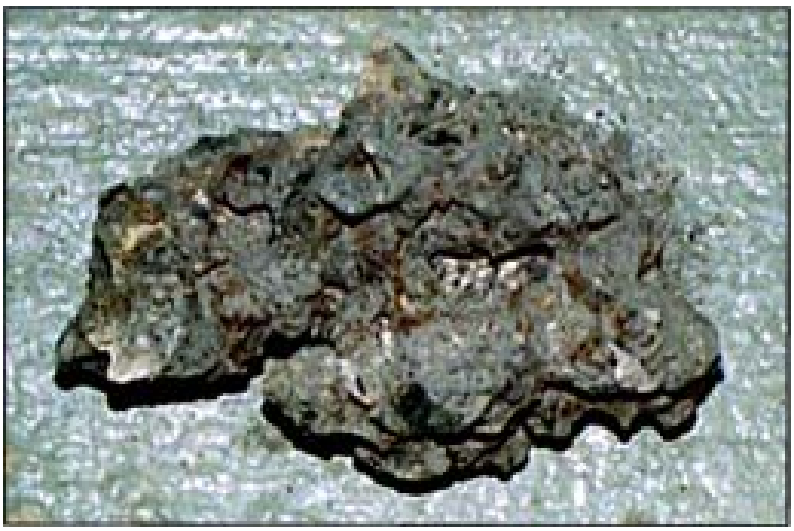

Figure 4.4 Sample of gasification ash clinker

4.3.1 Particle size distribution

Laser technology is used to investigate the particle size distribution of materials after grinding.

4.3.1.1 Particle size distribution parameters

By plotting the inverse of the cumulative percentage distribution, the cumulative % oversize particle distribution is obtained. Provision was made for statistical outliers by not

taking the five percent smallest diameters and five percent largest diameters into account.

For each sample a trend line is added to the cumulative % oversize graph (see figure 4.5).

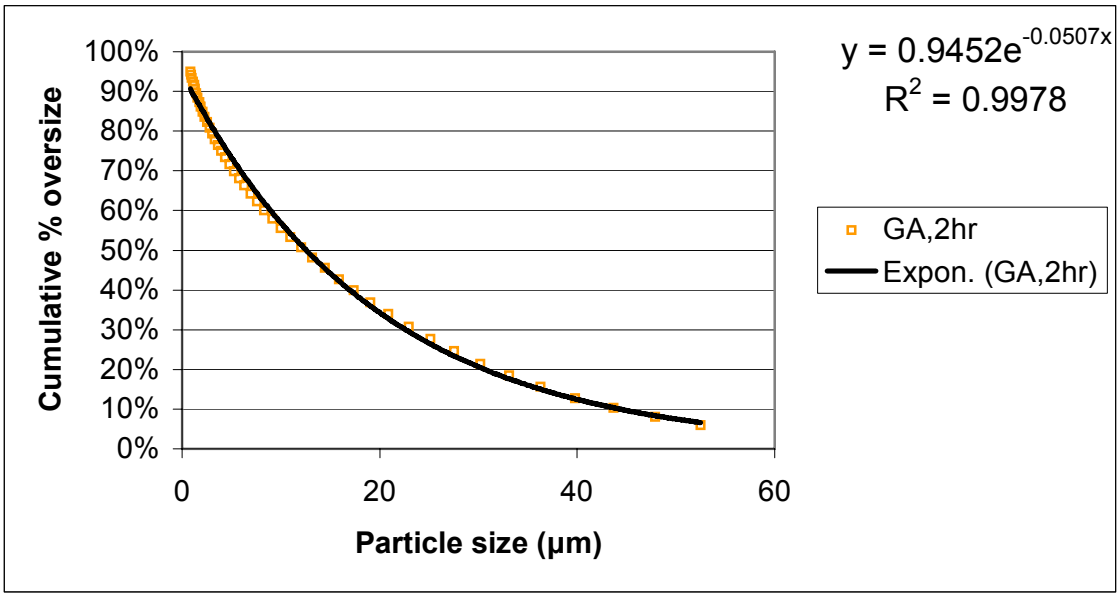

Figure 4.5 Exponential fit for cumulative % oversize particle size distribution

4.3.1.2 Rosin-Rammler particle size distribution parameters

The cumulative % oversize particle size distribution as discussed in 4.3.1.1 can be represented as a Rosin-Rammler distribution.

The Rosin-Rammler distribution graphs (Figure 4.6 and Figure 4.7) are examples of how the values for the particle size distribution parameters were derived. The modified Rosin-Rammler distribution graph $\ln\ln(1/y)$ versus $\ln x$ is plotted, with y the fitted functions $y = a\exp(bx)$ for the cumulative % oversize particle size distribution and x the particle size. A linear trend line and equation is also added to these graphs (see figure 4.6). The slope and interception with the horizontal axis of the line is taken as the n value and $\ln X_o$ value of the modified Rosin-Rammler function respectively.

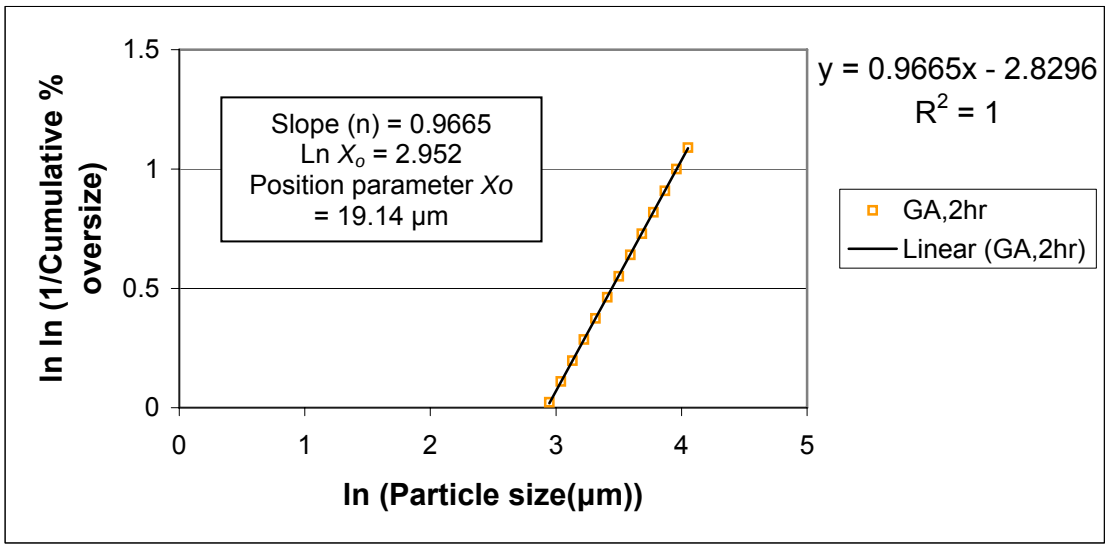

Figure 4.6 Rosin-Rammler distribution graph

With this analysis 36.8% of the particles (per mass) are greater than the X_o value (position parameter in µm). This parameter is an indicator of the particle size. The *n*-value represents the range of the particle size distribution of the particle sizes greater than X_o (see figure 4.7).

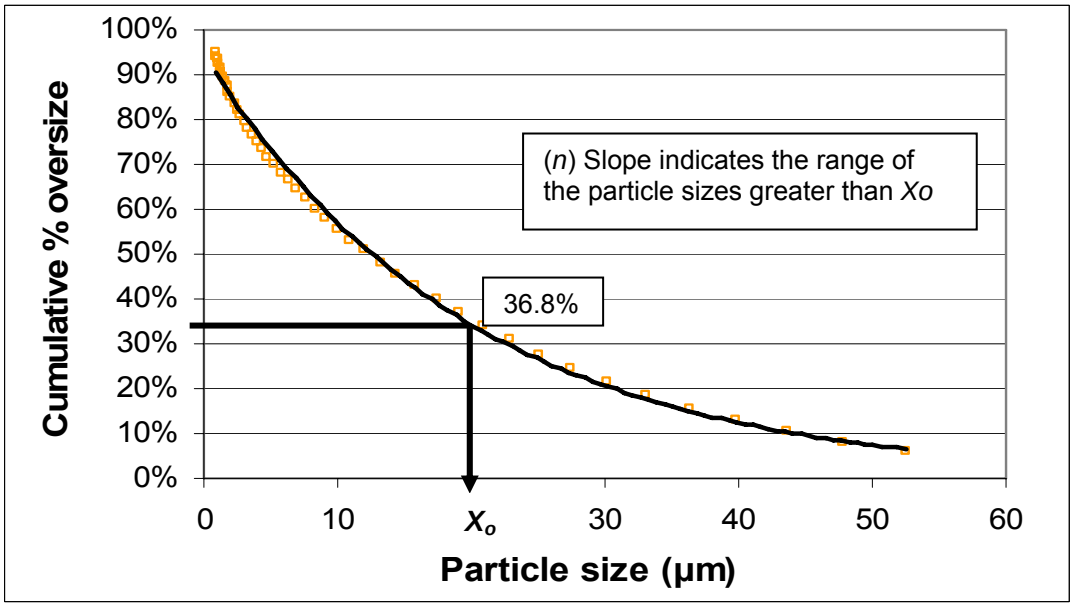

Figure 4.7 Explanation of Rosin-Rammler distribution parameters

4.3.1.3 Particle size distribution parameters

The corresponding 50% oversize particle size distribution in µm can be read from the exponential fit graph (See figure 4.8). This particle size gives an indication of the average particle size of each sample. In the same way the 10% oversize particle size (D10), which shows the difference in number of larger particles in each sample.

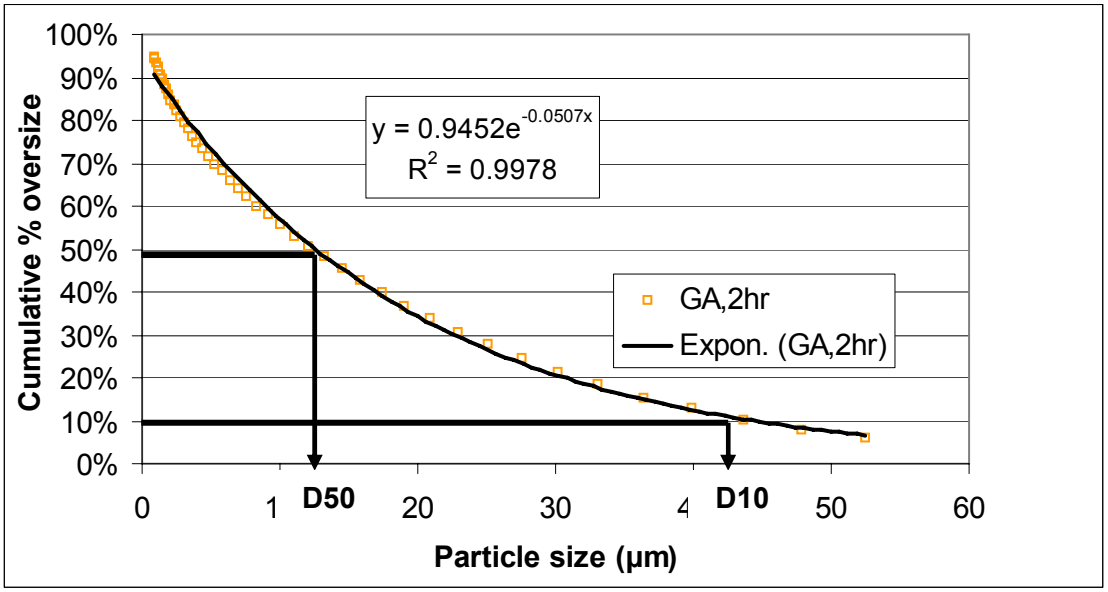

Figure 4.8 Cumulative % oversize distribution parameters

Figure 4.9 indicates the 3 µm and the 30µm oversize particle size distributions. This particle size can give an indication of the % of the particle which lies in the <3µm and 3-30µm intervals, which can correspond to the values cement manufacturer's currently use to limit the fineness of cement.

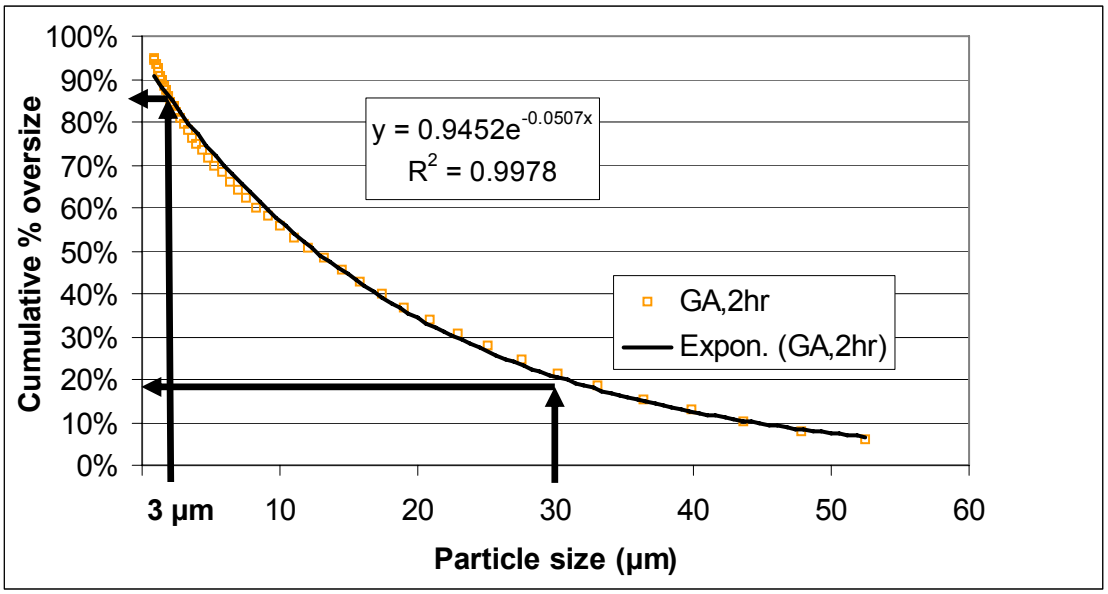

Figure 4.9 Cumulative % oversize intervals for 3µm and 30µm

4.3.2 Specific surface area

A standard method of determining the specific surface area of cement which is based on the resistance to air flow through a compact of cement and was developed by Blaine. Figure 4.10 shows the apparatus used to determine specific surface area.

A constant volume method where the time, t, required to pass a fixed volume of air through a compact bed of cement (12.7 mm diameter and 15 mm in depth), of standard porosity is related to the specific surface of cement by the following relationship:

$$S_w = K\sqrt{t} \qquad \text{(equation 4.1)}$$

Where K= 281.3915 (constant for apparatus)

Figure 4.10 Apparatus to determine specific surface area

4.3.3 Scanning electron microscopy (SEM)

A Hitachi X-650 Scanning Electron Microanalyzer was used to take the micrographs of the samples. Samples were mounted on aluminium stubs using conductive glue and were then coated with a thin layer of gold.

4.3.4 X-ray fluorescence spectroscopy (XRF)

An XRF Spectrometer was used to investigate the characteristic spectra of elements present in the solid sample. For quantification analysis, the intensity of characteristic line of the element analysed was measured.

The coarse solid sample was initially ground to a particle size of 100% <200µm. The powdered sample was calcined at 850°C for 4 hours in order to remove all organic compounds and water contained in the sample. The calcined sample was converted

into a solid solution by fusion with lithium tetra borate ($Li_2B_4O_7$). The prepared solid solution and standard were placed in sample holders and placed in the sample compartment of the XRF spectrometer. The intensity of a characteristic line of the element to be determined was measured. The concentration of the element in the sample was calculated from the intensity measured.

4.3.5 X-ray diffraction spectroscopy (XRD)

All the samples were received as dry, fine powder. A mass of approximately 4g of each sample, were further ground and homogenised by hand in an agate mortar.

The additional grinding, as required for a quantitative XRD analysis, was done using the agate segments in a McCrone micronising mill over 10 minutes. This fine grinding followed by spiking the samples with 10% (by mass) CaF_2 as an internal standard, was required to conduct the quantitative XRD analyses.

Approximately 0.5g of the ground sample was placed in a stainless steel sample holder and exposed to the X-ray beam to generate the sample's diffraction pattern.

4.4 STANDARD TESTS FOR CEMENTITIOUS MATERIALS

Fly ash complying with the requirements of the South African standard specification for Portland cement extenders (SANS 1491-2:2005 / SABS 1491-2:2005) conforms to the following tests:

- Sulphur trioxide content
- Loss on ignition
- Free water content
- Fineness
- Water requirement

- Strength Factor
- Soundness

4.4.1 Sulphur trioxide content (SANS 50196-2:1994 / SABS EN 196-2:1994)

1 g of the sample is weighed; 90mℓ of water and 10 mℓ of HCl is added while stirring vigorously. The solution is heated and left to digest just below boiling point for 15 minutes. The solution is filtered and washed where after the solution is heated while $BaCl_2.2H_2O$ is added to the solution. The solution is digested for 12 hours and then filtered and washed. Paper is placed in crucible and precipitate is ignited to constant mass at 300°C. The sulphate content is now determined for the sample.

$$SO_3 \text{ content} = (a - b) \times \frac{34.3}{c} \qquad \text{(equation 4.2)}$$

where:
a = mass of barium sulphate found (g)
b = mass of barium sulphate found in blank determination (g)
c = mass of sample taken (g)

4.4.2 Loss on ignition (SANS 50196-2:1994 / SABS EN 196-2:1994)

Weigh about 1g of sample into crucible and ignite at 850°C for 15 minutes. Allow cooling in desiccator and ascertaining whether constant mass is obtained by weighing the sample. Determine the LOI.

$$LOI\ \% = (a - b) \times \frac{100}{a} \qquad \text{(equation 4.3)}$$

where:
a = mass of sample taken (g)
b = mass of residue (g)

4.4.3 Free water content (SANS 6151:1989 / SABS 1151:1989)

Weigh about 1g of sample into crucible and dry the sample for 1 hour in oven at 100°C to a constant mass. Allow cooling in desiccator and determining the mass of the dry sample.

$$\textit{Free water content \%} = (a - b) \times \frac{100}{b} \qquad \text{(equation 4.4)}$$

where:
a = mass of sample (g)
b = mass of dried sample (g)

4.4.4 Test for fineness of cement and Portland cement extenders (SANS 6157:2002 / SABS 1157:2002)

A mass of 1 g of the sample is taken after being dried in an oven and placed on a 45µm sieve. The sample is washed with the use of a nozzle spraying water under a pressure of 70-80kPa. Remove the sieve from under the nozzle and dry the sieve with the residue in an oven. Determine the mass of the sieve and residue.

$$\textit{Fineness, \% (m/m)} = \frac{c - b}{a} \times 100 \qquad \text{(equation 4.5)}$$

where:
a = dried mass of specimen (g)
b = mass of sieve (g)
c = mass of sieve plus residue (g)

4.4.5 Water requirement (SANS 6156:1989 / SABS SM 1156:1989)

The mortar was mixed according to SABS Method 866 and the flow test was performed on the sample. The mix composition for mortar prisms is seen in Table 4.1.

Table 4.1 Mix composition for mortar prisms

Material	Quantity
Water	225 g
Cement	450 g
Standard reference sand	1350 g

In this project 35% of the cement was replaced with gasification ash as can be seen in Table 4.2.

Table 4.2 Mix composition used in test

Material	Quantity
Water	225 g
Gasification Ash	140 g
Cement	310 g
Standard reference sand	1350 g

The flow table is dried and the mould is placed in the centre. The mould is half-filled with a layer of mortar (25 mm) and tamped 20 times with a tamper. The mould is filled and again tamped 20 times. Excess mortar is cut off and mould is lift vertically. In a period of 25 seconds, the table is raised and dropped 25 times through a height of 12.7 mm. A photo of the flow table test can be seen in Figure 4.11.

Figure 4.11 Photo of sample on flow table after mould is removed

The diameter of the mortar is measured at four approximately equal-spaced intervals. The average diameter is calculated and taken as the flow. The increase in diameter is expressed as a percentage of the original nominal diameter of the lower part of the mortar specimen (100 mm). The diameter measurements on the flow table can be seen in the photo in Figure 4.12.

Calculate to the nearest 1% the water requirement of the material as follows:

$$\textit{Water requirement} = \frac{Wt \times 100}{Wr} \qquad \text{(equation 4.6)}$$

where:

Wt = mass of water to produce flow value of the mortar to within 5% points of the reference mix (g)

Wr = actual mass of water used in reference mix (g)

Figure 4.12 Photo of diameter measurements of flow table test

4.4.6 Strength factor test (SANS 50196-1:1994 / SABS EN 196-1:1994)

The strength of cement can be determined by casting mortar prisms. The specification prescribes a standard mix composition as indicated in Table 4.1. The mortar composition for the strength test was as indicated in Table 4.2. Mortar was mixed according to SABS Method 866. The test specimens are 40 mm x 40 mm x 160 mm prisms as seen in Figure 4.13.

Figure 4.13 Photo of mould used

The specimens are moulded after mixing of the mortar. Moulds are filled with the first of two layers of mortar, spread equally in each mould compartment and then compacted with the vibrating table for 20 seconds. After compacting the second layer, the surface of the specimen is levelled and the specimen are covered with plastic and placed in a constant temperature room at 22°C and 55% relative humidity (RH) overnight.

Mortar prisms are cast as for the strength factor test (see 4.4.6 strength factor test) and the flow table test (see 4.4.5) is conducted on each different mortar mix. Each batch of mortar is mixed mechanically using a mixer. Materials are added into the mixing bowl and mixed for a constant time of 30 seconds where after the water is added and mixed for a further 90 seconds. Samples are cast in sets of three prisms to obtain strengths on 2, 7, 28 days to study the strength development over a long period.

Specimens are demoulded after 24 hours and placed in water at 25˚C for curing.

Firstly the flexural strength is determined. Prisms are supported on supports 100 mm apart and loaded with a point load at midspan.

The flexural strength is calculated as follows:

$$R_f = \frac{1.5 \times F_f \times l}{b^3} \qquad \text{(equation 4.7)}$$

where:
R_f = flexural strength (MPa)
F_f = load applied to the middle of the prisms (kN)
l = distance between the supports (mm)
b = side of the square section of the prism (mm)

The same prisms tested in the flexural test are tested for compressive strength. The two halves of each prism are tested

in the press and the average of the six results obtained is taken as the compressive strength. The compressive strength of a prism is calculated as follows:

$$R_c = \frac{F_c}{1600} \qquad \text{(equation 4.8)}$$

where:

R_c = compressive strength (MPa)

F_c = maximum load at fracture (N)

1600 = 40 mm x 40 mm, area of the platens (mm)

4.4.7 Soundness (SANS 50196-3:1994 / SABS EN 196-3:1994)

The purpose of this test is to determine the risk of expansion due to hydration. Prepare a cement paste of standard consistency and fill a lightly oiled Le Chatelier mould, using only the hands and not vibration. Place the apparatus in a humidity (98%) cabinet for 24 hours at 20°C. Figure 4.14 shows the Le Chatelier apparatus in a water bath in a humidity cabinet. Measure the distance between the indicator points.

Figure 4.14 Le Chatelier moulds in humidity cabinet

Heat mould for 30 minutes and maintain the water-bath at boiling temperature for three hours. Measure the distance between the indicator points and allow mould to cool to 20°C. Measure distance between indicator points.

$$Soundness = c - a \qquad \text{(equation 4.9)}$$

where:

a = measurement after 24 hours in humidity cabinet (mm)

c = measurement after cooling specimen to 20°C (mm)

4.4.8 Relative density (LSA Method)

The relative density of the sample is determined by:

$$Relative\ density = \frac{c}{(c + e) - d} \qquad \text{(equation 4.10)}$$

where:

c = mass of sample (g)

d = mass of flask and sample and water (g)

e = mass of pyknometer and water (g)

4.5 FACTORS INVESTIGATED BY CASTING MORTAR PRISMS

4.5.1 Different Grinding Times

Mortar prisms were cast for the different grinding time intervals with a constant replacement of cement with gasification ash of 35%. Mortar prisms were water cured and compressive and flexural strengths were determined after 2, 7 and 28 days. The mix composition for both interblending cement and gasification ash after grinding each material separately, and intergrinding

of cement and gasification ash by interblending the two materials in the ball mill and grinding it together is seen in Table 4.3 and Table 4.4. The gypsum content was constant at 2.5% replacement of the cement content.

Table 4.3 Mortar prism mix composition for interblending cement and Gasification ash

Material	Mass (g)
Cement	292.5
Gasification ash	157.5
Gypsum	7.31
Water	225
Standard reference sand	1350

Table 4.4 Mortar prism mix composition for intergrinding cement and Gasification ash

Material	Mass (g)
Cement and Gasification ash interground	450
Gypsum	7.31
Water	225
Standard reference sand	1350

4.5.2 Different Gypsum Percentages

Mortar prisms were cast for in the ball mill to test the effect of different gypsum percentages and to establish the difference between the laboratory interblended and interground cements with a commercially available CEM I 42.5. Table 4.5 shows the different weights for gypsum as a percentage of the cement content.

Table 4.5 Gypsum replacement weights for mortar prisms

Gypsum replacement %	Gypsum content (g)
0.0%	0.00
0.5%	1.46
1.0%	2.93
1.5%	4.39
2.0%	5.85
2.5%	7.31
3.0%	8.78

4.5.3 Isothermal Conduction Calorimetry

In isothermal conduction calorimetry, the heat of hydration of cement is directly measured by monitoring the heat flow from the specimen when both the specimen and the surrounding environment are maintained at approximately isothermal conditions. Approximately 3g of water were inoculated into an equivalent mass of reactant powder that had been placed in a copper sample cup and placed within the calorimetry cavity. The cups were sealed with plastic film to minimize evaporation of water. Each reactant was allowed to equilibrate separately to 25°C, prior to mixing. The water was equilibrated in a syringe and when equilibrium had been achieved the plastic film was penetrated and the water injected over the solids. The rates of heat evolution, dQ/dt in mW/g were measured and recorded using a computer data acquisition system.

The heat of hydration of a mortar mix was also investigated. Mortar mixes were mixed and cast into a steel cylinder. Thermocouples were inserted into the pocket of the steel cylinders' lid. The cylinder and thermocouple were placed into a temperature isolation flask and left in a constant temperature room at 25°C.

The thermocouples recorded the temperature of the mortar over 112 hours. Afterwards the thermocouples were removed and the data were downloaded with a computer system.

4.5.3 Different replacements percentages of Gasification Ash

Mortar prisms were cast for different replacement percentages of Gasification ash. Gasification ash were replaced in the ball mill and grounded with cement. These replacement percentages were: 0%, 10%, 20%, 35% and 55%. The replacement percentages were selected as the highest interval currently used in commercially available CEM I (0%), CEM II (6-10% and 21-35%) and CEM IV (36-55%).

5. EXPERIMENTAL PROGRAMME AND TEST PROCEDURES FOR CONCRETE

5.1 INTRODUCTION

The aim of this study is to determine whether gasification ash can be used as a cement extender in concrete. Currently pulverised fuel ash (also called fly ash) is widely used as a cement extender in concrete and the effect of this type of ash is well established. In this study the properties of cement and concrete containing gasification ash will be compared to the properties of cement and concrete containing fly ash.

The aim of this chapter is to discuss the testing methods used in the practical analysis of the reactivity of a gasification ash. The mix design for different mixes of concrete will be discussed. The testing of concrete cubes, cylinders and shrinkage beams will be discussed with reference to the testing apparatus, as well as the standardised testing methods used.

5.2 MIX DESIGN FOR CONCRETE MIXES

Concrete was batched for three different mixes to investigate cube strengths, tensile strengths, E-values, shrinkage, creep, porosity and permeability.

Each mix (see Table 5.1) had a water/cement ratio of 0.6. The aggregate content was made up of dolomite sand and 1/3 of 9.5mm and 2/3 19mm granite stone. A 35% substitution of cementitious materials was considered where applicable for the mixes. The size of the mixes was 43 ℓ.

Table 5.1 Mix composition for concrete mixes

Materials	Quantity 43ℓ	Per kg/m³
Water	9 ℓ	210 ℓ
Cement	9.8 kg	227 kg
Cementitious material	5.3 kg	123 kg
Dolomite Sand	37.7 kg	875 kg
9.5mm Granite Stone	14.2 kg	330 kg
19mm Granite Stone	28.4 kg	660 kg

The mix composition remained constant and only the type of cementitious material used was changed. The cement used in the mixes can be seen in Table 5.2.

Table 5.2 Concrete mix composition

Mix	Description	Abbreviation
Mix 1	Intergrinding of cement and gasification ash	IG
Mix 2	Interblending of cement and gasification ash	IB GA
Mix 3	Interblending of cement and fly ash	IB FA

5.3 TEST CONDUCTED ON FRESH CONCRETE MIXES

5.3.1 Slump Test (SANS 586 / SABS SM 82:1994)

The slump test is a method to measure the consistency of the concrete. It does however not test all the consistency requirements and has a limited application.

In the slump test the mould is filled in three equal layers, subjecting each layer to 25 blows from the tamping rod while the mould is firmly held down by standing on the foot pieces. The surface is smoothed, the cone is removed and the slump is measured to the nearest 5 mm. The slump is the distance

between the top of the inverted mould and the highest point of the concrete as indicated in Figure 5.1.

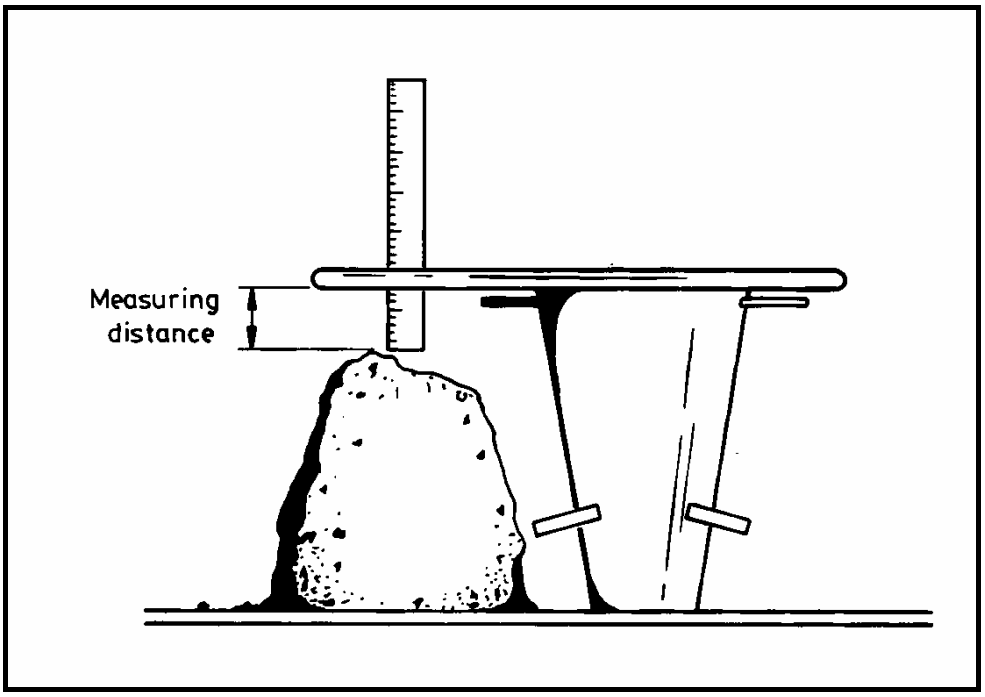

Figure 5.1 Measuring the slump (Addis, 2001)

5.4 STRENGTH TESTS

5.4.1 Compressive Strength Test (SANS 5863-1/SABS 863-1994)

Test specimens are crushed between two platens in a hydraulic press. The rate of load application influences the compressive strength results and is specified at a uniform rate of 0.3 MPa/s ± 0.1 MPa/s.

All the cubes were water cured. Three cubes (100x100x100) from each mix were crushed on 2, 7 and 28 days and the average of the three cube strengths was defined as the strength. The compressive strength is recorded to the nearest 0.5MPa.

5.4.2 Splitting Cylinder Test for Tensile Strength (SANS 625:1994/SABS SM 1253:1994)

In South Africa the tensile strength of concrete is determined indirectly by breaking beam specimens in flexure or by splitting cylinders by applying line loads.

The cylinder is placed with its axis horizontal between the platens of the testing machine, and the load is increased until failure occurs by indirect tension in the form of splitting along the vertical plane takes place. For each mix, two cylindrical samples were split.

The following equation was applied to determine the tensile strength of the concrete according to the elastic theory:

$$f = \frac{2 \times P}{\pi d \ell} \qquad \text{(equation 5.1)}$$

where:
f = tensile strength (MPa)
P = compression load at failure (N)
d = diameter of cylinder (mm)
ℓ = length of cylinder (mm)

All the cylinders were water cured and two cylinders from each mix were used to determine the tensile strength.

5.5 DEFORMATION AND VOLUME CHANGE OF CONCRETE

5.5.1 E-Value Test

Deformation takes place when a load is applied to a structural material. If the ratio of the applied compressive strength to the longitudinal strain produced is constant, the constant is called the modulus of elasticity (Young's modulus).

The non-linearity of the stress-strain relationship for concrete is mainly due to the non-linear stress-strain response of the paste. A portion of the curve may be regarded as being effectively linear, and at stresses within this range the elastic modulus may be taken as the slope of the linear portion. For this portion Hooke's law may be used to determine the modulus of elasticity.

There is no SABS test method to determine the static elastic modulus of concrete and therefore ASTM C 469-02 is used. The tests determine initial tangent modulus (Young's) as well as the secant modulus corresponding to one third of the compressive failure stress. The test involves loading a cylinder at a constant rate and recording the load (stress) and deformation (strain) of the specimen. A stress-strain curve is determined from which the modulus of elasticity is determined.

The modulus of elasticity was determined as follows:

$$\Delta L = \frac{G_L - G_F}{2} \qquad \text{(equation 5.2)}$$

$$\varepsilon = \frac{\Delta L}{L} \qquad \text{(equation 5.3)}$$

$$P = (P_L - P_F) \times 1000 \qquad \text{(equation 5.4)}$$

$$A = \frac{\pi d^2}{4} \qquad \text{(equation 5.5)}$$

$$\sigma = \frac{P}{A} \qquad \text{(equation 5.6)}$$

$$E = \frac{\sigma}{\varepsilon} \qquad \text{(equation 5.7)}$$

where:

G_L = Last reading of gauge (μm)

G_f = First reading of gauge (μm)

L = distance between measuring points (mm)

P_L = last strength interval (kN)

P_F = first strength interval (kN)

d = diameter of cylinder (mm)

E = static modulus of elasticity (GPa)

Cylinders were water cured for 28 days. For the determination of the modulus of elasticity, two cylinders of each mix were tested after the 28-day compressive results of the cubes were determined.

5.5.2 Shrinkage and Creep Test (ASTM C 512-02)

Volume change occurs in concrete in both the fresh and hardened state. Structural performance is most concerned by the volume change associated with an interchange of moisture between hardened concrete and the environment.

Swelling occurs when the net flow of moisture from the environment to the concrete cause a volume increase and shrinkage occurs when a net outflow from the concrete to the environment results in a decrease in volume. Conventional concrete usually contains more water than what can be chemically combined with the cement and there is a tendency for moisture to be lost from the concrete, resulting in shrinkage.

Creep is defined as the increase in strain (deformation) under a sustained stress (load). When loaded, concrete experiences an instantaneous elastic strain, which is recoverable. In addition, an inelastic creep strain takes place that is only partially recoverable.

Shrinkage is tested in conjunction with creep. Three cylinders were cast and cured in water for 28 days. For the test, one cylinder is used for shrinkage and two cylinders for creep testing. The shrinkage test is a natural drying method where the cylinder is dried in a controlled environment of 65±5% relative humidity and 22±2°C. The shrinkage movement is measured over a period of time.

The test method for creep measures the load-induced time dependent compressive strain at selected ages for concrete. The cube compressive strengths of the different mixes are determined on 28 days. The cylindrical samples are placed into a loading frame and loaded with 40% of the compressive load. Strain readings are taken immediately before and after loading, and thereafter at regular time intervals.

Figure 5.2 Photo of lab set-up for measuring shrinkage and creep

5.6 DURABILITY

Durability can be defined as, “the capability of maintaining the serviceability of a product, component assembly or construction over a specified time”.

The quality of concrete cannot be determined by only using the strength test as this approach does not give an adequate indication of the quality of the cover concrete. The cover concrete acts as a barrier between the reinforcing steel and

the external aggressive environment and its quality is of great importance in durability considerations.

The durability of concrete is a function of porosity. Strength increases with decreasing porosity and porosity is affected by capillary porosity and air-void porosity. Porosity may be defined as the percentage voids in a sample. Voids, which are spaces filled with water, are a result of the failure to expel all the air from the wet concrete.

The method that has been adopted is to measure a fluid transport parameter of the material such as permeability to liquids or gasses. Fluid transport properties are influenced by capillary porosity and the degree of interconnection capillaries. Permeability may be defined as the ease with which a liquid or gas can pass through a specific material.

5.6.1 Porosity Test

For each of the three mixes, two water-cured samples were tested after 28 days. A core was drilled from 150x150 cubes and oven-dried at a temperature of 100˚C for 24 hours to ensure that all moisture was removed. After determining the weight of the oven-dried samples, they were placed in a vacuum for 24 hours. The samples were then submerged in de-aired distilled water and once again placed in a vacuum for 3 hours. This was done to ensure that all the voids in the concrete samples were filled with water. Finally the submerged weight of the samples was determined. The porosity test set up can be seen in Figure 5.3.

Figure 5.3 Photo of porosity test set up

The following equation was applied to determine the porosity of the concrete:

$$Porosity = \frac{mass_{sat} - mass_{dry}}{mass_{sat} - mass_{wat}} \quad \text{(equation 5.8)}$$

where:

$mass_{sat}$ = weight of saturated sample (g)

$mass_{dry}$ = weight of oven-dried sample (g)

$mass_{wat}$ = weight of sample in water (g)

5.6.2 Oxygen Permeability Test

The oxygen permeability of the concrete was determined for two samples of each mix after 28 days. A core was drilled from the 150x150 cube and oven-dried at 100˚C for 24 hours to prevent expansion cracks, which would influence the permeability readings. The apparatus consists of a series of valves, which delivered oxygen at a known pressure through the samples, and calibrated glass tubes through which the rate

at which the oxygen bubbles moved could be measured with a stopwatch.

The following equation was applied to determine the permeability coefficient, *k*, of the concrete.

$$K = \frac{2 \times t \times Q \times e \times P}{A\,(P_2^2 - P_1^2)} \qquad \text{(equation 5.9)}$$

where:

t = sample thickness (m)

e = oxygen viscosity (2.02^{-5}N.s/m^2)

K = oxygen permeability (l/m^2)

Q = volume per second passing through sample (m/s^3)

A = cross sectional area of sample (m^2)

P_1 = atmospheric pressure (Pa)

P_2 = applied pressure (Pa)

The oxygen permeability index (OPI) can be calculated as:

$$OPI = -Log_{10}K \qquad \text{(equation 5.10)}$$

6. TEST RESULTS AND DISCUSSION ON CEMENT TESTS

6.1 INTRODUCTION

In chapter 6, the results of the experimental tests discussed in chapter 4 are reviewed and analysed to examine the reactivity of a gasification ash used as a cement extender.

Firstly the physical properties of the gasification ash will be discussed with reference to the particle size distribution and the shape of the particles. The chemical properties of the gasification ash will be analysed by considering the results from XRF, XRD and standard tests for extenders.

Thereafter the results of the mortar prism results for intervals of grinding times and different gypsum percentages will be illustrated and discussed. The discussion of the results takes into consideration that tests were conducted on a single set of samples. Limitations to the testing method will be discussed and possible improvements will be recommended.

6.2 PHYSICAL PROPERTIES

6.2.1 Particle Size Distribution Test

The water demand and workability of cement paste is controlled by the particle size distribution. As nothing can be done to alter the mineralogical characteristics, the control of particle size distribution is the only practical method by which the cementitious activity can be enhanced.

The particle size distribution of the cement and gasification ash ground for a two hour time interval can be seen in Figure 6.1. It is observed that the gasification ash, grinded separate and interground with cement had similar particle size distributions. There is a considerable difference in particle size

between the gasification ash and cement grinded separately for the same time interval. The gasification ash had a particle size range between 0.08 µm and 50µm, where the cement particles ranged between 2µm and 110 µm. The results for all the grinding time intervals can be seen in Appendix A. These results indicate that the cement clinker is harder than the gasification ash clinker. The particle size of intergrinding 65% cement and 35% gasification ash shows that the particle size distribution for time intervals 1,5 hours and 2 hours were identical. Further grinding did not reduce the fineness of the interground sample significantly (see Figure 6.2). Thus from the particle size distribution it is clear that an optimum grinding time can be established.

Higher fineness provides a greater surface area to be wetted, resulting in an acceleration of the hydration reaction. It was thus expected that the smaller particle size of the gasification ash should require the same or more water than fly ash.

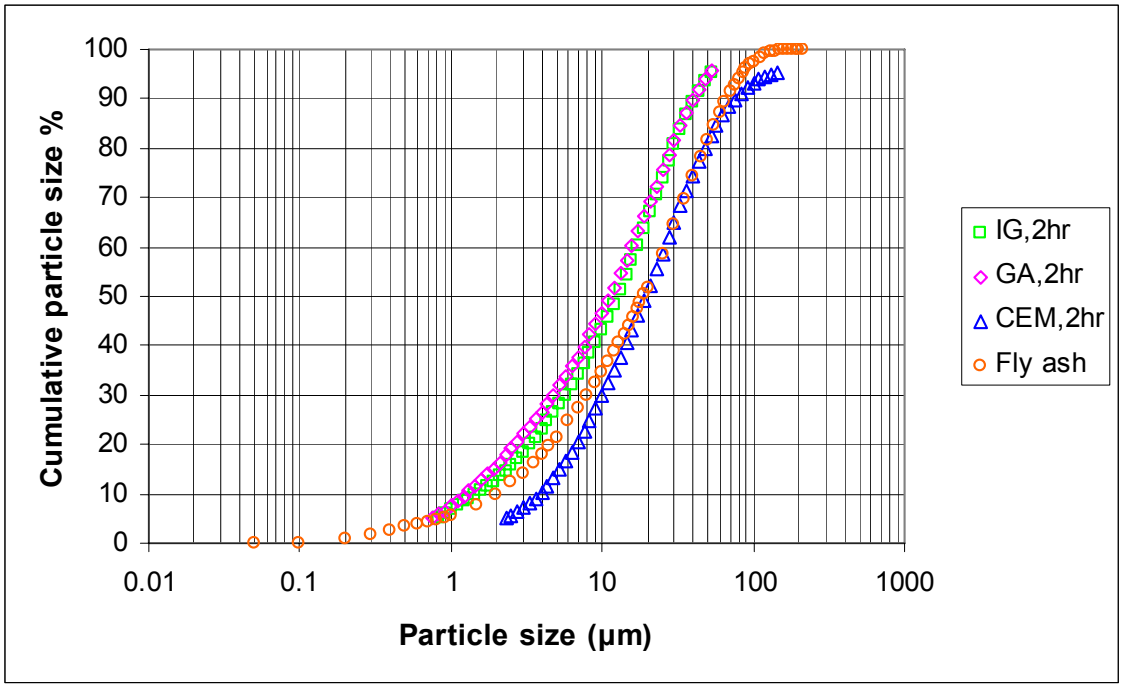

Figure 6.1 Graph of cumulative particle size distribution of cement and gasification ash (grinded separate and interground)

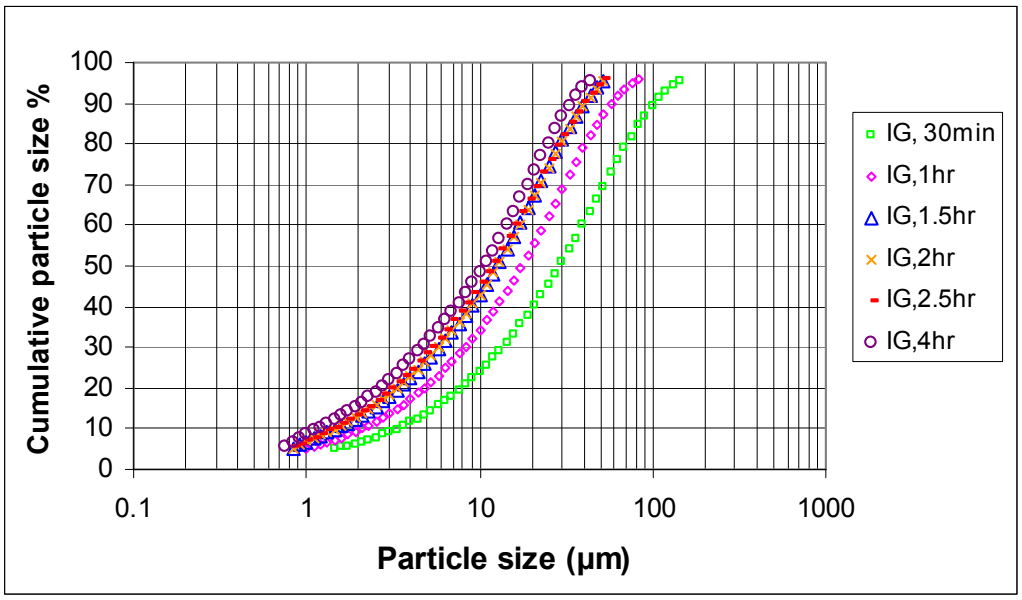

Figure 6.2 Cumulative particle sizes for gasification ash and cement interground

The relevance of the Rosin-Rammler particle size distribution parameters was evaluated by comparing the fitted functions for the cumulative % oversize particle size distributions for different grinding times. Both the constants in the equation vary with grinding time and therefore the constants as such cannot be used to compare the samples (See table 6.1). The functions for gasification ash are plotted in Figure 6.3. The rest of the particle size distributions can be viewed in Appendix B.

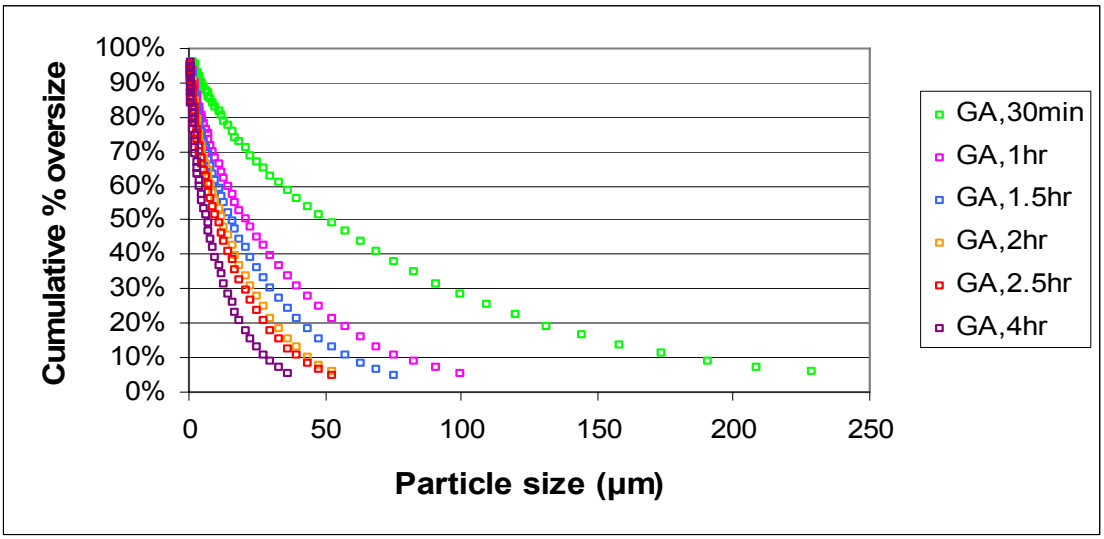

Figure 6.3 Summary of exponential fitted functions for the cumulative % oversize particle size distribution

According to Figure 6.3 the position parameter (X_o) and therefore the particle size distribution decrease as the grinding time increases for gasification ash. It is clear that the grinding time has a significant influence on the range of the particle size distributions greater than the position parameter (X_o). The shorter grinding times seem to have more of the larger (coarse) particles. This trend can also be seen when comparing the Rosin-Rammler slope (n) parameters (see Figure 6.4). See Appendix C for rest of graphs.

The graph clearly indicates that the particle size of gasification ash decreases as the grinding time increase. The fitted trend line that best describes the measured values is an exponential function. The statistical R-square value for all the samples of the exponential fit is between 0.995 and 0.999. The exponential equation is therefore a true representative of the cumulative % oversize particle size distribution.

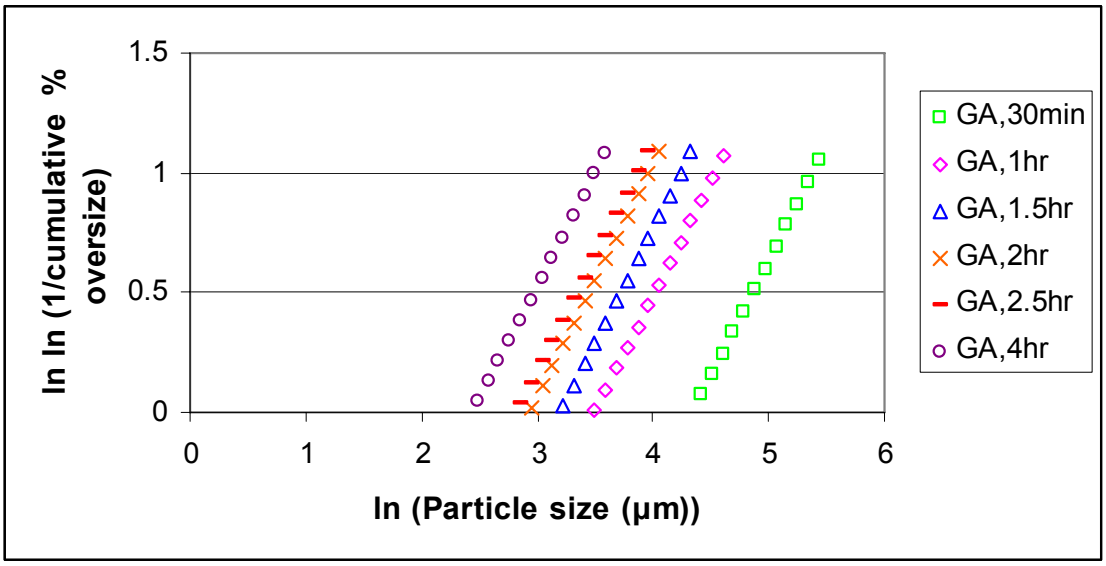

Figure 6.4 Summary of Rosin-Rammler distributions

Table 6.1 Fitted functions of oversize particle size distribution

Sample	Fitted function y = a e(bx)		R^2	X_o
	a	b		
IG,30 min	0.955	-0.0198	0.9996	47.90
IG,1hr	0.975	-0.0354	0.9997	28.01
IG, 1.5hr	0.9929	-0.0514	0.998	19.88
IG, 2hr	0.9835	-0.05	0.9983	20.00
IG, 2.5hr	0.9693	-0.0532	0.9986	18.20
IG, 4hr	0.9822	-0.0608	0.9963	16.69
GA,30min	0.9429	-0.0122	0.9991	78.35
GA, 1hr	0.9329	-0.0284	0.9989	33.05
GA, 1.5hr	0.9331	-0.0382	0.9986	24.51
GA, 2hr	0.9452	-0.0507	0.9978	19.14
GA, 2.5hr	0.9254	-0.0554	0.9981	16.64
GA, 4hr	0.8942	-0.0781	0.9952	10.93
Cem,30min	0.9675	-0.024	0.9936	37.71
Cem, 1hr	0.7121	-0.0144	0.8842	33.11
Cem, 1.5hr	0.9411	-0.0249	0.9858	37.29
Cem, 2hr	0.8794	-0.0237	0.9681	29.43
Cem, 2.5hr	0.9077	-0.0247	0.9791	32.04
Cem, 4hr	0.8179	-0.0179	0.9454	25.71
IB, 30 min	0.9031	-0.0165	0.9874	45.51
IB, 1hr	0.8898	-0.023	0.9792	31.66
IB, 1.5hr	0.9607	-0.03	0.9973	30.55
IB, 2hr	0.945	-0.033	0.9946	25.93
IB, 2.5hr	0.9142	-0.0321	0.9897	25.59
IB, 4hr	0.8079	-0.0256	0.9545	23.27

The values of the slope n and the position parameter X_o for all the samples can be seen in Table 6.2. The equations for the linear trend line fitted to the Rosin-Rammler distribution graph and the statistical R-square value of the linear fit are also listed in Table 6.2.

Table 6.2 Rosin-Rammler particle size distribution parameters

Sample	Fitted function y = cx +d		R^2	X_o	n
	c	d			
IG,30 min	0.9743	-3.7795	1	47.90	0.9743
IG,1hr	0.9848	-3.2664	1	28.01	0.9848
IG, 1.5hr	0.9959	-2.9494	1	19.88	0.9959
IG, 2hr	0.9902	-2.951	1	20.00	0.9902
IG, 2.5hr	0.9813	-2.8498	1	18.20	0.9813
IG, 4hr	0.9896	-2.7544	1	16.69	0.9896
GA,30min	0.9653	-4.0996	1	78.35	0.9653
GA, 1hr	0.958	-3.347	1	33.05	0.958
GA, 1.5hr	0.9589	-3.0666	1	24.51	0.9589
GA, 2hr	0.9665	-2.8296	1	19.14	0.9665
GA, 2.5hr	0.9543	-2.6897	1	16.64	0.9543
GA, 4hr	0.934	-2.2793	0.9999	10.93	0.934
Cem,30min	0.9816	-3.6309	1	37.71	0.9816
Cem, 1hr	0.816	-3.1629	0.9984	33.11	0.816
Cem, 1.5hr	0.9662	-3.5129	1	37.29	0.9662
Cem, 2hr	0.9307	-3.3684	0.9999	29.43	0.9307
Cem, 2.5hr	0.9469	-3.4172	0.9999	32.04	0.9469
Cem, 4hr	0.8908	-3.4053	0.9996	25.71	0.8908
IB, 30 min	0.9424	-3.7753	0.9999	45.51	0.9424
IB, 1hr	0.9348	-3.4207	0.9999	31.66	0.9348
IB, 1.5hr	0.9777	-3.3921	1	30.55	0.9777
IB, 2hr	0.9686	-3.2527	1	25.93	0.9686
IB, 2.5hr	0.9499	-2.0479	0.9999	25.59	0.9499
IB, 4hr	0.8839	-3.0507	0.9995	23.27	0.8839

The effect of grinding time on particle size distribution can be seen in Figure 6.5. From the graph it is observed that as the grinding time is extended the particles become finer, resulting in the position parameter decreasing. This trend is prominent for the gasification and as well as the blended cement. The cement clinker alone has no clear trend, since the position parameter of the cement after 30 minutes is less than that of intergrinding or gasification ash. After 1 hour the position

parameters for all three are approximately the same. Hereafter gasification ash and intergrinding continues to reduce as grinding time is extended, while the cement increases slightly.

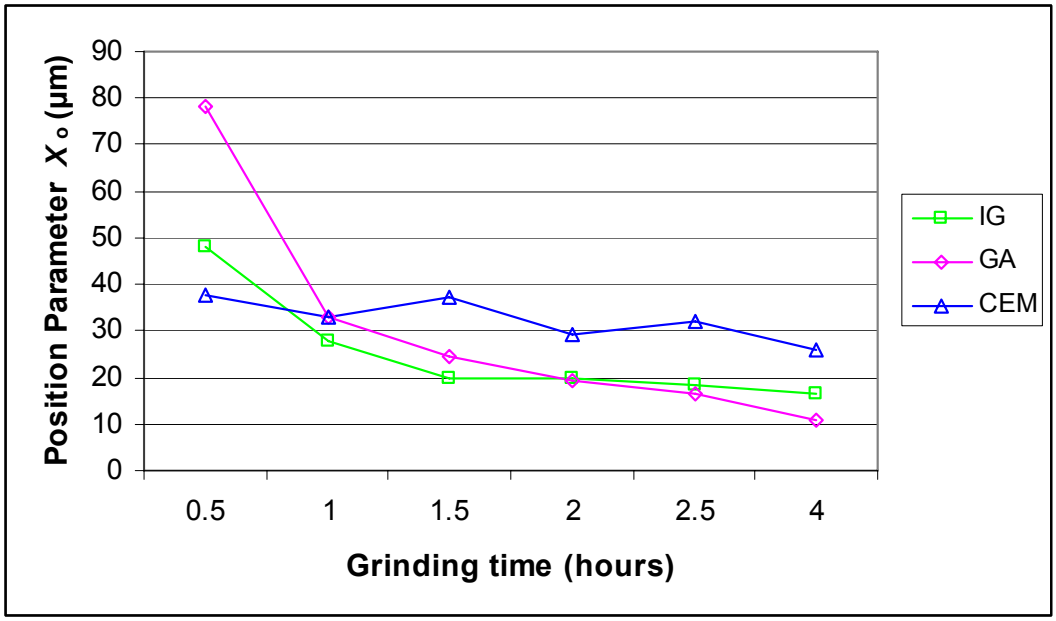

Figure 6.5 Relation between grinding time and position parameter X_o

The position parameters of cement range between 25µm and 38µm and there is no clear trend for the position parameter of cement to reduce with increased grinding time. The position parameter of gasification ash and intergrinding is significantly smaller than that of cement, even after 4 hours of grinding. After 2 hours of grinding the reduction in position parameter for gasification ash and intergrinding is not as noticeable as before. The graph indicates that an exponential relation exists between particle size and grinding time. It seems as if an optimum grinding time can be established. For both the intergrinding and gasification ash this optimum seems to be in the region of 2 hours. Grinding for longer than this optimum time would not decrease the particle size considerably more and would only add to the cost of grinding.

In Figure 6.6 the slope is plotted as a function of the grinding time. From this graph it can be seen that for intergrinding and

gasification ash the grinding time does not have an influence on the slope (*n*) value, which represents the range of the particle size distribution of the particle sizes greater than the position parameter. It is observed that for the gasification ash and intergrinding, the slope after 2 hours grinding is a maximum and thereafter the slope decreases. Thus after 2 hours the size range is narrow and any increase or decrease in grinding time make the size range wider. For cement the range varies for each grinding time interval. Intergrinding had the larger slope (*n*) and would have a narrower distribution than the gasification ash and the cement. This difference in slope is however very small and observed trends are not deemed to be significant.

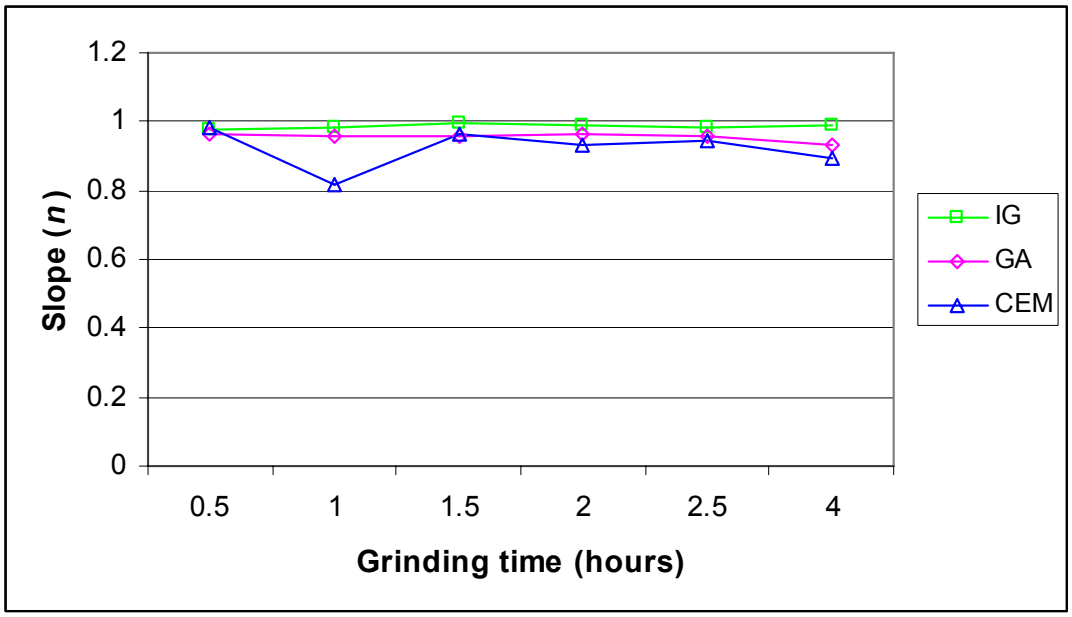

Figure 6.6 Relationship between grinding time and slope parameter (*n*)

The values of the oversize particle size distribution parameters (D50) and (D10) can be seen in Table 6.3. These parameters can be compared for different samples.

Table 6.3 Oversize particle size distribution parameters

Sample	Oversize particle size distribution parameters		3 - 30µm (%)	<3 µm (%)
	D50 (µm)	D10 (µm)		
IG,30 min	32.1	113.6	41.73	9.18
IG,1hr	19.4	64.2	55.20	13.76
IG, 1.5hr	14.0	44.4	62.05	18.01
IG, 2hr	13.9	45.4	62.18	18.48
IG, 2.5hr	12.7	43.1	62.74	19.65
IG, 4hr	11.6	37.3	64.44	22.07
GA,30 min	50.9	183.5	31.78	7.34
GA, 1hr	21.2	78.7	48.51	14.82
GA, 1.5hr	15.8	58.9	56.30	16.55
GA, 2hr	12.4	44.1	59.57	22.01
GA, 2.5hr	10.5	40.4	59.79	25
GA, 4hr	7.3	31.3	58.34	32.48
Cem,30 min	26.2	92.8	52.82	5.66
Cem, 1hr	22.2	100.9	57.08	6.32
Cem, 1.5hr	23.9	86.5	55.41	6.83
Cem, 2hr	21.4	83.4	57.94	7.13
Cem, 2.5hr	22.1	85.1	56.99	7.42
Cem, 4hr	22.7	106.7	53.25	7.97

The D50 and D10 results in the table indicate that for intergrinding of 35% gasification ash and 65% cement in the ball mil and for separately grounded gasification ash and cement the oversize particle size distribution parameters, D50 and D10, decrease for increased grinding time. This trend is more observable for the gasification ash. The gasification ash has a softer clinker than the cement and this is seen since the gasification ash is easier to grind. For the cement there is no clear trend. This is due to the harder cement clinker. It seems that increased grinding did not affect the particle size. The table also indicate the 30-3µm and <3µm percentage particles.

These results indicate that with increased grinding time the % of particles <3µm increase. The cement remained almost constant between 52 and 58µm. For both the intergrinding and gasification ash the % particles become more as grinding time increase. All of the results in the table indicate that with increased grinding time the particles become smaller.

6.2.2 Shape of Particles

Particle shape has a strong influence on the water requirement of concrete. The unique spherical shape of fly ash makes its water requirement lower and thus improves the workability (see Figure 6.7). The gasification ash has no unique structure and could be described as angular as can be seen in Figure 6.8. Angular shapes have higher water requirements, and an increase in porosity and a decrease in strength may be expected.

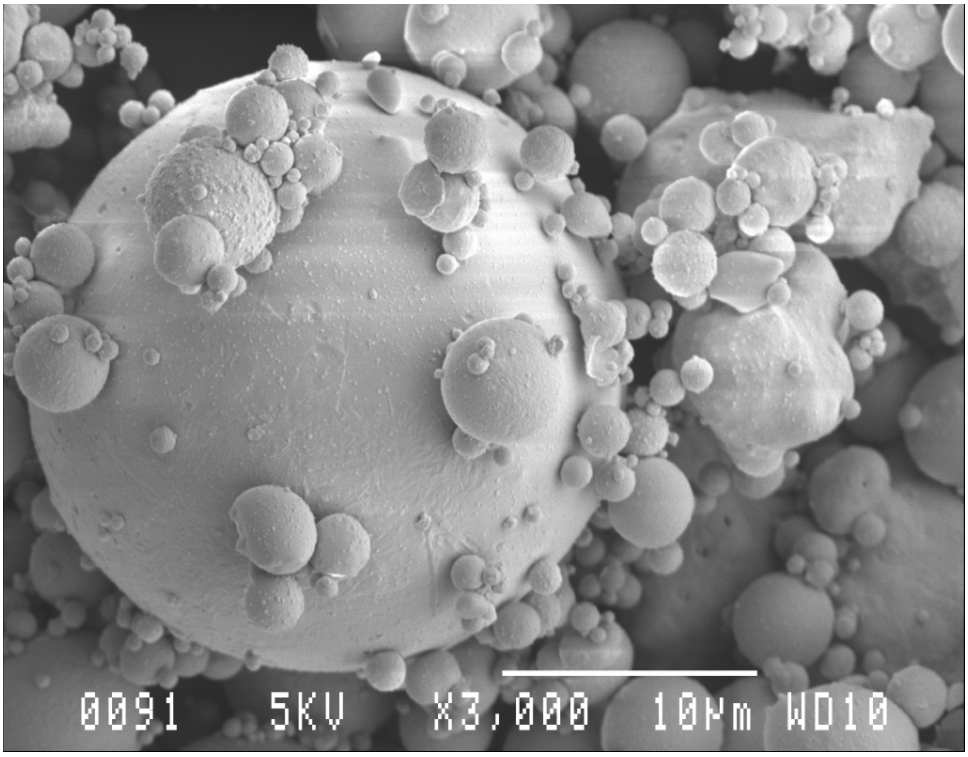

Figure 6.7 Scanning electron microscope photo of fly ash

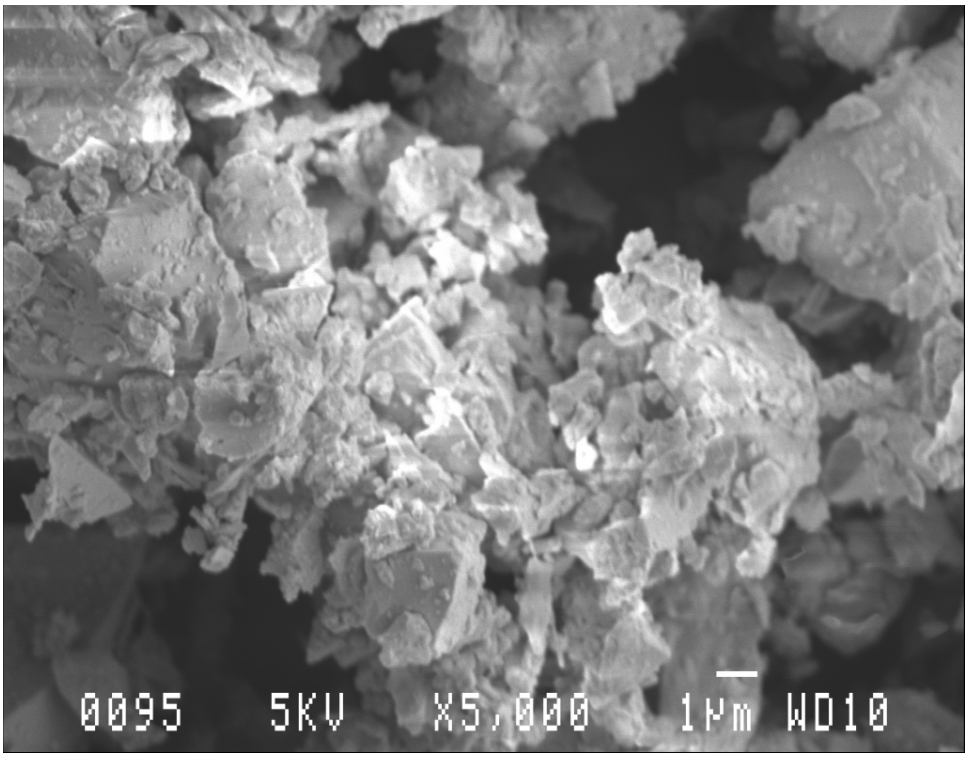

Figure 6.8 Scanning electron microscope photo of gasification ash

The Blaine surface area (Appendix D) for cement, gasification ash and interground cement and gasification ash is seen in Figure 6.9.

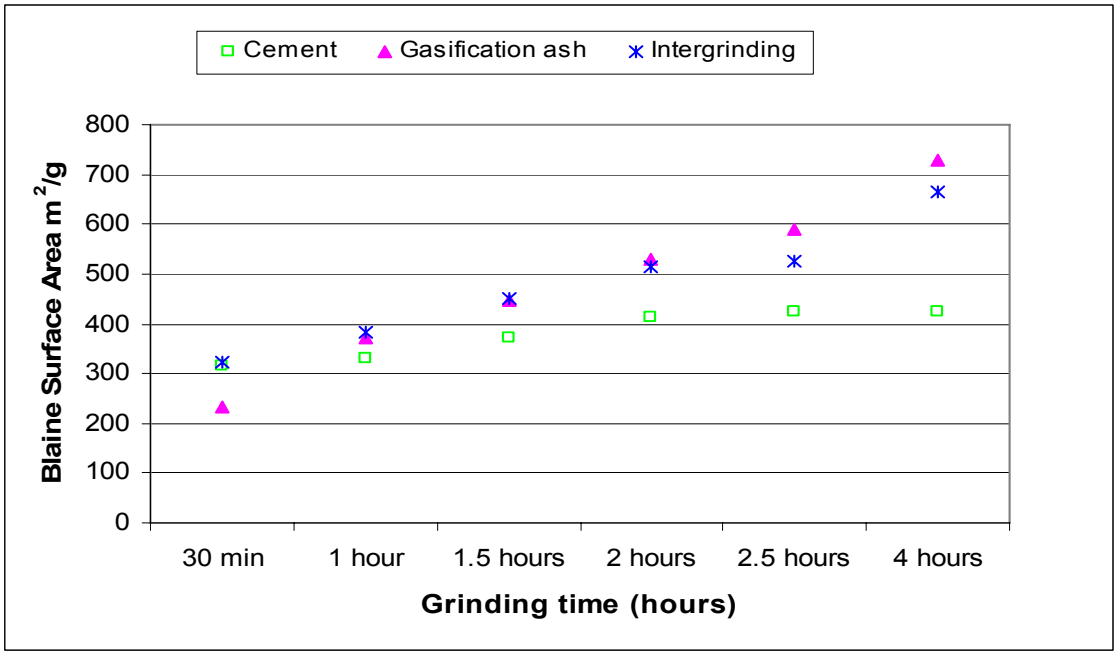

Figure 6.9 Graph indicating Blaine surface area

From the graph it can be seen that cement has a surface area ranging between 300m^2/g and 450m^2/g. This range of surface area corresponds to commercial cement as reported by Bhatty et al (2004). The surface area of cement increase for the grinding time intervals up to 2 hours, after which the surface area remains constant for 2.5 hours and slightly decreases for 4 hours grinding. This indicates that longer grinding does not keep increasing the surface area. There seems to be an optimum surface area for the cement. Initially after 30 minutes, gasification ash has the lowest surface area while the interground sample is close to the cement sample. From 1 hour grinding, both the gasification ash and interground gasification ash and cement sample has a higher surface area than the cement. The gasification ash and interground gasification ash and cement is approximately the same up to 2 hours of grinding, Thereafter the gasification ash's surface area increase more than the interground. This indicates that the surface area of gasification ash increase, while the cement reached an optimum surface area. After 2 hours, when cement reached an optimum surface area, the interground gasification ash and cement sample increased less in surface area.

6.3 CHEMICAL PROPERTIES

6.3.1 XRF

The XRF results of the gasification ash provided insight into the behaviour in reactivity in concrete. The chemical composition of both gasification and fly ash can be seen in Table 6.4.

These results indicate that gasification ash has a chemical composition similar to that of fly ash and it should thus be acceptable to use as a cement extender in concrete. There are

three elements in the form of oxides present in the gasification ash (MnO, Cr_2O_3 and V_2O_5) which are not in fly ash. These elements should have no effect on the reactivity. The P_2O_5 - content is lower in the gasification ash but was not considered to be significant. The varying amount of Al_2O_3 within the ashes is not so important in determining the influence on properties in concrete, thus the lower content of Al_2O_3 in gasification ash would not have detrimental effects on the concrete. These results indicate that gasification ash should be acceptable to use as a cement extender in concrete.

Table 6.4 XRF results

Elements	**Gasification Ash %**	**Typical values of South African Fly Ash* %**
Fe_2O_3	6.8	3.7-4.7
MnO	0.13	0
Cr_2O_3	0.63	0
V_2O_5	0.02	0
TiO_2	1.43	1.4-1.9
CaO	8.17	7.1-10.5
K_2O	0.83	0.5-1.2
P_2O_5	0.7	1.1-1.4
SiO_2	48.5	45-49
Al_2O_3	23.5	29-31
MgO	2.3	1.8-2.8
Na_2O	0.5	0.1-0.8
Cl	0	0
S	0.4	0
SO_3	0.49	0.5-1.0
Loss on ignition	5.18	5.0

*(SANS 1491-2:2005 / SABS 1491-2:2005)

6.3.2 XRD

The XRD results showed that gasification ash has high percentages of quartz (SiO_2) and mullite (Al_6SiO_{13}) which is similar to fly ash.

The XRD analysis of gasification ash shows that anorthite, sodian intermediate ($(Ca, Na)(Si, Al)_4O_8$), mullite (Al_6SiO_{13}), alpha-quartz (SiO_2), were found to be the major minerals present in ash, diopside ($Ca(Mg,Al)(Si,Al)_2O_6$), indialite ($Mg_2Al_4Si_5O_{18}$) and gehlenite ($Ca_2Al_2SiO_7$) were identified in small concentrations. These results indicate that gasification ash should be acceptable for use as a cement extender in concrete.

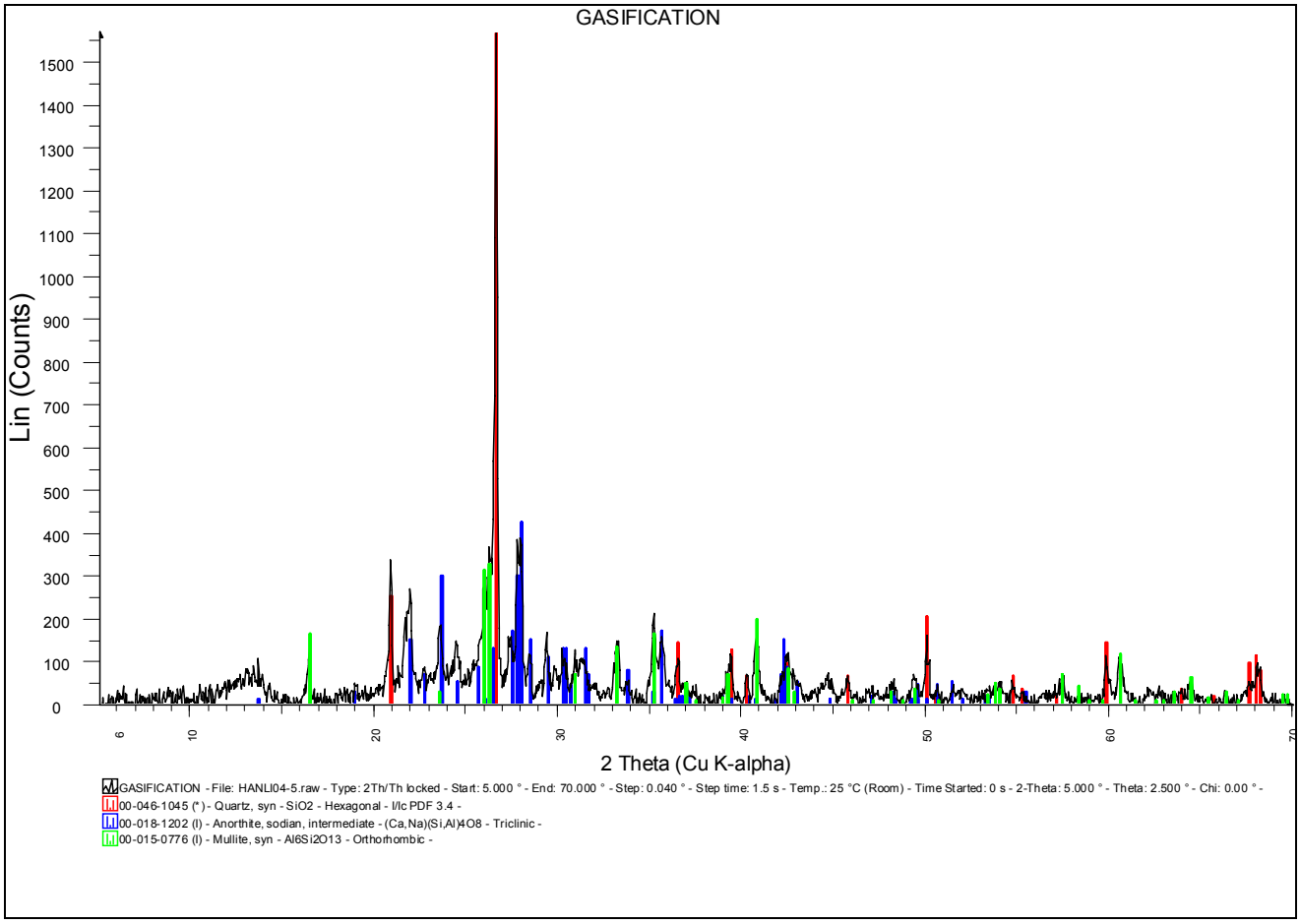

Figure 6.10 XRD results for gasification ash

6.3.3 Standard Tests for Cementitious Materials

The results of the standard tests conducted are summarized in Table 6.5. The chemical requirements of the gasification ash comply with the specification as set for fly ash in all but two cases. The gasification ash has a higher loss on ignition (LOI), due to the higher carbon content, which gives the ash a dark grey colour. The water requirement of gasification ash is more than 100% and this can be explained when considering the angular shape of the gasification ash. The strength factor of gasification ash is 2% higher than fly ash. The factors that do not meet the limits as set for fly ash do not cause a great concern but it should be investigated.

Table 6.5 Chemical test results

Test	Method	Gasification ash	Limits for Fly ash
Sulphur trioxide content, % (m/m)	SANS 50196-2	0.49	<2.5
Loss on ignition, % (m/m)	SANS 50196-3	5.18	<5.0
Free water content, % (m/m)	SANS 6151	0.19	1
Fineness, residue retained on a sieve with square apertures of nominal size 45um, % (m/m)	SANS 6157	6.5	12.5
Water requirement, % of control, max	SANS 6156	> 100	95
Strength factor, %	SANS 50196-1	8	>6
Soundness, expansion, mm, max	SANS 50196-3	0	<1
Relative density	LSA Method	2.59	2.3
Specific surface area, cm^2/g	LSA Method	7802	Not quantified

6.4 EFFECT OF GRINDING TIME ON THE PROPERTIES OF INTERBLENDED GASIFICATION ASH AND CEMENT

6.4.1 Mortar Prism Compressive Strength

Figure 6.11 shows the results for interblending gasification ash and cement manufactured in the laboratory. See Appendix E for the mortar prism strength summary. Both the gasification ash and cement clinker were ground for different time intervals. A mix of cement grinded for 2 hours and not interblended can also be seen in the graph. From the results it is observed that continually, throughout the strength development, the mix containing cement with 2 hours grinding time had the highest compressive strength. After 28 days the 2.5 hour mix was almost equal to the 2 hour mix. The mix made with cement containing only clinker achieved the same compressive strength after 28 days. The difference in compressive strength of mixes grinded for less than 2 hours was approximately 10 MPa. This difference clearly indicates than grinding time should not be shorter than 2 hours.

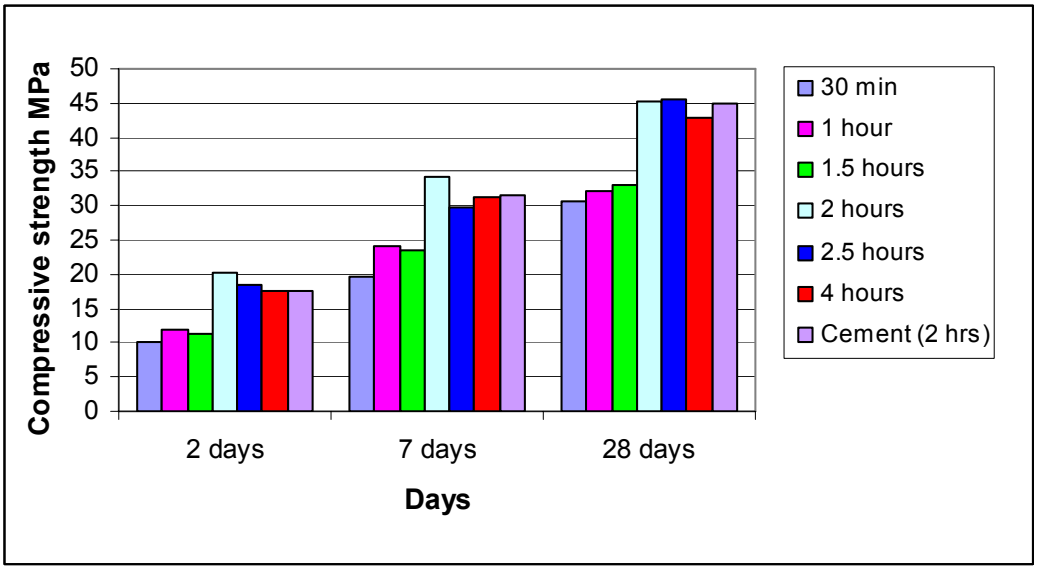

Figure 6.11 Compressive strengths for interblending gasification ash and cement for different grinding times

The compressive strength results of the mortar prisms are defined as a strength class in Table 6.6 from SANS 50197-1/SABS EN 197-1:2000.

Table 6.6 Strength classes of interblending mixes grinding time

	30 min	1 hour	1.5 hours	2 hours	2.5 hours	4 hours	cement (2hrs)
Strength class	N/A to 32.5 N	32.5R	32.5R	42.5 R	42.5 N	42.5 N	42.5 N
Percentage strength development after 7 days	63%	75%	71%	76%	65%	73%	70%

From the strength class requirements the difference in the compressive mortar strength for the mixes are highlighted. Grinding times shorter than 30 minutes does not achieve strengths for an acceptable strength class. Grinding times of 1 and 1.5 hours produce a cement strength class of 32.5R. A cement strength class of 42.5 R was produced for 2 hours grinding time and for the grinding times longer than 2 hours cement with a strength class of 42.5 N was achieved. When consideration is given to the cement grinded for 2 hours and not interblended, it is clear that gasification ash had a contribution to the early strength development of the mortar prisms. Table 6.6 also indicates the percentage of 28 day strength gained after 7 days, which indicates that mostly 70% of the strength is achieved after 7 days. Grinding for 2 hours increased the 7 day strength to 76% of the 28 day strength.

6.4.2 Mortar Prisms Flexural Strength

The flexural strengths of the interblended mixes (Figure 6.12) indicate the same trend as did the compressive strength for the mix grinded for 2 hours (Appendix E). After 28 days the interblended mixes grinded for longer than 2 hours exceeded the flexural strength of the cement only mix. The difference in flexural strengths for the mixes was approximately 1 MPa,

which is not a considerable difference. The flexural strength results shows that grinding times greater than 2 hours achieved better flexural strengths.

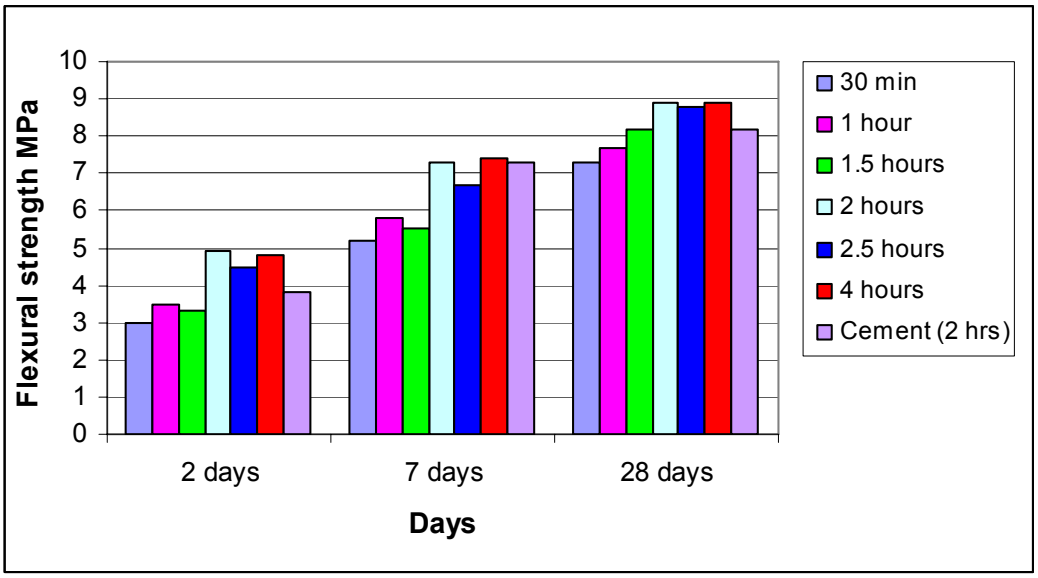

Figure 6.12 Flexural strengths for interblending gasification ash and cement for different grinding times

Table 6.7 gives a percentage of the compressive strength achieved by the flexural strength after 28 days. It is expected that the flexural strength should be 10% of the compressive strength. All of the mixes had a flexural strength of at least 19% of the compressive strength. The results indicate that interblending gasification ash and cement achieved better flexural strengths than a cement only mix.

Table 6.7 Percentage of compressive strength achieved for interblending

	30 min	1 hour	1.5 hours	2 hours	2.5 hours	4 hours	cement (2hrs)
Percentage of compressive strength achieved	24%	22%	21%	19%	19%	20%	18%

6.4.3 Particle Size Distribution

The effect of the particle size distribution on the 28-day compression strengths can be seen in Figure 6.13 and Figure 6.14. The Rosin-Rammler particle size distribution parameters (as discussed in 4.3.1.2) are plotted as a function of the 28-day compression strengths.

The graph indicates that the compressive strength increased with decreasing position parameters (X_o) for interblending of cement clinker and gasification ash. Thus finer particle achieved greater strengths. The interblended mix of 4 hours grinding time had the smallest position parameter (X_o), but achieved slightly lower strengths than the 2.5 hour and 2 hour mixes. It can be seen in Figure 6.13 that for grinding times longer than 2 hours the position parameter (X_o) decreases slightly while no significant increase in compressive strength is observed.

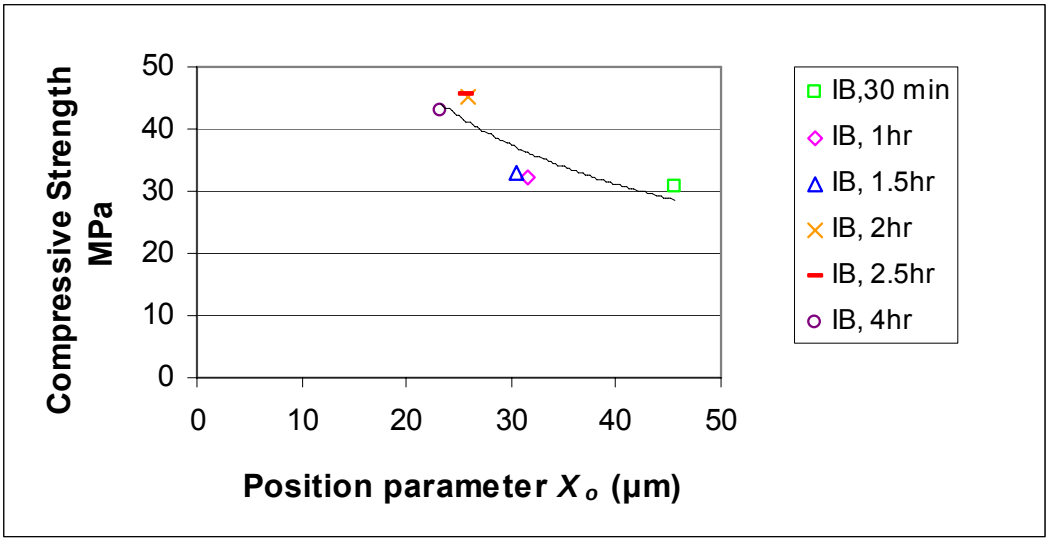

Figure 6.13 Relation between compressive strengths and Rosin-Rammler distribution position parameter (X_o) for interblending gasification ash and cement

Figure 6.13 indicates that position parameters larger than 30µm achieved lower compressive strengths. There was a considerable increase in compressive strength from 30µm to 25µm. From the graph it seems as if a peak is reached at 25µm, where the highest strengths were reached. It is thus concluded that 25µm, and thus 2 hours is an optimum when position parameters is compared to the compressive strength. However, the difference in compressive strength between the 2, 2.5 and 4 hours are small and thus a 2-hour grinding time seems the most effective when considering strength, particle sizes and cost of grinding.

In Figure 6.14 the slope (*n*) is plotted as a function of the 28-day compression strength. The smallest slope, after 4 hours grinding had high compressive strength. Grinding times of 2 and 2.5 hours had approximately the same compressive strengths but higher slopes. There is no clear trend to establish that smaller slopes give higher compressive strengths. However, the difference in compression strength between the 2 and 4 hour grinding time is small and optimally the 2 hour grinding time is most effective when strength, particle size and cost of grinding is considered.

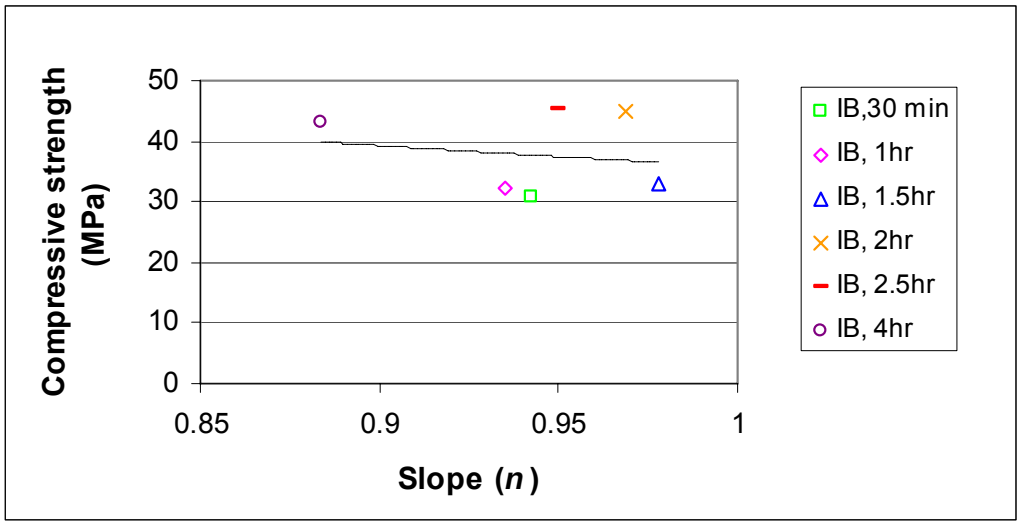

Figure 6.14 Relation between compression strengths and Rosin-Rammler distribution slope (*n*) parameter for interblending gasification ash and cement

In Figure 6.15, the oversize particle size distribution parameters (D50) and (D10) are plotted as a function of the 28-day compressive strength in order to find the influence of compressive strength on the particles size distribution.

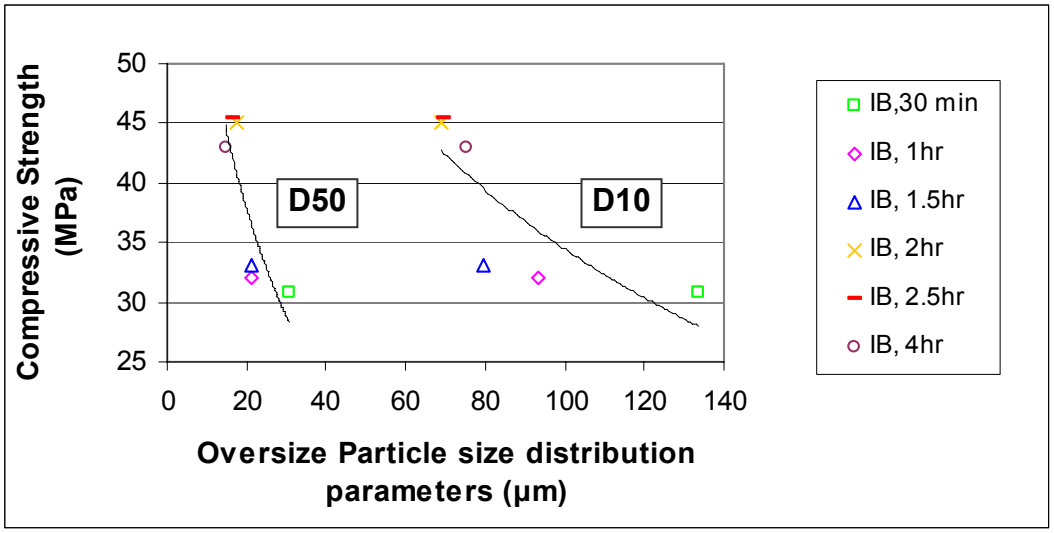

Figure 6.15 Relation between compression strength and particle size distribution parameters for interblending gasification ash and cement

As the average particle size becomes smaller the 28-day compression strength increases. As the 10% largest particle size for different grinding times become smaller compressive strengths also increases. After 2 hours grinding the maximum compressive strength is obtained. The difference in compressive strength between 2, 2.5 and 4 hours is small and thus an optimum limit is reached after 2 hours grinding for both the 50% and 10% largest particle size distribution parameters.

6.5 EFFECT OF GRINDING TIME ON THE PROPERTIES OF INTERGROUND GASIFICATION ASH AND CEMENT

6.5.1 Mortar Prism Compressive Strength

Figure 6.16 shows the results for gasification ash and cement clinker interground in the ball mill for different time intervals. See summary of strength results in Appendix F. The results indicate that intergrinding for 2 hours achieved the highest compressive strength during the strength development. Same as for the interblending, grinding for shorter than 1.5 hours achieved strengths of approximately 10 MPa less. The compressive strength of the cement only mix where slightly higher than the mixes interground for longer than 2 hours. This difference of 1 MPa is omissible. From the results it can be seen that intergrinding time should not be shorter than 1.5 hours.

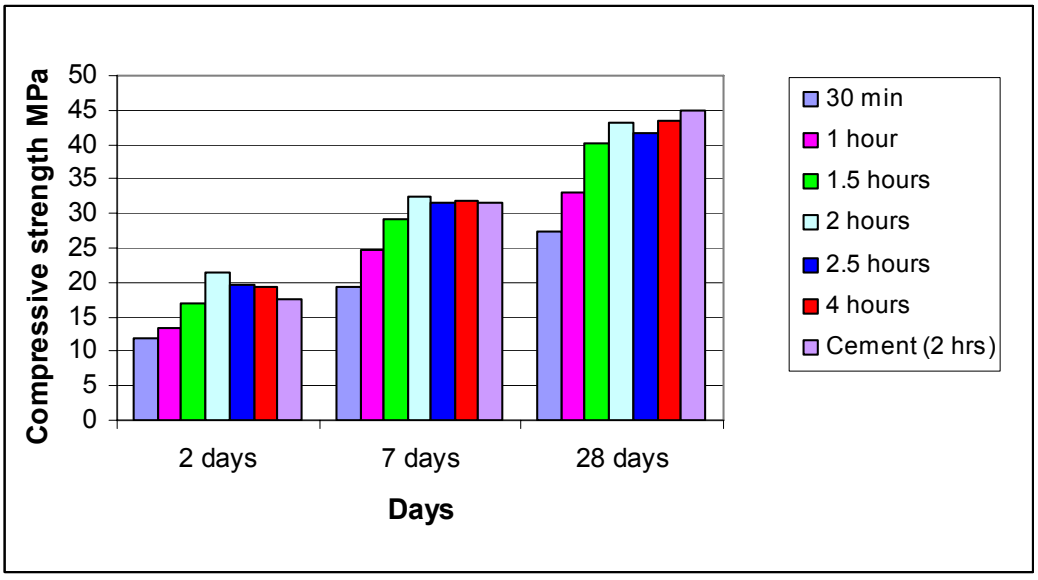

Figure 6.16 Compressive Strength for intergrinding gasification ash and cement for different grinding times

From the strength class requirements in Table 6.7 the difference in interblending and intergrinding can be observed in terms of strength. Grinding times shorter than 30 minutes for intergrinding did not achieve strengths for an acceptable

strength class. The same strength class were achieved for grinding 1, 1.5, 2 and 4 hours. For intergrinding the 2.5 hour grinding achieved a lower strength class than with the interblending at 32.5 R. This is similar to the 1 and 1.5 hour grinding time strength class. A cement strength class of 42.5 R was produced for 2 hours grinding time and for grinding 4 hours cement with a strength class of 42.5 N was achieved. When consideration is given to the cement grinded for 2 hours and not interblended, it is clear that gasification ash had a contribution to the early strength development of the mortar prisms.

Table 6.8 also indicates the percentage of 28 day strength gained after 7 days, which indicates that at least 70% of the strength is achieved after 7 days for all the mixes. Intergrinding achieved a faster rate of strength development after 7 days than the interblending mixes (Table 6.6).

Table 6.8 Strength classes for intergrinding mixes grinding time

	30 min	**1 hour**	**1.5 hours**	**2 hours**	**2.5 hours**	**4 hours**	**cement (2hrs)**
Strength class	N/A to 32.5 N	32.5R	32.5R	42.5 R	32.5 R	42.5 N	42.5 N
Percentage strength development after 7 days	71%	75%	73%	75%	76%	73%	70%

6.5.2 Mortar Prism Flexural Strength

The flexural strengths of intergrinding in Figure 6.17 indicate that grinding times longer than 1.5 hours achieved higher flexural strengths (Appendix F). The difference in flexural strengths is less than 1 MPa. The graph indicates that although the difference in flexural strength is omissible, grinding times longer than 1.5 hours achieved greater flexural strengths and thus grinding for less than 1.5 hours is not advisable.

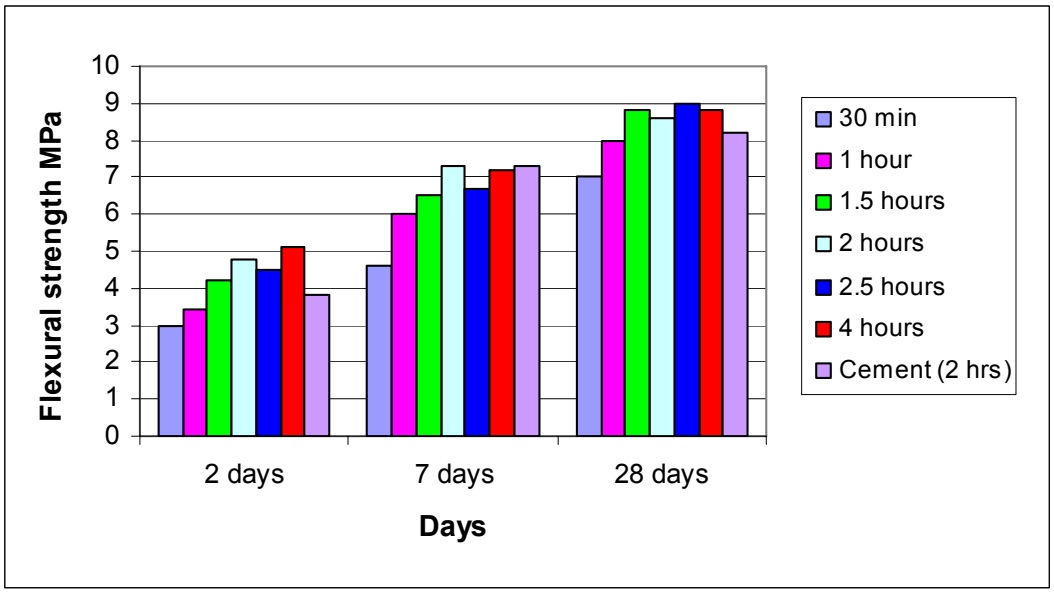

Figure 6.17 Flexural strengths for intergrinding gasification ash and cement

Table 6.9 gives a percentage of the compressive strength achieved by the flexural strength after 28 days for intergrinding. All of the mixes had a flexural strength of at least 20% of the compressive strength, which is higher than the expected 10%. The lowest percentage is achieved by the cement only mix. The results indicate that intergrinding gasification ash and cement achieved better flexural strengths than a cement only mix.

Table 6.9 Percentage of compressive strength achieved for intergrinding

	30 min	1 hour	1.5 hours	2 hours	2.5 hours	4 hours	cement (2hrs)
Percentage of compressive strength achieved	26%	24%	22%	20%	22%	20%	18%

6.5.3 Particle Size Distribution

The effect of the particle size distribution on the 28-day compression strengths can be seen in Figure 6.18 and Figure

6.19. The Rosin-Rammler particle size distribution parameters (as discussed in 4.3.1.2) are plotted as a function of the 28-day compression strengths.

The graph indicates that compressive strength increase with decreasing position parameters (X_o) for intergrinding of cement clinker and gasification ash. Thus finer particle achieved greater strengths. It can be seen in Figure 6.18 that for grinding times longer than 2 hours the position parameter (X_o) decreases slightly while no significant increase in compressive strength is observed.

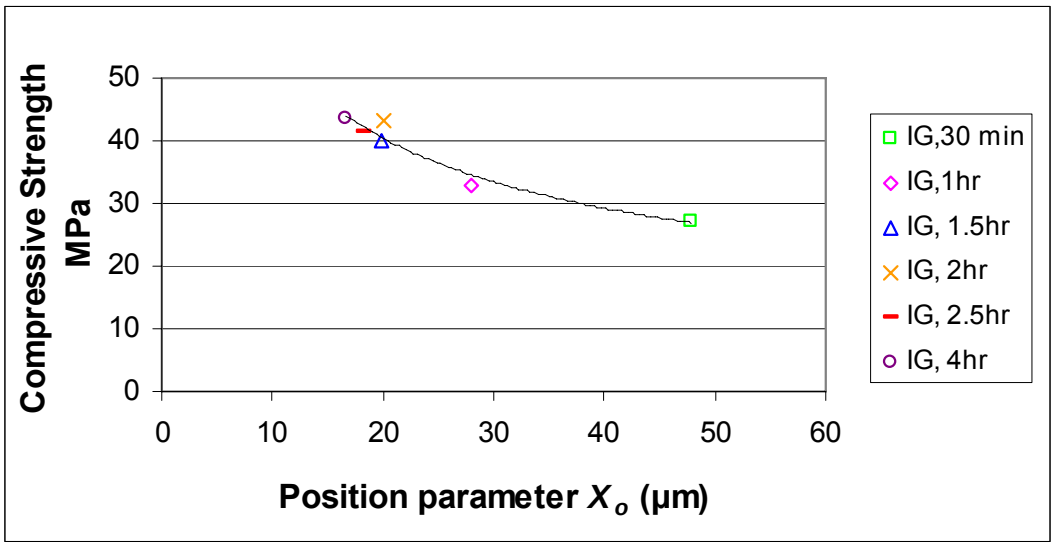

Figure 6.18 Relation compressive strengths and Rosin-Rammler distribution position parameter (X_o) for intergrinding gasification ash and cement

Figure 6.19 indicates that position parameters larger than 20µm achieved considerably lower compressive strengths. There was a considerable increase in compressive strength from 30µm to 20µm. The highest strengths were reached at 20µm and 16µm. The 30-3µm used by cement manufacturers as a limit on fineness, effectively show that after 1.5 hours the % particle almost remained constant (Table 6.3) as did the compressive strength. From the graph it seems as if a peak is reached at 20µm. It is thus concluded that 20µm, and thus 2

hours is an optimum when position parameters is compared to the compressive strength.

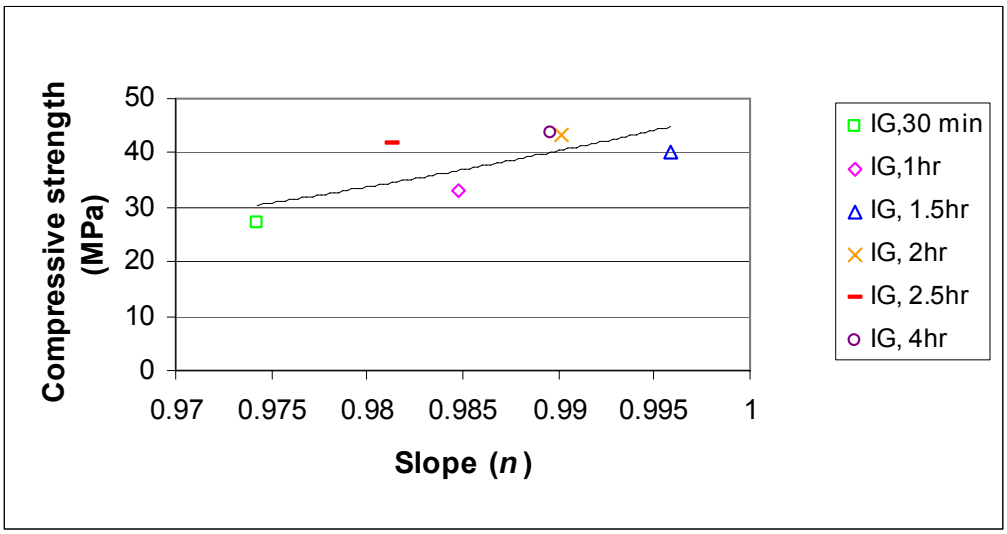

Figure 6.19 Relation between 28-day compression strengths and Rosin-Rammler distribution slope (*n*) parameter

In Figure 6.19 the slope (*n*) is plotted as a function of the 28-day compression strength. From this graph it seems that with increased grinding time the slope (n) decrease and the compression strengths increase. The smallest slope, after 4 hours grinding had the greatest compression strength. Again the difference in compression strength between the 2 and 4 hour grinding time is small and optimally the 2 hour grinding time is most effective when strength, particle size and cost of grinding is considered.

In Figure 6.20, the oversize particle size distribution parameters (D50) and (D10) are plotted as a function of the 28-day compressive strength in order to find the influence of compressive strength on the particles size distribution.

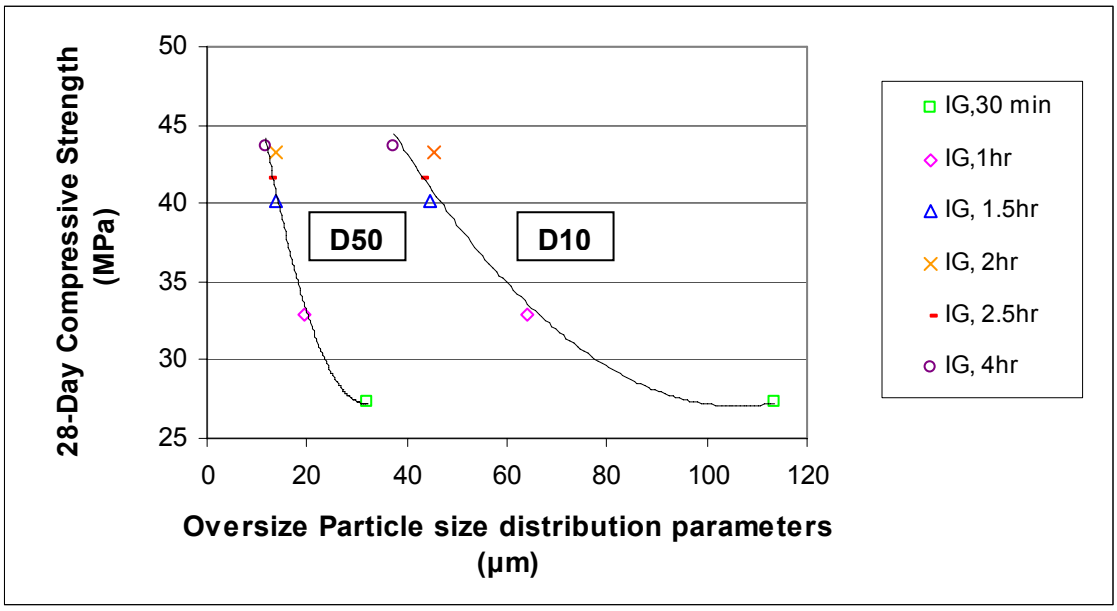

Figure 6.20 Relation between 28-day compression strength and particle size distribution parameters

As the average particle size becomes smaller the 28-day compression strength increases. As the 10% largest particle size for different grinding times become smaller compressive strengths also increases. It is interesting to note that the distribution curves converge, indicating that the particle sizes become smaller and more uniform in size at higher strengths. After 4 hours grinding the maximum compressive strength is obtained. However the compressive strength difference between 4 hours and 2 hours is small and thus an optimum limit is reached after 2 hours grinding for both the 50% and 10% largest particle size distribution parameters.

6.6 EFFECT OF GYPSUM CONTENT ON THE PROPERTIES OF INTERGROUND GASIFICATION ASH AND CEMENT

6.6.1 Mortar Prism Compressive Strength

Figure 6.21 shows the compressive results for different gypsum contents. See Appendix G for a summary of the strengths. The highest compressive strength is achieved by 3% gypsum content but the difference in compressive strength for the different gypsum contents is not significant. All of the mixes

can be classified as 32.5R in strength class. From the results there is no clear indication that there is an optimum gypsum content.

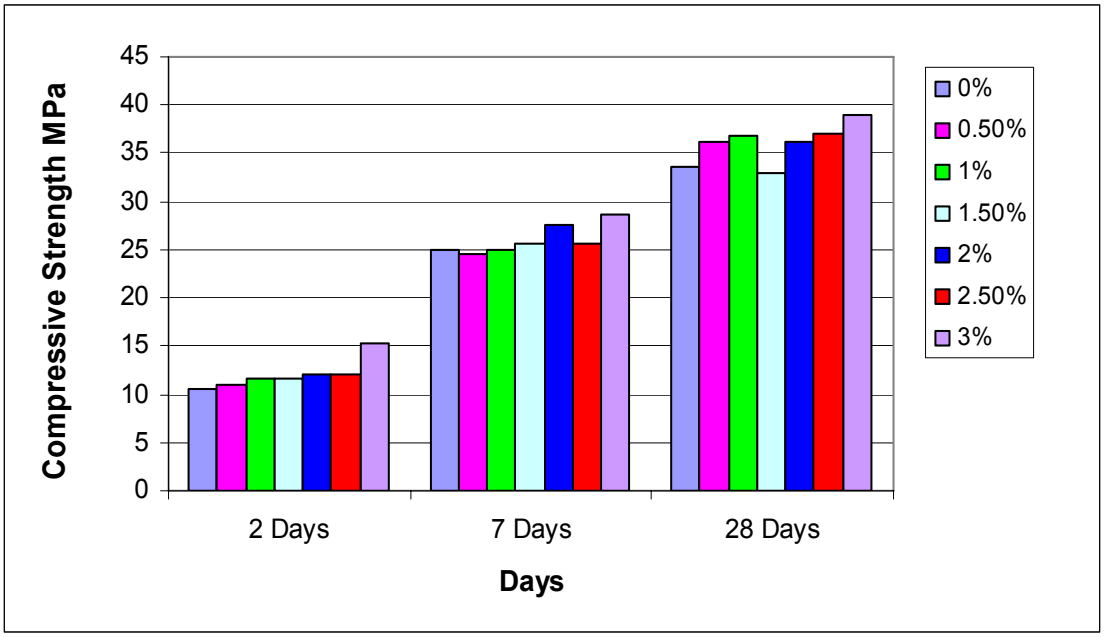

Figure 6.21 Compressive strengths for gypsum content

6.6.2 Mortar Prism Flexural Strength

The flexural strengths (Appendix G) for different gypsum contents can be seen in Figure 6.22. All of the mixes were a blend of 35% gasification ash, intergrinded with cement. After 28 days the highest compressive strength is achieved by 2% gypsum content. The difference in compressive strength for the different mixes is small. From the flexural strength results there is no clear indication that there is an optimum gypsum content.

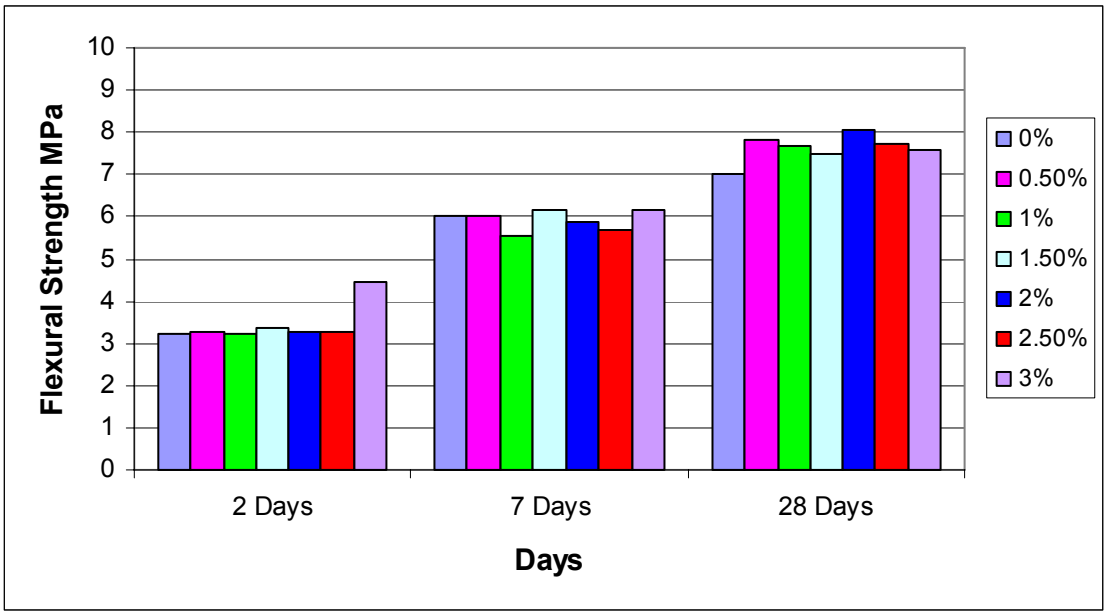

Figure 6.22 Flexural strengths for gypsum content

6.6.3 Heat of Hydration

Figure 6.23 shows the rate of heat development for different gypsum percentages. From the graph it is observed that the first peak (initial reaction) is delayed for low percentages of gypsum. All the first peaks for the gypsum percentages have a lower heat evolution than the reference 100% cement mix. A 3% replacement of gypsum peaks at the same time as the 100% cement, however at a lower heat evolution. For all the curves it is observed that the curves are smooth and no shoulders is observed after the first heat peak which would indicate flash or false set. The duration for testing was 36 hours and restricts the complete curve of hydration.

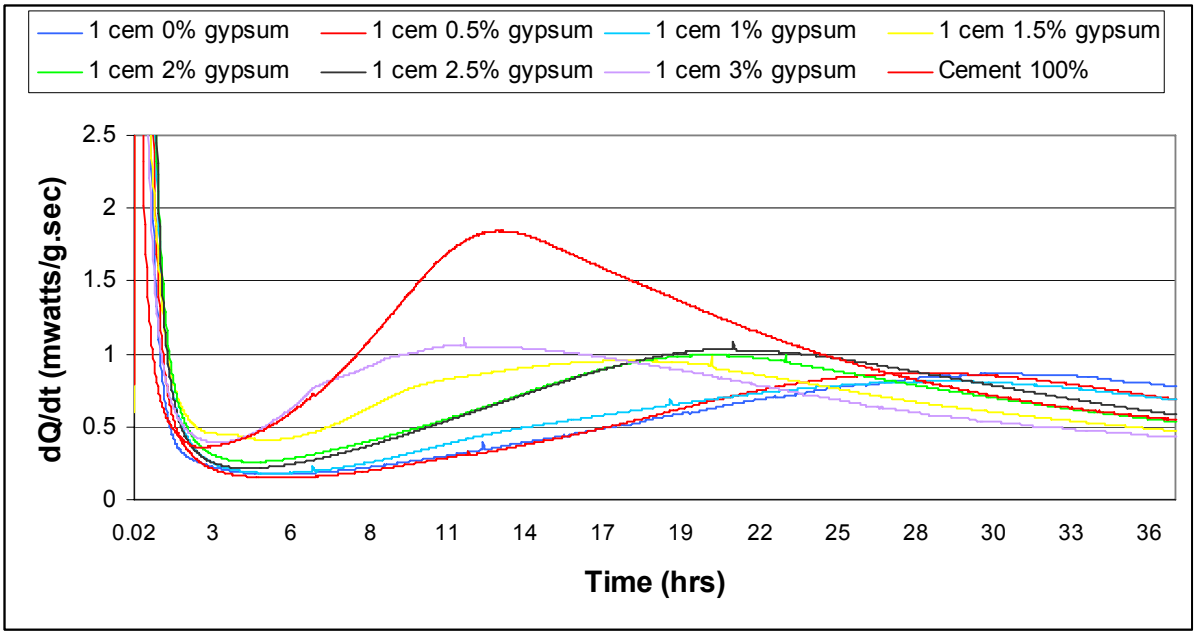

Figure 6.23 Rate of heat development for different gypsum percentages

Figure 6.24 represents the evolution of the hydration heat of mortars made with the different percent of gypsum substitution relative to 100% PC mortar, with a reference point of zero being assigned to the hydration heat developed by the 100% PC mortar. This representation of the data shows clearly the effect of different percentages of gypsum on the heat development. Low percentages of gypsum decrease the heat output after the induction period. The heat difference with respect to the pure cement paste is positive for these mixes after the induction period. For higher gypsum percentages the initial heat output is less than for low gypsum percentages. After the induction period the heat difference for the higher gypsum percentages as negative. Higher gypsum percentages seem to have a constant heat output after the induction period.

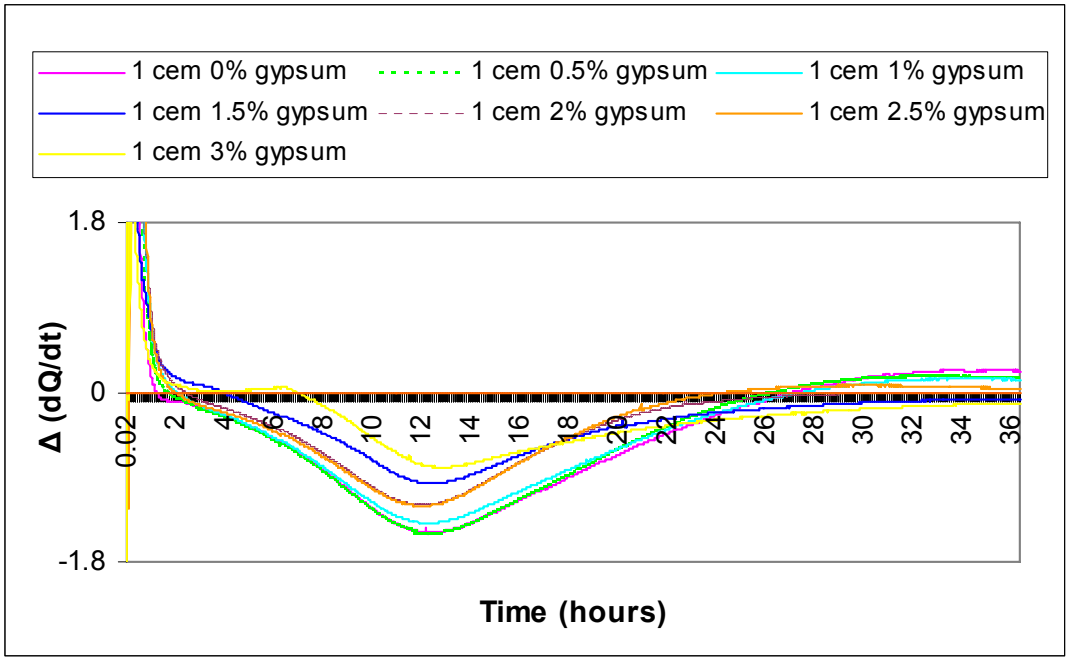

Figure 6.24 The difference in the rate of heat evolution for different gypsum percentages cement and pure PC cement

This was further confirmed by the plotting the total heat evolved with time in Figure 6.25. The total heat evolved at the first 10 hours increased with decreasing gypsum contents. After 10 hours the pure cement has a considerable increase in heat where low gypsum percentages decrease the heat evolution. Higher gypsum percentages have a constant heat evolution which is lower than the pure cement. From the results it is clearly observed that gypsum decrease the heat evolution of cement pastes. This is true for the smallest percentages of gypsum. There is no clear indication that gypsum percentages considerably enhance the hydration of cement. It can be deduced that a 2.5% gypsum addition is a good average to use in further testing when heat of hydration and compressive strength is considered.

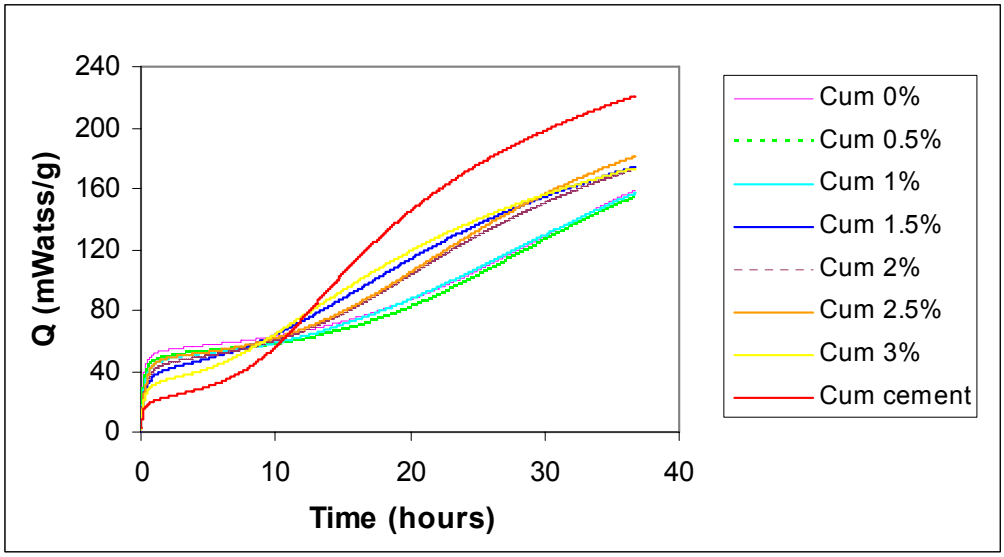

Figure 6.25 Total heat of hydration of different gypsum percentage cements at 25°C

6.7 EFFECT OF REPLACEMENT LEVEL ON THE PROPERTIES OF INTERGROUND GASIFICATION ASH AND CEMENT

6.7.1 Mortar Prism Compressive Strength

Figure 6.26 shows the results for gasification ash and cement clinker interground for different replacement levels. See Appendix H for summary of strength results. The results indicate that a replacement level of 10% achieved the highest compressive strength. Replacement levels more than 10% were gradually lower in compressive strength. Replacing 10% of cement with gasification ash achieved a higher compressive strength than the mix with 0% replacement. This clearly indicates that gasification ash replacement can increase the compressive strength of mortar pastes. The difference in compressive strength between 35% and 55% is approximately 15MPa, which is considerable. From the results it can be seen that a 10% replacement of gasification ash had the highest compressive strength. The 20% and 35% replacement had lower compressive strengths but was still considered as sufficient for use in cement. A replacement of 55% had low

compressive strengths and is not recommended as a replacement for cement.

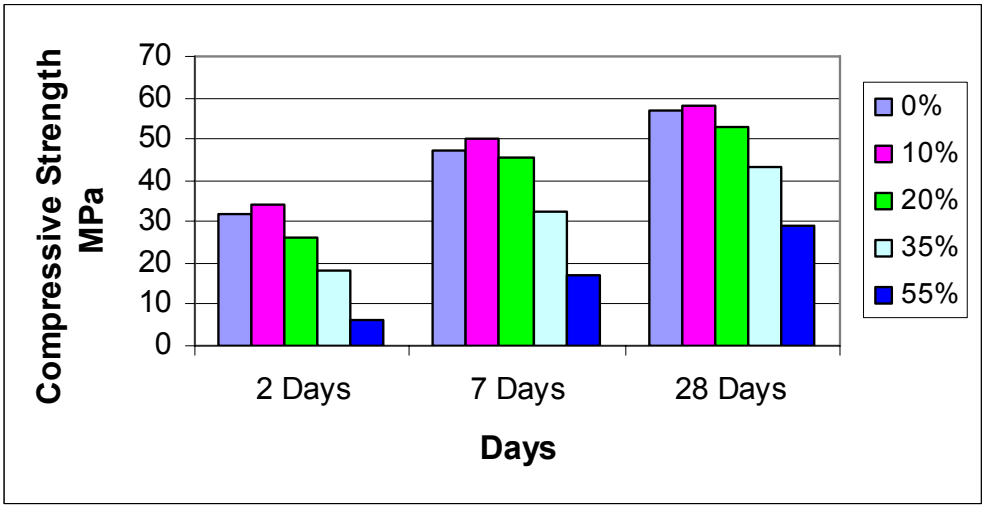

Figure 6.26 Compressive strength for different replacement levels of gasification ash

From the strength class requirements in Table 6.10 the difference in replacement level can be observed in terms of strength. Replacement levels of 0% to 20% achieved the same strength class, 52.5N. The 35% replacement achieved strengths for a lower strength class, 42.5N. The 55% did not achieve a compressive strength to be classified. The results indicate that gasification ash replacement has no detrimental effect on the compressive strength development of cement paste. Low replacement levels achieved higher compressive strengths than high replacement levels.

Table 6.10 also indicates the percentage of 28 day strength gained after 7 days, which indicates that at least 75% of the strength is achieved after 7 days for mixes with a replacement level between 0% and 35%. The 10% and 20% replacement level achieved a faster rate of strength development after 7 days than the 0% replacement level. The 55% replacement level achieved lower strength development than the expected 70%.

Table 6.10 Strength classes for different replacement levels of gasification ash

	0%	10%	20%	35%	55%
Strength class	52.5 N	52.5 N	52.5 N	42.5 N	N/A to 32.5N
Percentage strength development after 7 days	83%	87%	85%	75%	58%

6.7.2 Mortar Prism Flexural Strength

The flexural strengths (Appendix H) of different replacement levels of gasification ash in Figure 6.27 indicate that replacement levels lower than 35% achieved higher flexural strengths. The difference in flexural strengths is approximately 1 MPa. The graph indicates that although the difference in flexural strength is small, replacement levels less than 35% achieved greater flexural strengths and thus a 55% replacement level is not advisable.

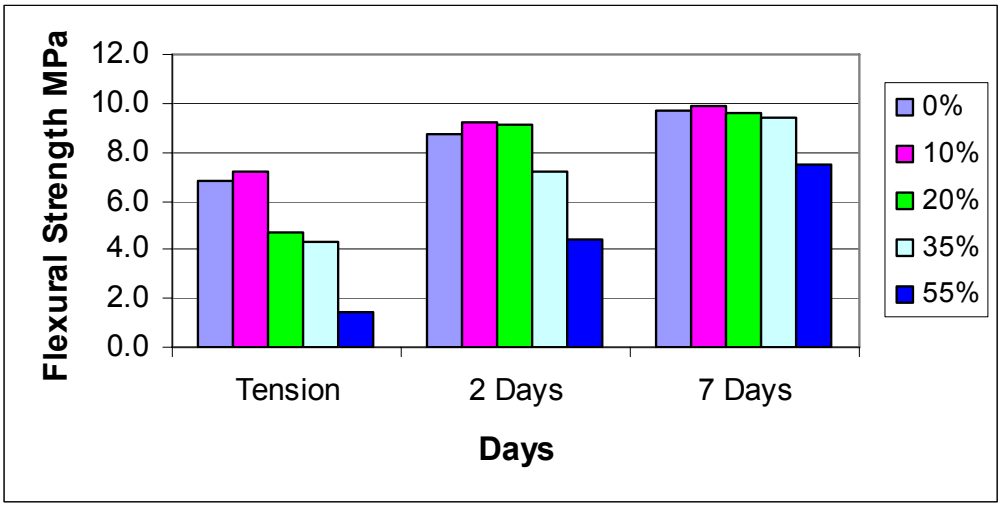

Figure 6.27 Flexural strengths for different replacement levels of gasification ash

Table 6.11 gives a percentage of the compressive strength achieved by the flexural strength after 28 days for intergrinding. All of the mixes had a flexural strength of at least 20% of the compressive strength, which is higher than the expected 10%. The cement only mix seen in Table 6.7 and 6.9 had a percentage of 18% while the 0% replacement was 17%. The ratio varied with repeating and further testing should be done to establish limits on the strengths. The lowest percentage is achieved by the cement only mix. The results indicate that intergrinding gasification ash and cement achieved better flexural strengths than a cement only mix.

Table 6.11 Percentage of compressive strength achieved for different replacement levels of gasification ash

	0%	10%	20%	35%	55%
Percentage of compressive strength achieved	17%	17%	18%	22%	26%

6.7.3 Particle Size Distribution

The effect of the particle size distribution on the 28-day compression strengths can be seen in Figure 6.28 and Figure 6.29. The Rosin-Rammler particle size distribution parameters (as discussed in 4.3.1.2) are plotted as a function of the 28-day compression strengths.

The graph indicates that compressive strength decrease with decreasing position parameters (X_o) for replacement levels of gasification ash. It can be seen in Figure 6.28 that for a 10% replacement level of gasification ash the position parameter (X_o) is smaller than the 0% replacement. Replacement levels of 20% and 55% had the same position parameter (Xo) as the 10% replacement level, but with lower compressive strengths. The 35% replacement level had a smaller position parameter (Xo)

than the other replacement levels. There is no indication that finer particle achieved greater strengths.

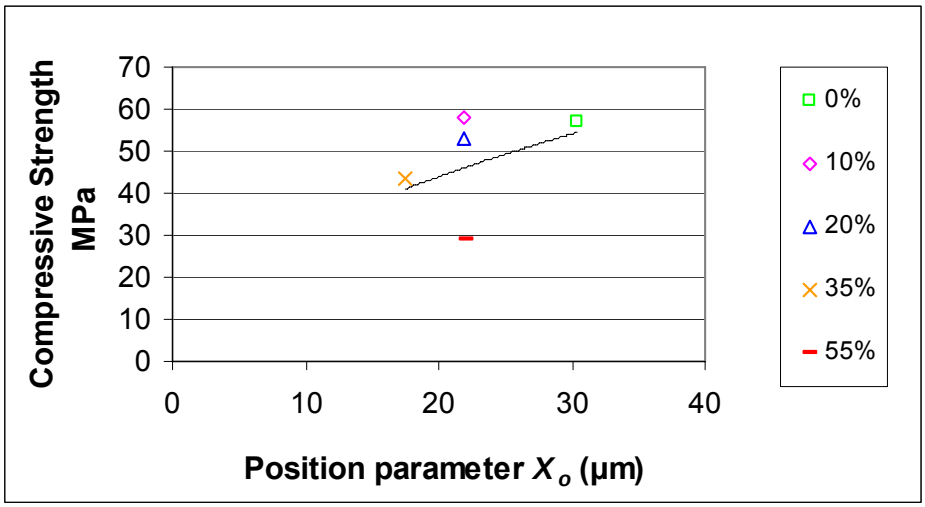

Figure 6.28 Relation compressive strengths and Rosin-Rammler distribution position parameter (X_o) for replacement levels of gasification ash

Figure 6.28 indicates that there is no significant indication that position parameters had an effect on the compressive strength development of the mortar mixes.

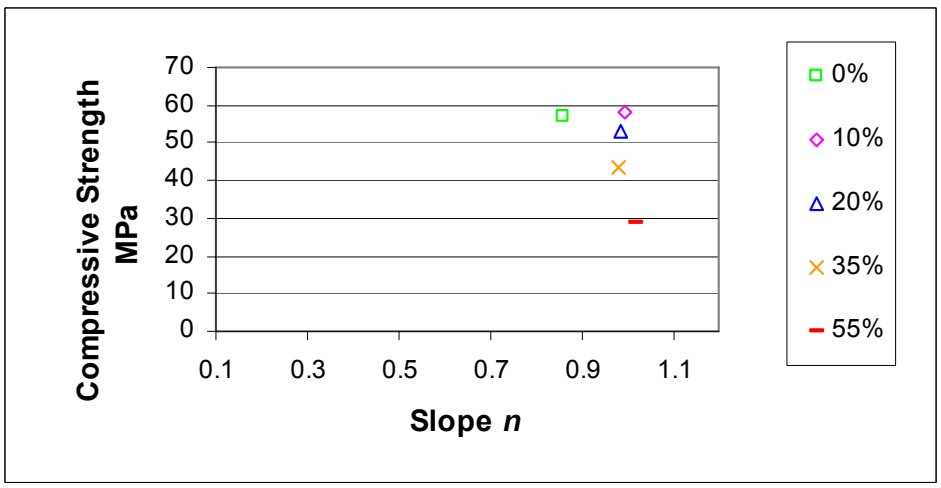

Figure 6.29 Relation between 28-day compression strengths and Rosin-Rammler distribution slope (n) parameter

In Figure 6.29 the slope (n) is plotted as a function of the 28-day compression strength. From this graph it seems that the

slope (*n*) is approximately 1 for all the replacement levels of gasification ash but 0%. The compressive strength decreased for different replacement level while the slope (*n*) remained the same. There is no significant indication that the slope (*n*) had an effect on the compressive strength of the mortar mixes.

In Figure 6.30, the oversize particle size distribution parameters (D50) and (D10) are plotted as a function of the 28-day compressive strength in order to find the influence of compressive strength on the particles size distribution.

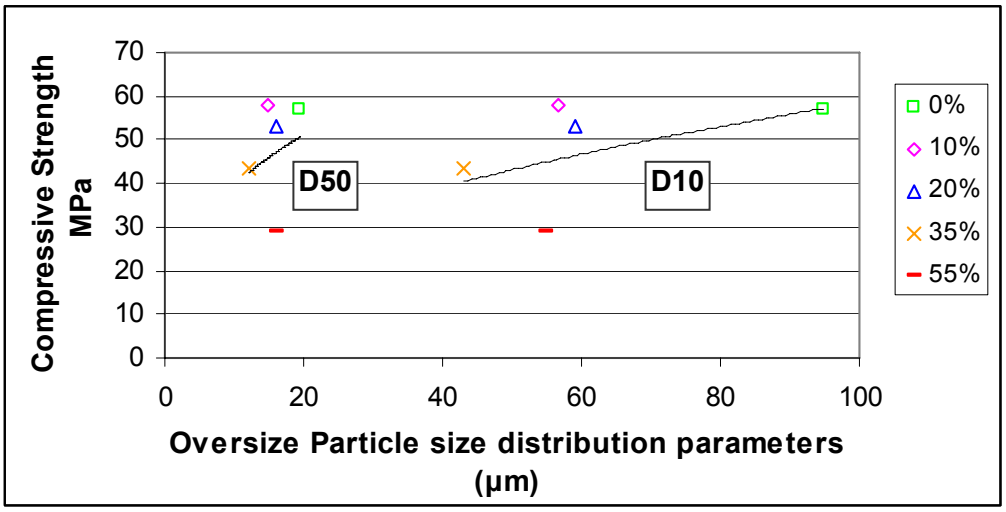

Figure 6.30 Relation between 28-day compression strength and particle size distribution parameters of replacement level of gasification ash

As the average particle size becomes smaller the 28-day compression strength decreases. As the 10% largest particle size for different replacement levels become smaller compressive strengths also decreases. It is however interesting to note that there is no clear indication that the average particle size or the 10% largest particle size becomes smaller for different replacement levels. The average particle size for the different replacement levels range between 15µm and 20µm, while the 10% largest particle size range between 40µm and 95µm. From the graph there is no optimum limit for

both the 50% and 10% largest particle size distribution parameters.

6.8 COMPARISON BETWEEN MANUFACTURED AND COMMERCIAL CEMENT

6.8.1 Mortar Prism Compressive Strength

The cement manufactured in the lab was compared to commercially available CEM I 42.5R. See Appendix I for a summary of strengths. The cement manufactured in the laboratory was either interblended (interblend in mixer) or interground (interblend in ball mill and ground together) for 2 hours with a 2.5% gypsum content. Figure 6.31 indicates the compressive strengths for interblended and interground cement manufactured in the lab and a commercially available CEM I 42.5R. From the graph it is observed that intergrinding cement and gypsum achieved compressive strengths higher than the CEM I 42.5R, while interblending achieved lower compressive strengths than the CEM I 42.5R.

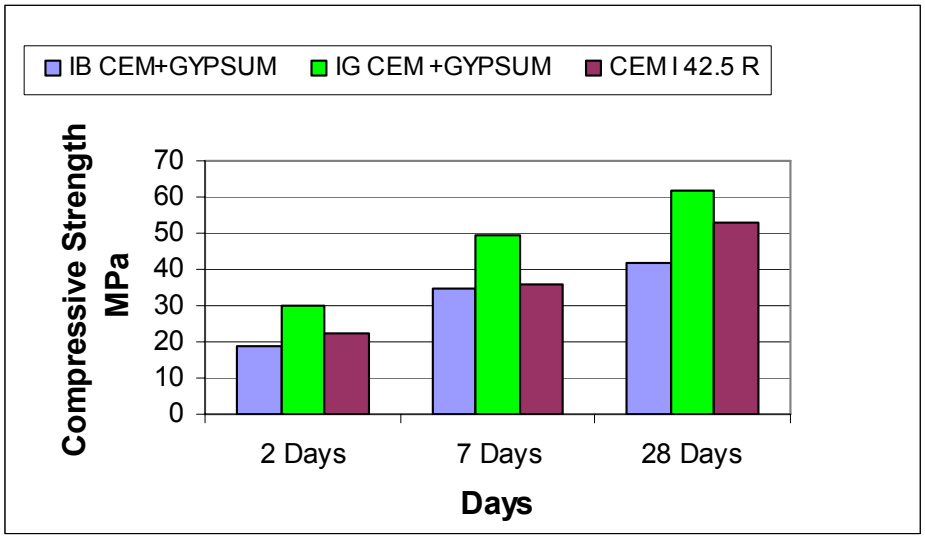

Figure 6.31 Compressive strengths for manufactured and commercially available cement

From the strength class requirements in Table 6.12 the difference can be observed in terms of strength. Interblending

can be classified as 42.5N while intergrinding is classified as 52.5N.

Table 6.12 also indicates the percentage of 28 day strength gained after 7 days, which indicates that interblending and intergrinding achieved at least 80% of the strength after 7 days. The CEM I 42.5 R achieved only 68% of its strength development after 7 days. From the results it is clear that the interground cement manufactured in the lab performed better than a commercially available 42.5R. The interblended cement manufactured cement performed like a 42.5N but had a faster strength development after 7 days than the 42.5R.

Table 6.12 Strength classes for different replacement levels of gasification ash

	IB CEM + Gypsum	**IG CEM + Gypsum**	**CEM I 42.5R**
Strength class	42.5 N	52.5 N	42.5 R
Percentage strength development after 7 days	82%	80%	68%

6.8.2 Flexural Mortar Prism Strengths

Figure 6.32 shows the flexural strengths (Appendix I) for interblended and interground cement manufactured in the lab and a commercially available CEM I 42.5N. From the graph it is observed that interground cement achieved similar flexural strengths than the CEM I 42.5N.

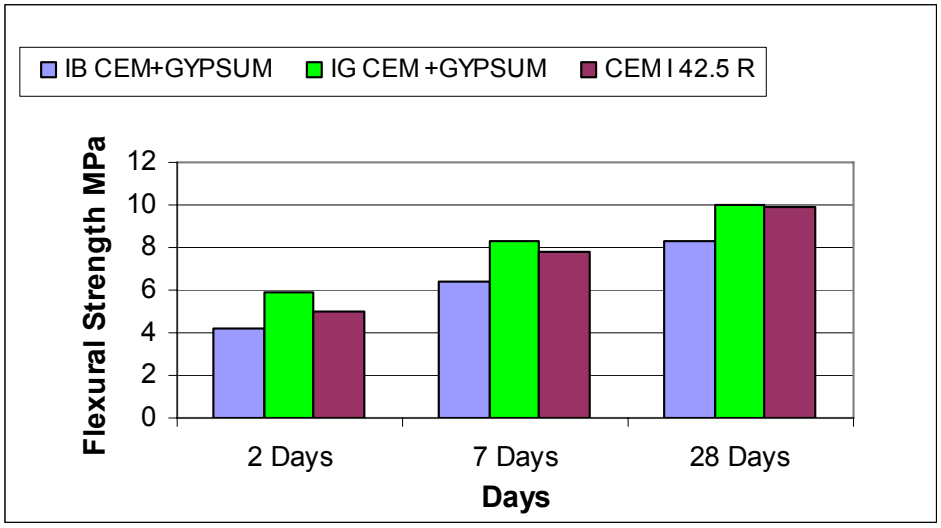

Figure 6.32 Flexural strengths for manufactured and commercially available cement

Table 6.13 gives a percentage of the compressive strength achieved by the flexural strength after 28 days. Interblending achieved the highest percentage of flexural strength compared to compressive strength. The interground and CEM I 42.5R mixes achieved smaller percentages but all three of the mixes achieved a percentage higher than 10% which is expected. The results indicate that the both the interblended and interground cement performed similar to the commercially available CEM I 42.5R.

Table 6.13 Percentage of compressive strength achieved for different replacement levels of gasification ash

	IB CEM + Gypsum	**IG CEM + Gypsum**	**CEM I 42.5R**
Percentage of compressive strength achieved	20%	16%	19%

6.8.3 Heat of Hydration

Figure 6.33 shows the rate of heat development for the manufactured and commercially available cement. From the graph it is observed that the cement manufactured in the lab peak at the same time as the CEMI 42.5R but at a lower heat evolution. After the first peak both the mixes decrease without any shoulders which indicate flash or false set. The results indicate that the cement manufactured in the lab performed similar to the commercially available CEM I 42.5R but lower heat of hydration temperatures is observed for the cement manufactured in the lab.

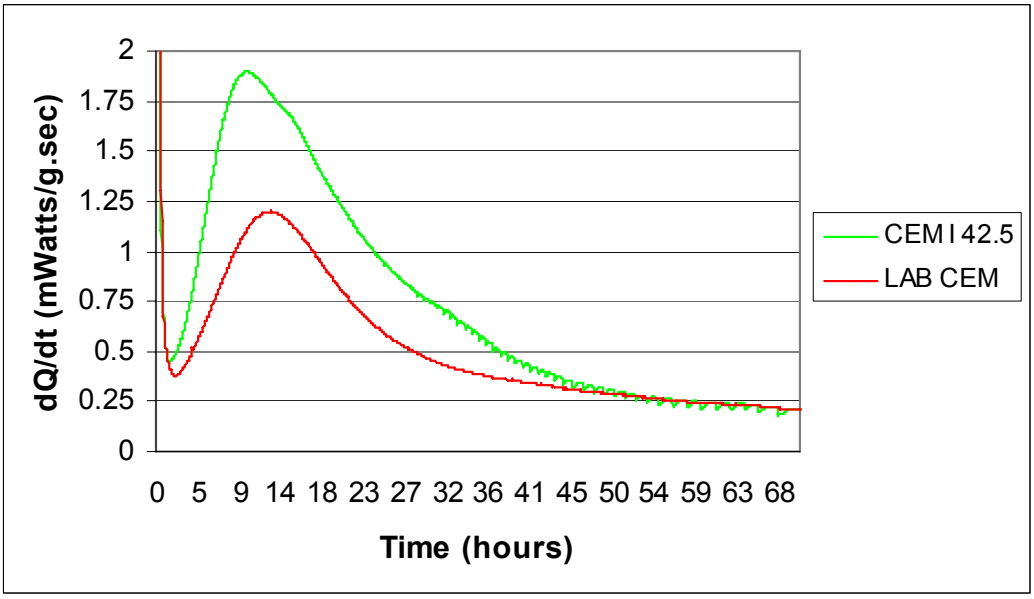

Figure 6.33 Rate of heat development for manufactured and commercially available cement

6.9 CONCLUSION

- It is observed that the gasification ash, grinded separate and interground had similar particle size distributions. The particle size of gasification ash ground separately is considerably finer than that of cement ground separately for the same time interval. This indicates that the cement clinker is harder than the gasification ash clinker.

- The position parameter (X_o) and therefore the particle size distribution decrease as the grinding time increases for gasification ash.
- It seems as if an optimum grinding time can be established. For both the intergrinding and gasification ash this optimum seems to be in the region of 2 hours.
- The gasification ash has no unique structure and could be described as angular.
- The XRF, XRD and chemical specification results indicate that gasification ash should be acceptable to use as a cement extender in concrete.
- The compressive strength, flexural strength, particle size and Rosin-Rammler distribution parameters clearly indicate that grinding time should not be shorter than 2 hours for interblending and intergrinding of gasification ash and cement.
- It can be deduced that a 2.5% gypsum addition is a good average to use in further testing when heat of hydration and compressive strength are considered.
- The compressive strength, flexural strength, particle size and Rosin-Rammler distribution parameters confirm that replacement levels of gasification ash should range between 10% and 35%.
- The cement manufactured in the laboratory performed similar in strength development to the commercially available CEM I 42.5R but lower heat of hydration temperatures are observed for the cement manufactured in the laboratory.

7. TEST RESULTS AND DISCUSSION ON CONCRETE TESTS

7.1 INTRODUCTION

In chapter 7, the results of the experimental tests discussed in chapter 5 on concrete are reviewed and analysed to examine the reactivity of a gasification ash when used in concrete.

Thereafter the results of the concrete cast are illustrated and discussed. The results include slump, compression strength, tensile strength, E-value, shrinkage, creep, porosity and oxygen permeability test results. The discussion of the results takes into consideration that tests were conducted on a single set of samples. Limitations to the testing method will be discussed and possible improvements will be recommended.

7.2 TESTS CONDUCTED ON FRESH CONCRETE

7.2.1 Slump Test

The slump test results (as indicated in figure 7.1) illustrate that the concrete mix interblended with fly ash had the highest slump and thus a high workability. It is expected that due to the filler effects characteristic of fly ash it will exhibit a slightly lowered paste water demand. This increases the cohesiveness of the mix which improves its workability (Holcim, 2005). The mixes with gasification ash were less workable. Results indicate that the water demand of concrete containing gasification ash is higher than that of the mix interblended with fly ash. The slump test results indicate that the use of gasification ash as cement extender will results in a reduction in the workability of concrete.

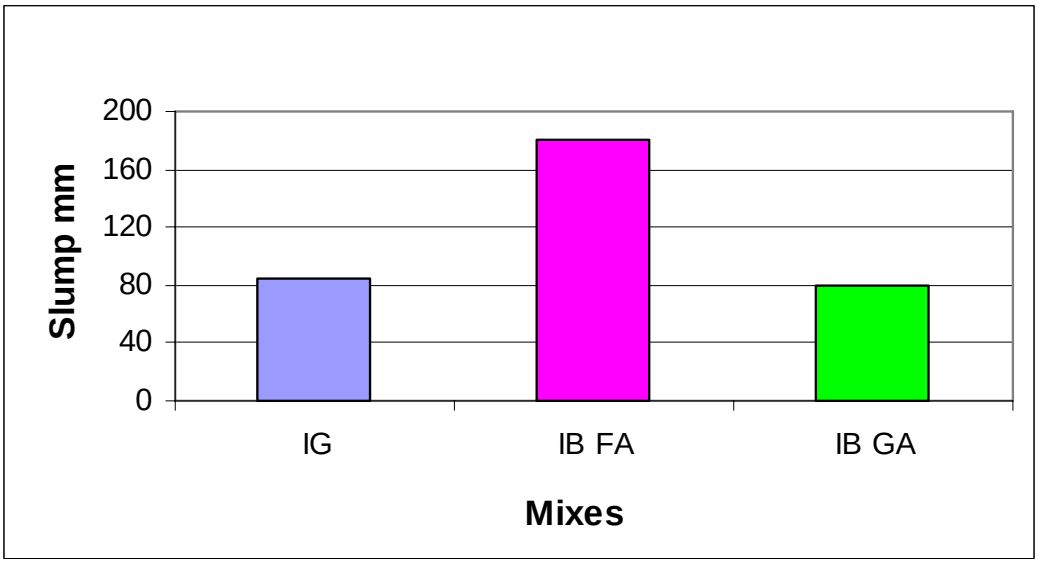

Figure 7.1 Slump test for concrete mixes

7.3 STRENGTH TESTS

7.3.1 Concrete Cube Compression Test Results

Figure 7.2 shows the compressive strength of the different concrete mixes. The highest strength was achieved by the intergrinded gasification ash mix, but the strength difference is not greater than 5 MPa for all the mixes after 28 days (see Appendix J). The lowest strengths were achieved by the interblending with fly ash. These results clearly indicate that the use of gasification ash as cement extender does not have a negative impact on the strength development of concrete.

After 7 days the gasification ash intergrinded achieves a high compressive strength. This value could statistically be considered as an outlier but no trends can be concluded from the results as only one set of samples were tested. This value visibly indicates that more testing should be done so that statistical conclusions could be drawn about the behaviour of compressive strength of gasification.

The compressive strength test is however not a good indicator of concrete durability as no direct relationship exists between

the two characteristics. The quality of concrete, in terms of durability, should therefore not be deduced from the compressive strength, as is often the case in the construction industry.

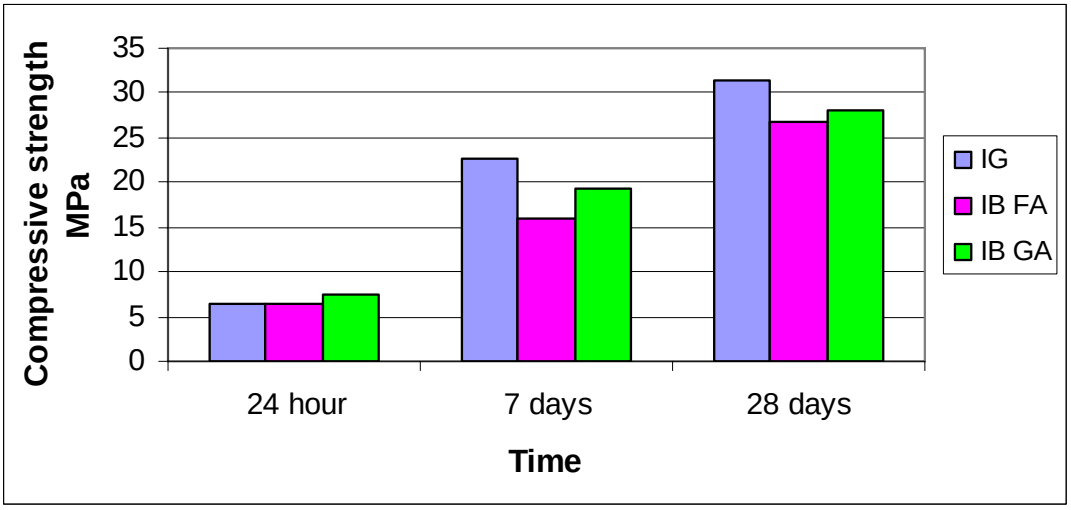

Figure 7.2 Concrete cubes compression strength results

7.3.2 Tensile Strength Results

Theoretically the tensile strength is expected to be 10% of the compressive strength. Results in Table 7.1, shows that the tensile strength of the mixes was all approximately 3 MPa. All of the mixes had a flexural strength to compressive strength comparison of 10% to 12%. Higher than 10% for the interblending mixes was due to a lower compressive strength than the intergrinding mix. The flexural strength results of gasification ash, intergrinded or interblended was marginally higher than the mix interblended with fly ash. The tensile results are however within 0.3 MPa of each other and therefore the difference is not considerable. Interblending with gasification ash has a slightly higher tensile strength than the fly ash.

Table 7.1 Table comparing tensile and compressive strengths

Mixes	Tensile strength MPa	Compression Strength MPa	Comparison %
IG	3.3	31.5	10%
IB FA	3.02	26.7	11%
IB GA	3.35	28.0	12%

From Figure 7.3, it can be seen that interblending and intergrinding with gasification ash achieved the highest tensile strengths. These results indicate that the use of gasification ash as cement extender does not results in a reduction in the tensile strength of concrete.

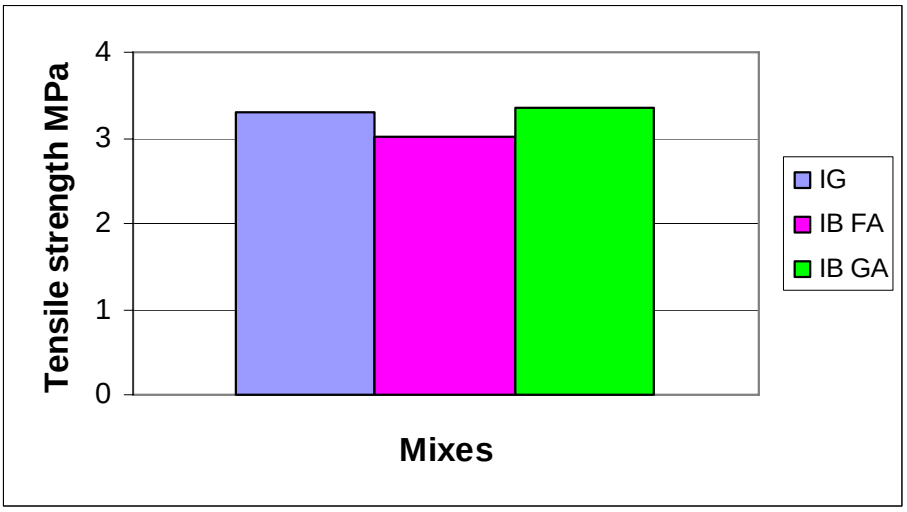

Figure 7.3 Tensile strength results for concrete mixes

7.4 DEFORMATION AND VOLUME CHANGE OF CONCRETE

7.4.1 E-value test results

The elastic modulus represents the material stiffness of the concrete to an imposed stress. Figure 7.4 shows the average of two results for each mix. The results for the E-value show that intergrinding with gasification ash achieved the highest

modulus of elasticity. Interblending with gasification ash achieved the lowest modulus of elasticity.

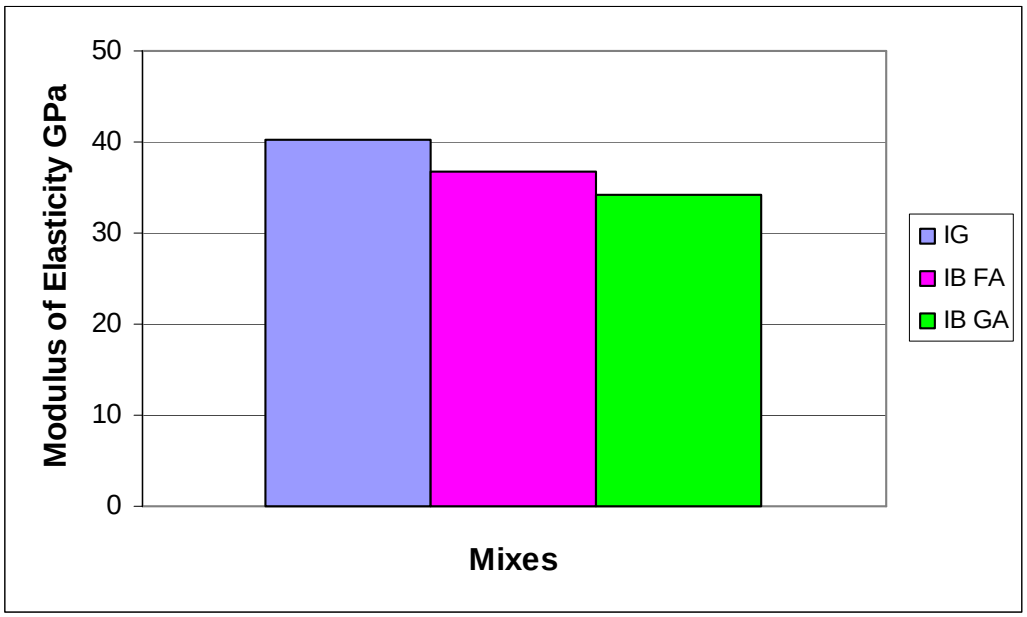

Figure 7.4 E-value test results for concrete mixes

Gasification ash intergrinded achieved a higher modulus of elasticity than the interblending mixes (see table 7.2). This could be due to the better interface of the particles already mixing when grinded together and due to the higher compressive strength of intergrinding. There is a constant difference of 2 GPa between each of the cylinders for all three mixes. No trends can be concluded from the results as only one set of samples were tested. The high stiffness of intergrinding gasification ash indicates that more testing should be done so that statistical conclusions could be drawn about the stiffness of concrete when gasification ash is intergrinded with cement. These results indicate that the use of gasification ash as cement extender does not have a detrimental effect on the stiffness of concrete.

Table 7.2 E-value results of the different cylinders for the different mixes

Mix	E-value Cylinder 1	E-value Cylinder 2
IG	38.8 GPa	40.3 GPa
IB FA	37.8 GPa	35.9 GPa
IB GA	35.4 GPa	33 GPa

7.4.2 Shrinkage and Creep Test

Shrinkage is caused by drying therefore factors that contribute to the drying of concrete such as relative humidity, size and shape of the concrete member as well as the concrete mix proportions and materials will influence shrinkage.

Table 7.3 indicates the shrinkage, creep and specific creep for each of the mixes after 309 days. From the results it is observed that intergrinding and interblending of gasification ash achieved higher shrinkage, creep and specific creep results than the interblended fly ash mix. These differences are only marginal.

Table 7.3 Shrinkage, Creep and Specific Creep Results for the different mixes

MIX	Shrinkage (microstrain)	Creep (microstrain)	Specific Creep (microstrain/Mpa)
IG GA	413.4	830.7	201.1
IB FA	326.8	643.7	169.8
IB GA	378.0	783.5	184.6

Previous studies conducted by Badenhorst (2003) showed that for a 70/30 FA blended cement it is expected that for different aggregate the shrinkage differs. A dolomite sand and granite stone was used in the mix design of the concrete for all three

mixes. Granite has an expected shrinkage of 500 microstrain while dolomite has an expected shrinkage of 300 microstrain. The results of the three mixes fall in this range and thus the difference in shrinkage for the mixes is not considerable. Figures 7.5, 7.6 and 7.7 indicate the shrinkage and creep for each of the three mixes. The results for shrinkage indicate the gasification ash did not shrink significantly more than fly ash.

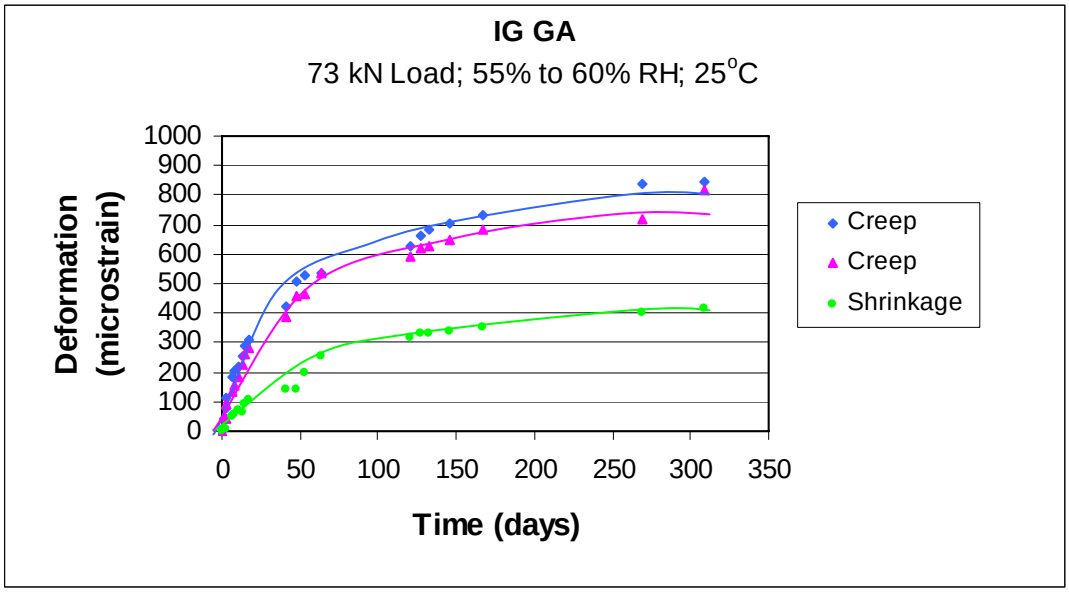

Figure 7.5 Shrinkage and creep results for interground gasification ash mix

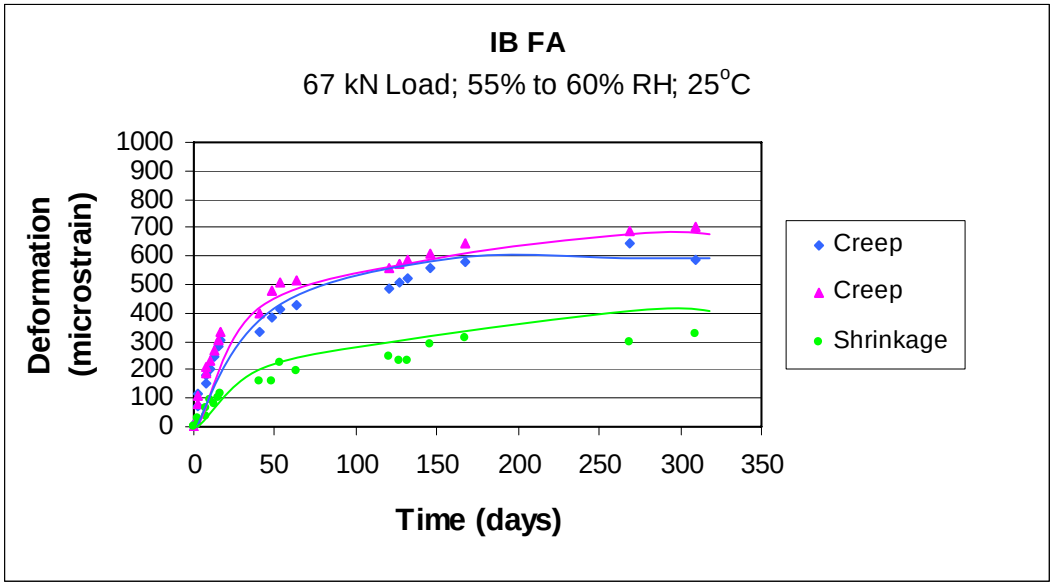

Figure 7.6 Shrinkage and creep results for interblended fly ash mix

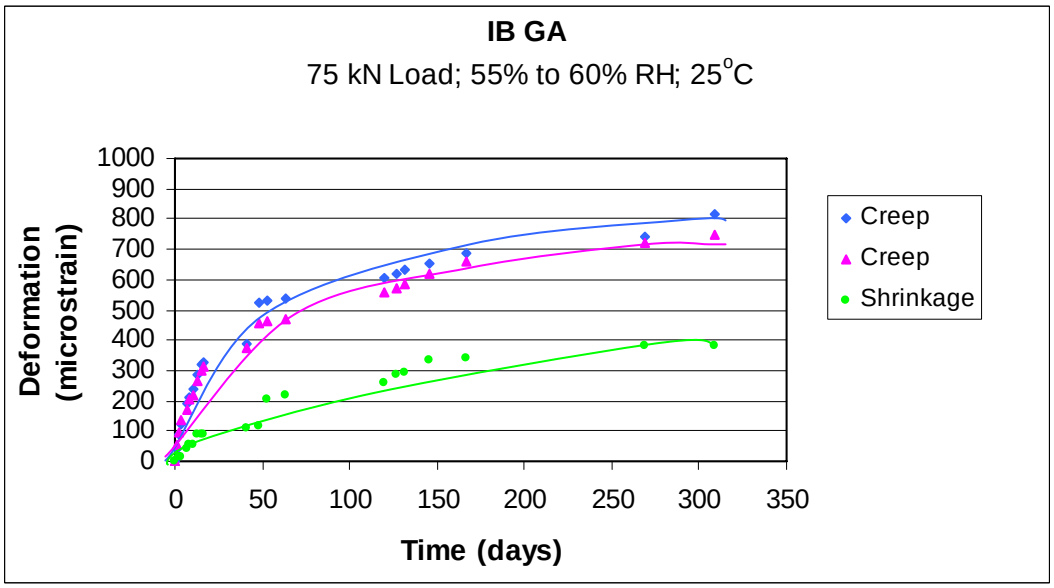

Figure 7.7 Shrinkage and creep results for interblended gasification ash mix

Creep of concrete is load induced, and is influenced by factors associated with the application of load and the ability of the concrete to withstand the load. The potential of the concrete to creep is determined by mix materials and proportions of the concrete.

Table 7.3 indicate that interground and interblended gasification ash mixes had higher creep values than the interblended fly ash mix. The difference in the creep values are however not considerable (see figure 7.5, 7.6 and 7.7). The results for creep indicate the gasification ash did not creep significantly more than fly ash.

Figure 7.8 indicate the specific creep (See Appendix K) for the three mixes. It is observed that over time the specific creep for the three mixes is approximately the same. The specific creep results indicate that gasification ash has a specific creep similar to fly ash.

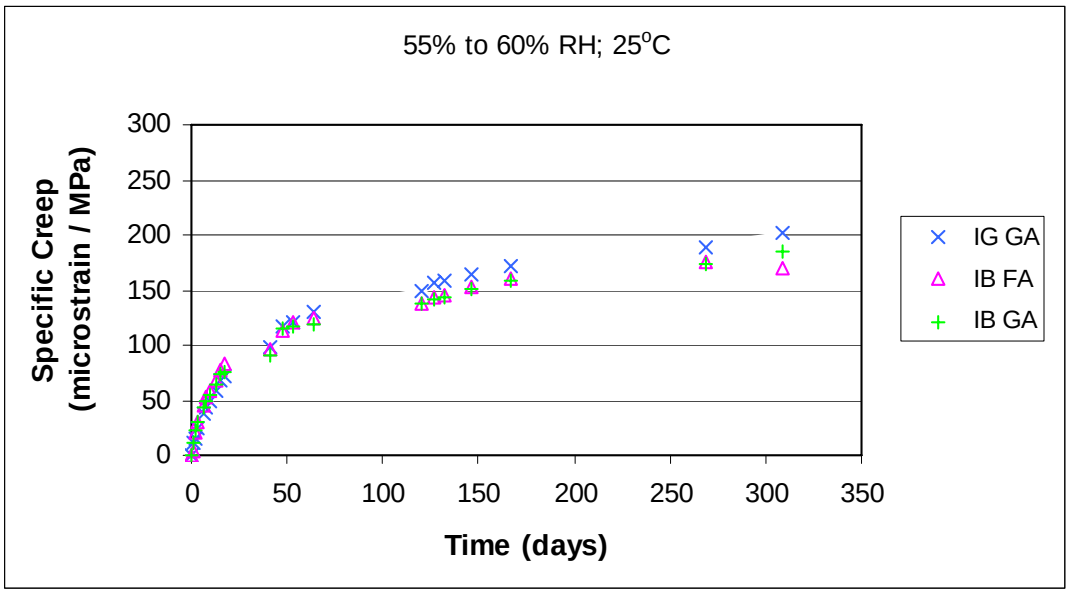

Figure 7.8 Specific creep results for the three different mixes

7.5 DURABILITY TESTS

7.5.1 Porosity Test Results

It can be observed from Figure 7.7 that for interblending the porosity of the gasification ash was lower than fly ash. This is due to a finer particle size of the gasification ash than the fly ash, which results in a more even distribution of solid particles in the concrete.

The concrete mix interblended with fly ash has the highest porosity, which shows that the cement particles did not disperse uniformly through the water resulting in agglomerations and leaving large spaces which do not contain cement. These spaces form capillary pores and entrain air. The result of this is a lower strength of the concrete. The intergrinding with fly ash had a finer particle size and results in a lower porosity. Interblending with gasification ash had a slightly higher porosity than the intergrinding with gasification ash; this could be due to better interlocking of particles grinded together. See Appendix L for Porosity summary.

The difference in porosity between all three mixes is between 15% and 16%. Porosity values (British Concrete Society, 2000) for a highly porous concrete is greater than 15%. Al three of the mixes fall into this category and thus the difference in results is omissible. The results indicate that the use of gasification ash as cement extender does not results in an increase in porosity. It is therefore anticipated that the concrete containing gasification ash will be no less durable than concrete currently manufactured.

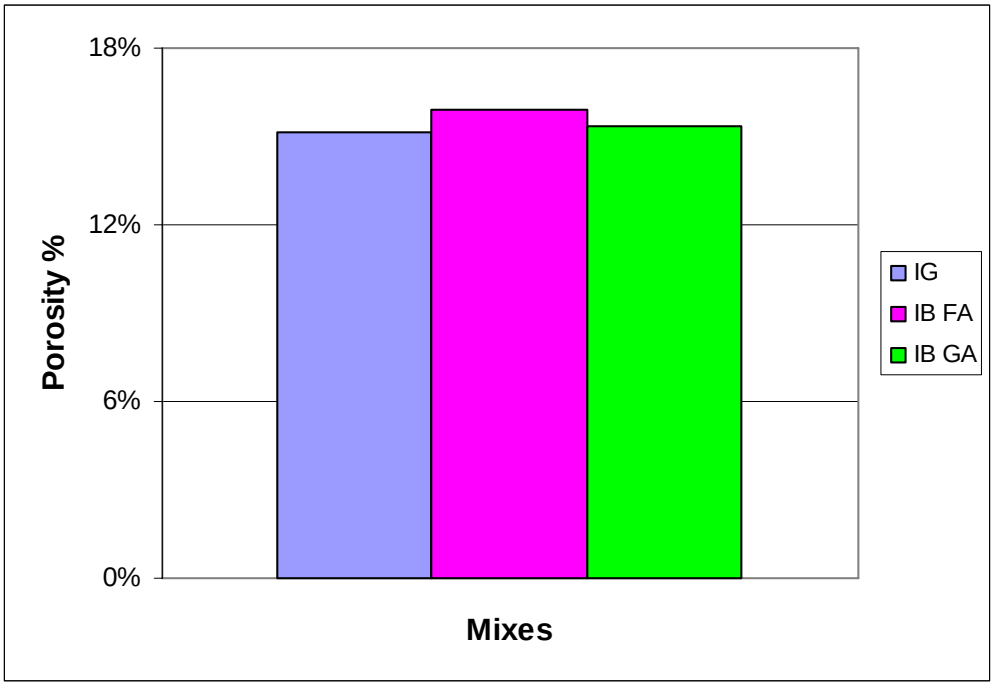

Figure 7.7 Porosity results of concrete mixes

7.5.2 Oxygen Permeability Test Results

The results of the permeability test (as indicated in figure 7.8) show that the type of ash used did not affect the permeability of mixes. The mix interblended with fly ash achieved the lowest permeability. High permeability is due to a poor quality of cement paste-aggregate interface. Fly ash has the effect of reducing the permeability, which is observed from the results. Intergrinding had the highest permeability and would absorb the most water. See Appendix M for Permeability calculations.

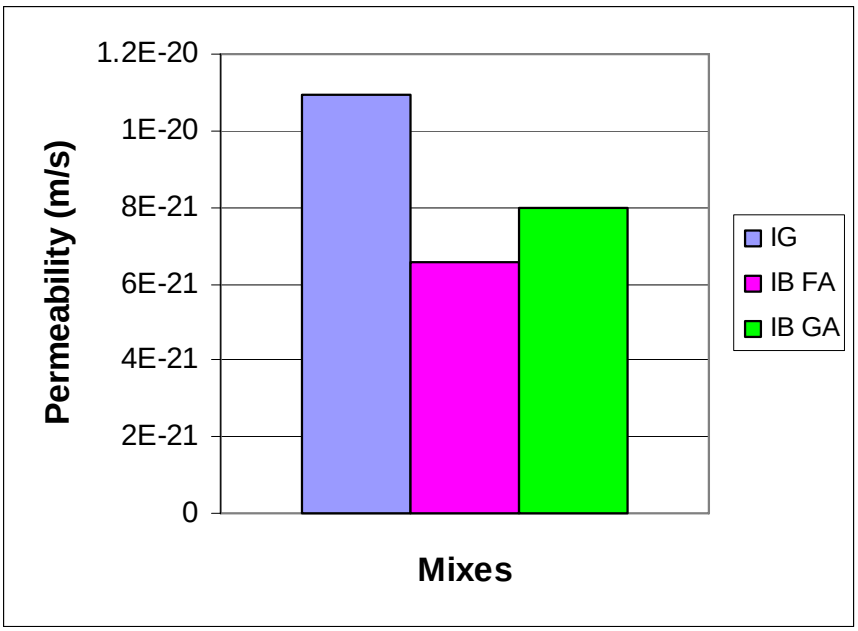

Figure 7.8 Oxygen permeability test results for concrete mixes

Permeability values (British Concrete Society, 2000) for a good quality concrete with a low permeability is smaller than 2×10^{-18} and all of the results fall into this category. OPI values as seen in Figure 7.9 indicate an excellent class of durability for concrete with a greater than 10 OPI (Alexander, 1999). These results indicate that the use of gasification ash in concrete achieves a low permeability and a durable concrete can be expected.

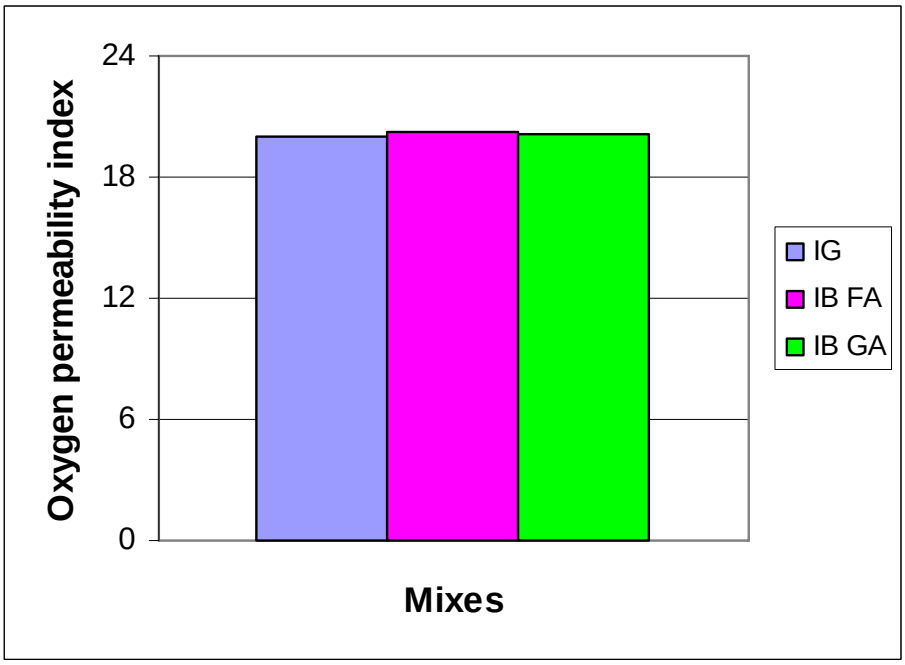

Figure 7.9 Oxygen permeability index results for the concrete mixes.

7.6 CONCLUSION

- The use of gasification ash as a cement extender in concrete would have ecological and economical benefits in the cement industry.
- The slump test results indicate that the use of gasification ash as cement extender will results in a reduction in the workability of concrete.
- The use of gasification ash as cement extender does not have a negative impact on the strength development of concrete. There was no reduction in the tensile strength of concrete.
- The use of gasification ash as cement extender does not have a detrimental effect on the stiffness of concrete.
- The results for shrinkage indicate the gasification ash did not shrink significantly more than fly ash. Creep results indicate that gasification ash did not creep significantly more than fly ash. The specific creep results indicate that gasification ash has a specific creep similar to fly ash.

- The results indicate that the use of gasification ash as cement extender does not results in an increase in porosity. It is therefore anticipated that the concrete containing gasification ash will be no less durable than concrete currently manufactured.
- The use of gasification ash in concrete achieves a low permeability and a durable concrete can be expected.

8. CONCLUSIONS AND RECOMMENDATIONS

8.1 CONCLUSIONS

The aim of the research is fulfilled and explained by giving consideration to each of the following conclusions.

Investigating the physical, chemical and mineralogical composition of a gasification ash sample had the following results:

- The gasification ash has no unique structure and could be described as angular.
- The chemical and mineralogical composition of gasification ash indicates that the ash have similar elements than fly ash and is within the allowable range for use as a cement extender in cement and concrete.
- The physical properties of gasification ash indicated that the gasification ash, ground separate and interground with cement in the ball mill had similar particle size distributions. There is a considerable difference in particle size between the gasification ash and cement ground separately for the same time interval. This indicates that the cement clinker is harder than the gasification ash clinker.
- The position parameter (X_o) and therefore the particle size distribution decrease as the grinding time increases for gasification ash.

Investigating the physical properties of cement manufacturing with specific reference to grinding time, the optimisation of gypsum, specific surface area and particle size distribution had the following results:

- It seems as if an optimum grinding time can be established. For both the intergrinding and gasification ash this optimum seems to be in the region of 2 hours.
- The compressive strength, flexural strength, particle size and Rosin-Rammler distribution parameters clearly indicate than grinding time should not be shorter than 2 hours for interblending and intergrinding of gasification ash and cement.
- It can be deduced that a 2.5% gypsum addition is a good average to use in further testing when heat of hydration and compressive strength is considered.

The effect of replacement level on the properties of interblended and interground gasification ash and cement shows that:

- The compressive strength, flexural strength, particle size and Rosin-Rammler distribution parameters confirm that replacement levels of gasification ash should range between 10% and 35%.
- The cement manufactured in the lab performed similar in strength development to the commercially available CEM I 42.5R but lower heat of hydration temperatures is observed for the cement manufactured in the lab.
- Intergrinding of gasification ash and cement in the ball mill is in my opinion better than interblending gasification ash and cement in the mixer.

The effect of interblended and interground gasification ash and cement on the short and long term properties of concrete had the following results:

- The use of gasification ash as a cement extender in concrete would have ecological and economical benefits in the cement industry.

- The slump test results indicate that the use of gasification ash as cement extender will results in a reduction in the workability of concrete.
- The use of gasification ash as cement extender does not have a negative impact on the strength development of concrete. There was no reduction in the tensile strength of concrete.
- The use of gasification ash as cement extender does not have a detrimental effect on the stiffness of concrete.

- The results for shrinkage indicate the gasification ash did not shrink significantly more than fly ash. Creep results indicate that gasification ash did not creep significantly more than fly ash. The specific creep results indicate that gasification ash has a specific creep similar to fly ash.

The effect of the gasification ash on the durability of concrete showed:

- The use of gasification ash as cement extender does not results in an increase in porosity. It is therefore anticipated that the concrete containing gasification ash will be no less durable than concrete currently manufactured.
- The use of gasification ash in concrete achieves a low permeability and a durable concrete can be expected.
- Gasification ash can be used as a cement extended in concrete.

8.2 RECOMMENDATIONS

- The environmental impact of decreasing CO_2 in the manufacturing of cement can benefit from using gasification ash as a cement extender.

- The use of gasification ash as a cement extender in concrete is highly recommended due to characteristics like increased strength development and reduced permeability.

- The effect of variability in chemical properties of gasification ash should be further investigated.

- The effect of admixtures on gasification ash could influence the water demand of concrete and cause concrete to be expensive.

- Long term testing should be done on gasification ash to determine the effect on concrete durability.

- Testing should be repeated on gasification ash to determine a trend for the behavior of gasification ash when used as a cement extender in concrete.

- The grinding times and results are not necessarily the only answer since the laboratory equipment has a influence on this.

9. REFERENCES

ACI Committee 232.1R-94. Use of Natural Pozzolans in Concrete. ACI Journal, February 1995,

Addis, B.J. and Owens, G. 2001. Fulton's Concrete Technology. Eight Edition. Cement and Concrete Institute. Midrand, South Africa.

Alexander, M.G Mackechnie, J.R and Ballim, Y. Guide to the use of durability indexes for achieving durability in concrete structures. University of Cape Town and University of Witwatersrand. Research Monograph No.2. Cape Town. 1999.

American Coal Ash Association. 1997. Coal combustion Product-Production and Use. Alexandria. Virginia.

ASTM C 469-02. Standard test method for static modulus of elasticity and poisson's ratio of concrete in compression. West Conshohocken. American Society for Testing and Materials. 2002.

ASTM C 512-02. Standard test method for Creep of Concrete in Compression. American Society for Testing Materials. West Conshohocken. Pennsylvania. 2002.

ASTM C 1861-97. Standard Guide for Use of Coal Combustion By-Products in Structural Fills. American Society for Testing Materials. West Conshohocken. Pennsylvania. 2002.

Babcock and Wilcox. 1978. Steam. Its Generation and Use. New York, NY.

Badenhorst, S. 2003. A Critical review of concrete drying shrinkage, test methods, factors influencing and shrinkage prediction. Johannesbug. University of the Witwatersrand. July 2003. (MSc Project Report).

Ballim, Y. 1999. Localising international concrete models – the case of creep and shrinkage prediction. Proceedings of the 5th International conference on concrete technology for developing countries. New Delhi. Volume 1. Pt 7. November 1999. pp 66-78.

Bhatty, J.I. Miller, F.M. and Kosmatka, S.H. 2004. Innovations in Portland Cement Manufacturing. Portland Cement Association. Illinois.

Bouzoubaâ, N. Zhang, M.H. Bilodeau, A. and Malhotra, V.M. 1997. The effect of grinding on the physical properties of fly ashes and a Portland cement clinker. Cement and Concrete Research. Volume 27, Number. 12. pp 1862 – 1874.

British Concrete Society. 2000. British Concrete Society technical report number 54. Diagnosis of deterioration in concrete structures. Identification of defects, evaluation and development of remedial action. Concrete Society. London.

Brown, J.H. 1982. The strength and workability of concrete with PFA substitution. In Proceedings, International Symposium on the Use of PFA in Concrete. University of Leeds, UK. Apr 14-16. Edited by J.G. Cabrera and A.R. Cusens. Department of Civil Engineering. University of Leeds, Leeds, UK. pp 151-161.

Bye, G.C. Portland cement. 1999. Composition, production and properties. 2nd edition. Thomas Telford.

Carette, G.G and Malhotra, V.M. 1986. Characterization of Canadian fly ashes and their relative performance in concrete. Energy, Mines and Resources Canada. CENMET Report 86-6E. Ottawa. ON.

Chindaprasirt, P. Homwuttiwong, S and Sirivivatnanon, V. 2004. Influence of fly ash fineness on strength, drying shrinkage and sulphate resistance of blended cement mortar. Cement and Concrete Research. Volume 34. pp 1087 – 1092.

Davis, R.E Carlson, R.W Kelly, J.W and Davis, H.E. 1937. Properties of cements and concretes containing fly ash. Journal of the American Concrete Institute, Volume 33, pp 577-612.

Diamond, S. and Lopez-Flores, F. 1981. On the distribution between physical and chemical characteristics between lignitic and bituminous fly ashes. Proceedings, Symposium on Effects of Fly Ash Incorporated in Cement and Concrete. Edited by S. Diamond. Materials Research Society. Boston, MA. pp 34-44.

Erdogdu, K. Tokyay M. and Türker, P. 1999.Comparison of intergrinding and separate grinding for the production of natural pozzolan and GBFS-incorporated blended cements. Cement and concrete research, Volume 29, pp 743-746.

Escalante-Garcia, and Sharp, J.H. 2004. The chemical composition and microstructure of hydration products in blended cements. Cement and concrete composites, Volume 26, pp 967-976.

Frigione, G. 1983. Gypsum in Cement. In: Ghosh SN ed. Cement Technology. Pergamon Press.New York. pp 485-535.

Frigione, G. and Mara, S. 1976. Relationship between particle size distribution and compressive strength in Protland Cement. Cement and Concrete Research. Volume 6. pp 113-128.

Ghosh, R.S. and Timusk, J. 1981. Creep of fly ash concrete. Journal of the American Concrete Institute. Volume 87. pp 351-357.

Grieve, G.R.H. 1991. The influence of two South African fly ashes on the engineering properties of concrete. PhD thesis. Johannesburg. Univeristy of the Witwatersrand.

Hect, N.L. and Duvall, D.S. 1975. Characterisation and Utilization of Municipal and Utility Sludges and Ashes: Volume III–Utility Coal Ash. National Environmental Research Center. U.S. Environmental Protection Agency.

Holcim. 2005. Materials Handbook. Holcim South Africa.

Illston, J.M. and Domone, P.L.J. 2001. Construction Materials. Their nature and behaviour. Third Edition. Spon Press, London.

Joshi, R.C. 1982. Effect of coarse fraction (+ #325) of fly ash on concrete properties. In Proceedings, 6th International Symposium on Fly Ash Utilization. Reno, NV. March 1982. U.S. Department of the Environment. Washington, DC. DOE/METC/82-52. pp 77-85.

Krüger, J.E. 1999. Guide 2: Origin, History and Properties of South African Fly Ash and Portland Fly Ash Cements. Guides on the use of South African fly ash as a cement extender. The South African Coal Ash Association, South Africa.

Lane, R.O. and Best, J.F. 1982.Properties and use of fly ash on Portland cement concrete. Concrete International. Volume 4, Number 7. pp 81-92.

Lea FM. 1970. Chemistry of cement and concrete. 4th ed. Edward Arnold Publishers Ltd. Great Britain.

Lee, S.H. Kim, H.J. Sakai, E and Daimon, M. 2003. Effect of particle size distribution of fly ash-cement system on the fluidity of cement pastes. Cement and concrete research, Volume 33, pp 763-768.

Lerch, W. 1946. The influence of gypsum on the hydration and properties of Portland cement pastes. PCA Bulletin. Number 12.

Locher, F.W. Sprung, S. and Korf, P. 1973. The effect of particle size distribution on the strength of Portland cement. Zement-Kalk-Gips. Volume 26. pp 349-355.

Massazza, F. 1998. Chemical analysis of Portland cements. Chapter 4: Lea's Chemistry of Cement and Concrete, Fourth Edition, Edited by Hewlett, P.C. Arnold, London.

Malhotra, V.M. and Mehta, P.J. 1996. Pozzolanic and Cementitious Materials. First Edition. Gordon and Breach Publishers, Amsterdam.

Metha, P.K. 1989. Pozzolanic and cementitious by-products in concrete – Another look. Proceedings, 3rd CANMET/ACI International Conference on the use of Fly Ash, Silica Fume, Slag and Other Mineral By-Products in Concrete, Trondheim, Norway. June 18-23. Edited by V.M. Malhorta. American Concrete Institute. Detroit, MI. Special Publication SP-114, Volume 1, pp 1-43.

Naik, T.R. and Ramme, B.W. 1990. Effect of high-lime fly ash content on water demand, time of set and compressive strength of concrete. ACI Materials Journal. Volume 87. pp 619-626.

Neville, A.M. 1995. Properties of Concrete. Fourth Edition. Longman Group Ltd. London.

Newman, J. 2003. Advanced concrete technology. Elsevier Ltd.

Olorunsogo, F.T. 1990. Effect of particle size distribution of ground granulated blast furnace slag on some properties of slag cement mortar. PhD thesis, University of Leeds.

Owens, P.L. 1979. Fly ash and its usage in concrete. Concrete: The Journal of the Concrete Society. Volume 13. pp 21-26.

Pandey, S.P. 1983. The Particle Size Distribution Analysis: Science and Applications in Cement Technology. In: Ghosh SN ed. Cement Technology. Pergamon Press.New York. pp 735-775.

Rosin, P. and Rammler, E. 1933. The laws governing the fineness of powdered coal. Journal of the Institute of Fuel. Volume 7. pp 29-33.

Sandberg, P. 2005. The use of Isothermal calorimetry to optimise cement sulphate Part 1 – Cement without admixtures. Internal Document. Grace Construction Products.

SANS 1491/SABS 1491:1989. Portland cement extenders, Part 1: Ground granulated blastfurnace slag, Part 2: Silica fume, Part 3: Fly ash. South African Bureau of Standards. Pretoria.

SANS 50196-1/SABS 196-1:1994. Methods of testing cement, Part 1: Determination of strength. South African Bureau of Standards. Pretoria.

SANS 50196-2/SABS 196-1:1994. Methods of testing cement, Part 1: Sulphur trioxide content and loss on ignition. South African Bureau of Standards. Pretoria.

SANS 50196-3/SABS 196-1:1994. Methods of testing cement, Part 1: Soundness. South African Bureau of Standards. Pretoria.

SANS 50197-1/SABS 197-1:2000. Cement Part 1: Composition, specification and conformity criteria for common cements. South African Bureau of Standards. Pretoria.

SANS 5862/SABS SM 862:1994. Concrete tests – Consistence of freshly mixed concrete, Part 1: Slump tests, Part 2: Flow test, Part 3: Vebe test, Part 4: Compacting factor and compaction index. South African Bureau of Standards. Pretoria.

SANS 5863/SABS Method 863-1994. Concrete tests – Compressive strength of hardened concrete. 1st Revision. South African Bureau of Standards. Pretoria.

SANS 6151/SABS Method 863-1994. Freewater content of Portland cement extenders. 1st Revision. South African Bureau of Standards. Pretoria.

SANS 6156/SABS Method 863-1994. Water requirement of Portland cement extenders. 1st Revision. South African Bureau of Standards. Pretoria.

SANS 6157/SABS Method 863-1994. Fineness of cement and Portland cement extenders. 1st Revision. South African Bureau of Standards. Pretoria.

SANS 6253/SABS Method 863-1994. Concrete tests – Compressive strength of hardened concrete. 1st Revision. South African Bureau of Standards. Pretoria.

Schwartz, K.P. 2003. The outlook for CCPs. Electric Perspectives. July/August 2003.

Steffan, P. and Dean, G. 1991. FGD Gypsum Utilization: Survey of current practices and Assessment of Market Potential. Proceedings, Air Waste Management Conference. p. 1.

Tang, F.J. and Gartner, E.M. 1988. Influences of Sulphate Source on Portland Cement Hydration. Advances in Cement Research. Volume 1. Number 2. April 1988.

Taylor, H.F.W. 1982. Cement Chemistry, 2nd ed. Telford. Reprinted 1982.

Uchikawa, H. 1986. Effect of blending components on hydration and structure formation. Proceedings, 8th International Congress on the Chemistry of Cements. Rio de Janeiro, Brazil. Sept, 22-27. Specials Report Volume 1.

Van Dyk, J.C. Keyser, M.J. and Coertzen, M. 2005. World of Coal Ash Conference. SASOL's unique position in SYNGAS Production in South Africa. Coal Sources using SASOL Lurgi Fixed Bed Dry Bottom Gasifiers. Paper Presented.

Wainwright, P.J. and Olorunsogo, F.T. 1999. Effects of PSD of GGBS on some durability properties of slag cement mortars. Journal of the South African Institution of Civil Engineering. Volume 41, Number 1 First Quarter 1999. pp 9-17.

Wainwright, P.J. 2004. Portland Cement. School of Civil Engineering. University of Leeds. Lecturer Notes.

www.wbcsdcement.org, agenda for sustainable development. 2005.

Yuan, R.L and Cook, J.E. 1983. Study of Class C fly ash concrete. Fly Ash, Silica Fume, Slag and Other Mineral By-products in Concrete, first international conference. Montebello, Canada. SP-79. pp 307-319.

APPENDIX A

CUMULATIVE PARTICLE SIZE DISTRIBUTION OF GASIFICATION ASH, CEMENT AND GASIFICATION ASH AND CEMENT INTERGROUND AND INTERBLENDED

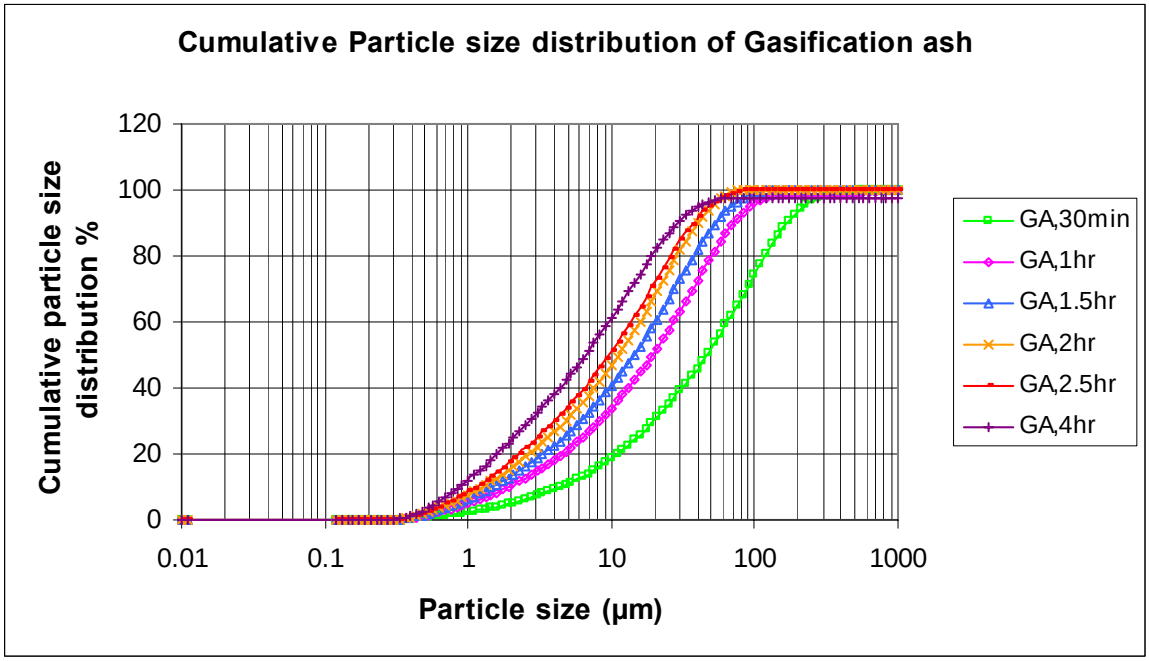
Cumulative Particle size distribution of Gasification ash
Cumulative particle size distribution %
120
100
80
60
40
20
0
0.01
0.1
1
10
100
1000
Particle size (µm)
GA,30min
GA,1hr
GA,1.5hr
GA,2hr
GA,2.5hr
GA,4hr

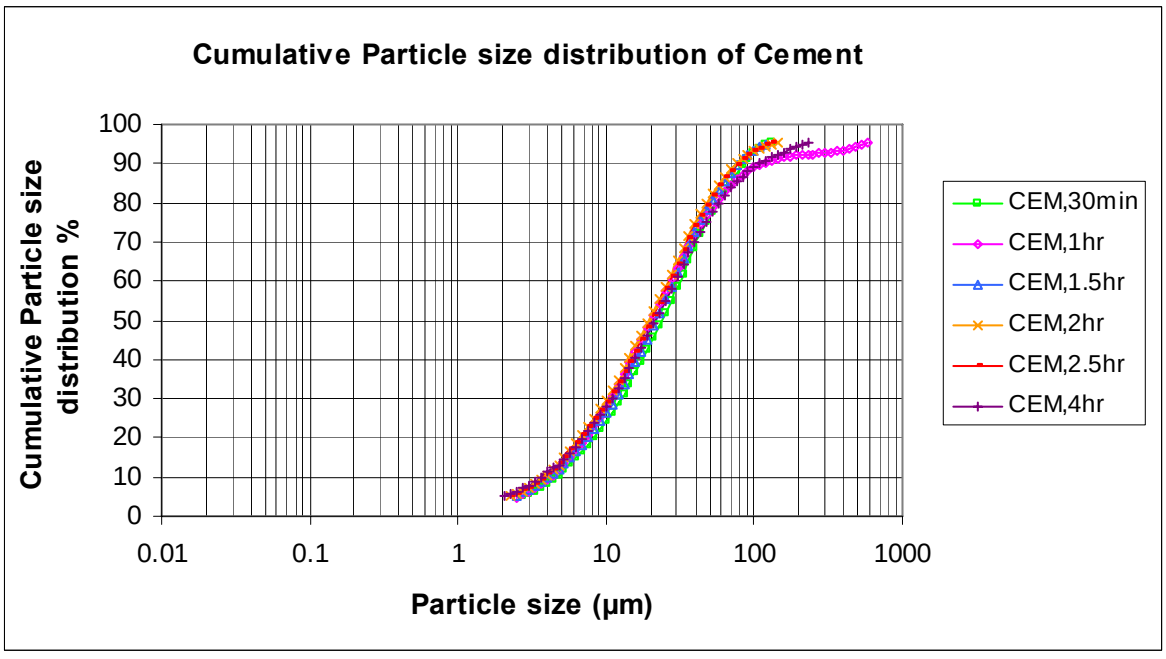
Cumulative Particle size distribution of Cement
Cumulative Particle size distribution %
100
90
80
70
60
50
40
30
20
10
0
0.01
0.1
1
10
100
1000
Particle size (µm)
CEM,30min
CEM,1hr
CEM,1.5hr
CEM,2hr
CEM,2.5hr
CEM,4hr

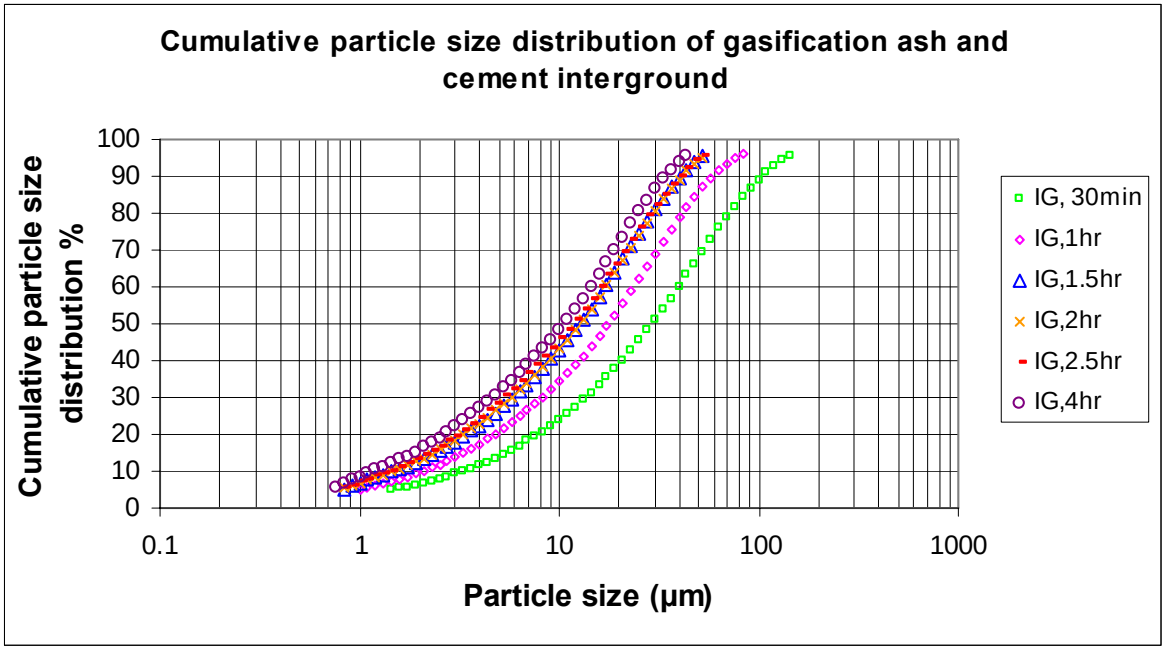
Cumulative particle size distribution of gasification ash and cement interground
Cumulative particle size distribution %
100
90
80
70
60
50
40
30
20
10
0
0.1
1
10
100
1000
Particle size (µm)
IG, 30min
IG,1hr
IG,1.5hr
IG,2hr
IG,2.5hr
IG,4hr

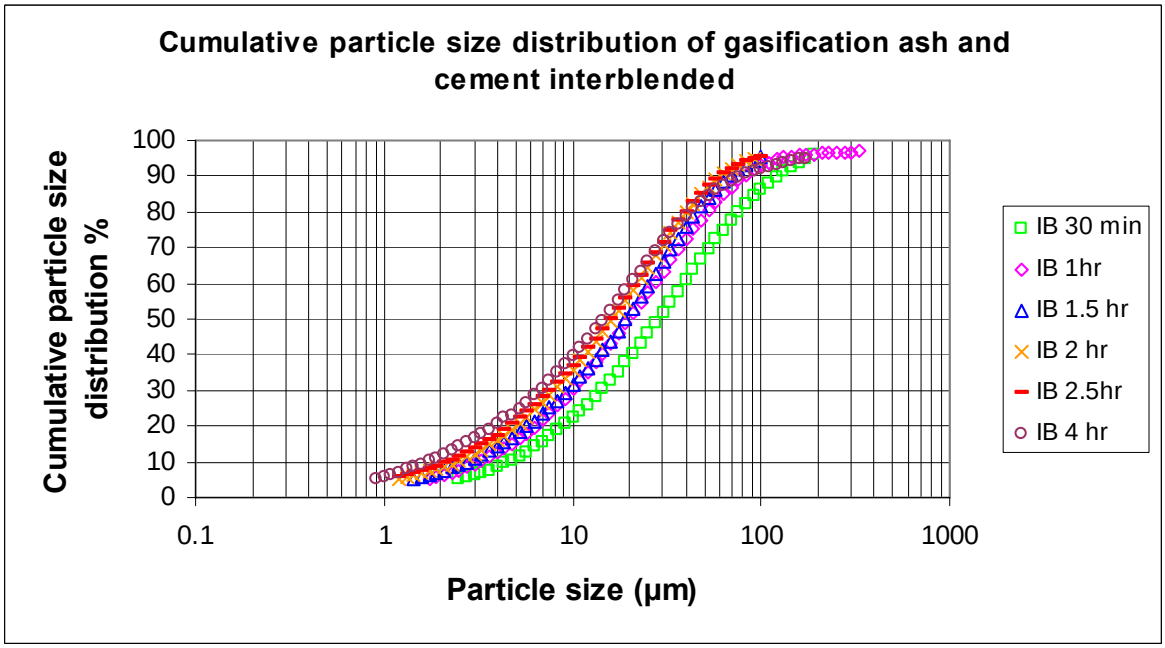
Cumulative particle size distribution of gasification ash and cement interblended
Cumulative particle size distribution %
100
90
80
70
60
50
40
30
20
10
0
0.1
1
10
100
1000
Particle size (µm)
IB 30 min
IB 1hr
IB 1.5 hr
IB 2 hr
IB 2.5hr
IB 4 hr

APPENDIX B

CUMULATIVE % OVERSIZE PARTICLE SIZE DISTRIBUTIONS FOR GASIFICATION ASH, CEMENT AND GASIFICATION ASH AND CEMENT INTERGROUND AND INTERBLENDED

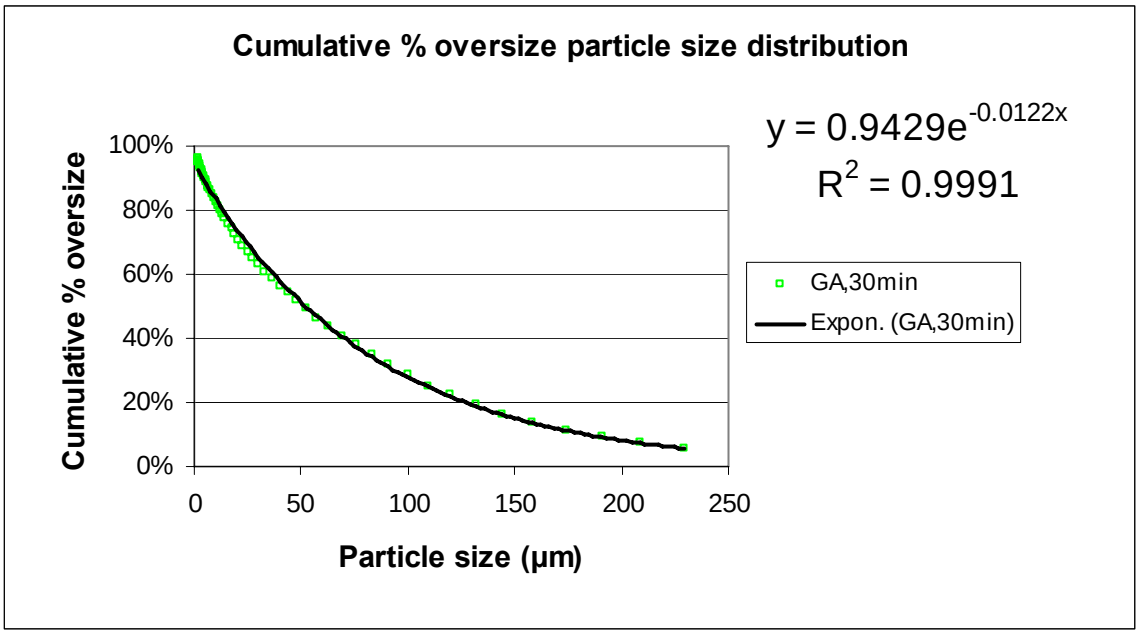
Cumulative % oversize particle size distribution
y = 0.9429e-0.0122x
R2 = 0.9991
Cumulative % oversize
100%
80%
60%
40%
20%
0%
0
50
100
150
200
250
Particle size (µm)
GA,30min
Expon. (GA,30min)

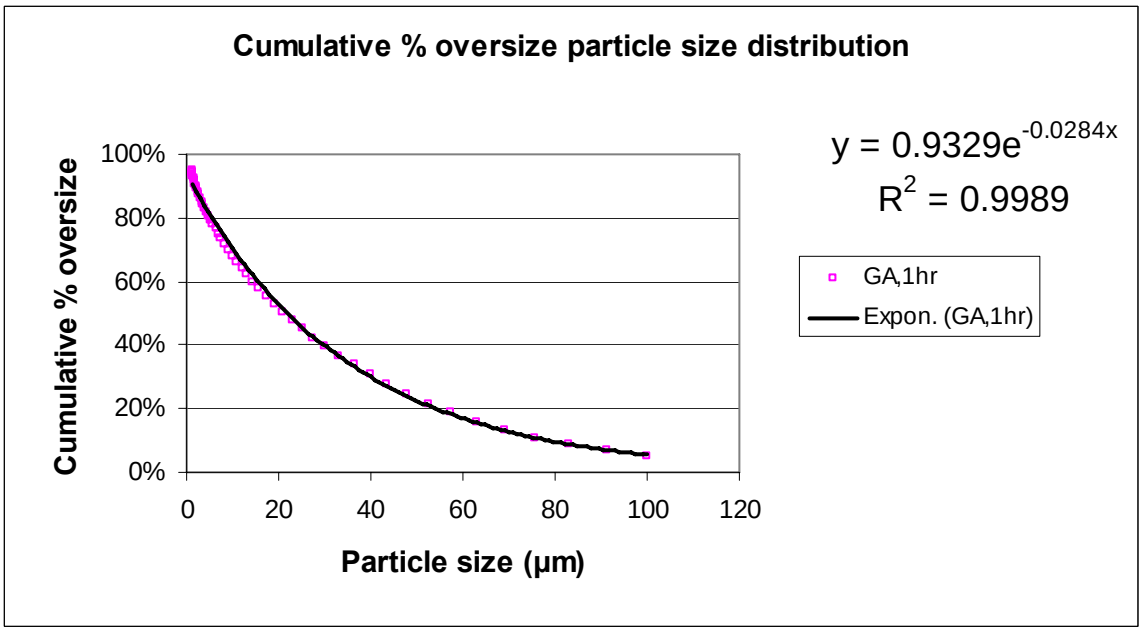
Cumulative % oversize particle size distribution
y = 0.9329e-0.0284x
R2 = 0.9989
Cumulative % oversize
100%
80%
60%
40%
20%
0%
0
20
40
60
80
100
120
Particle size (µm)
GA,1hr
Expon. (GA,1hr)

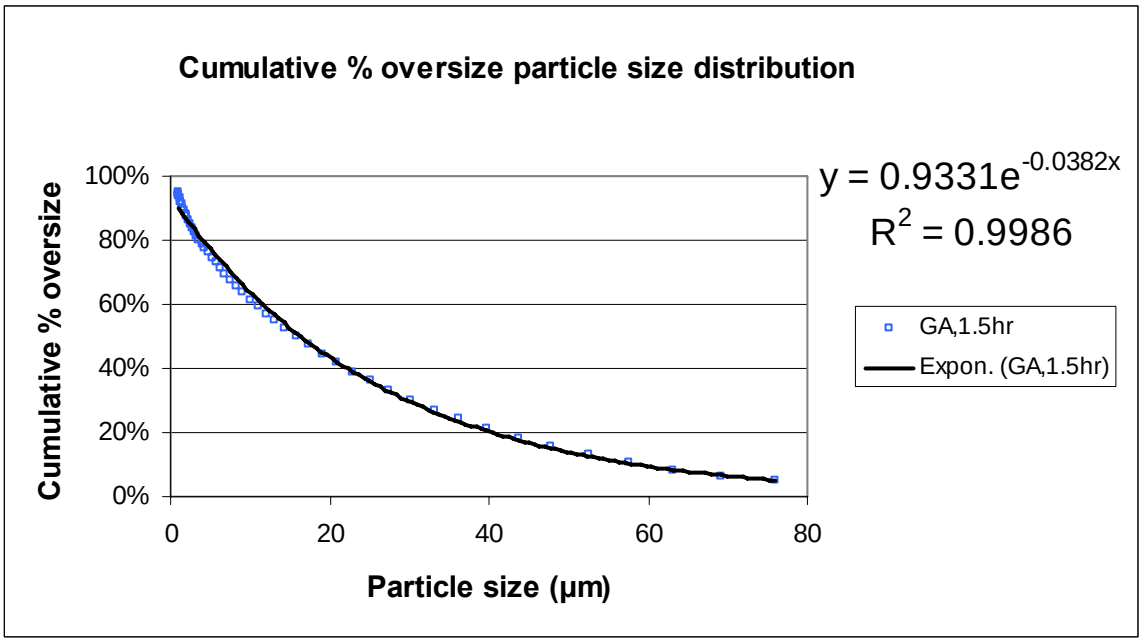
Cumulative % oversize particle size distribution
Cumulative % oversize
100%
80%
60%
40%
20%
0%
0
20
40
60
80
Particle size (µm)
y = 0.9331e-0.0382x
R2 = 0.9986
GA,1.5hr
Expon. (GA,1.5hr)

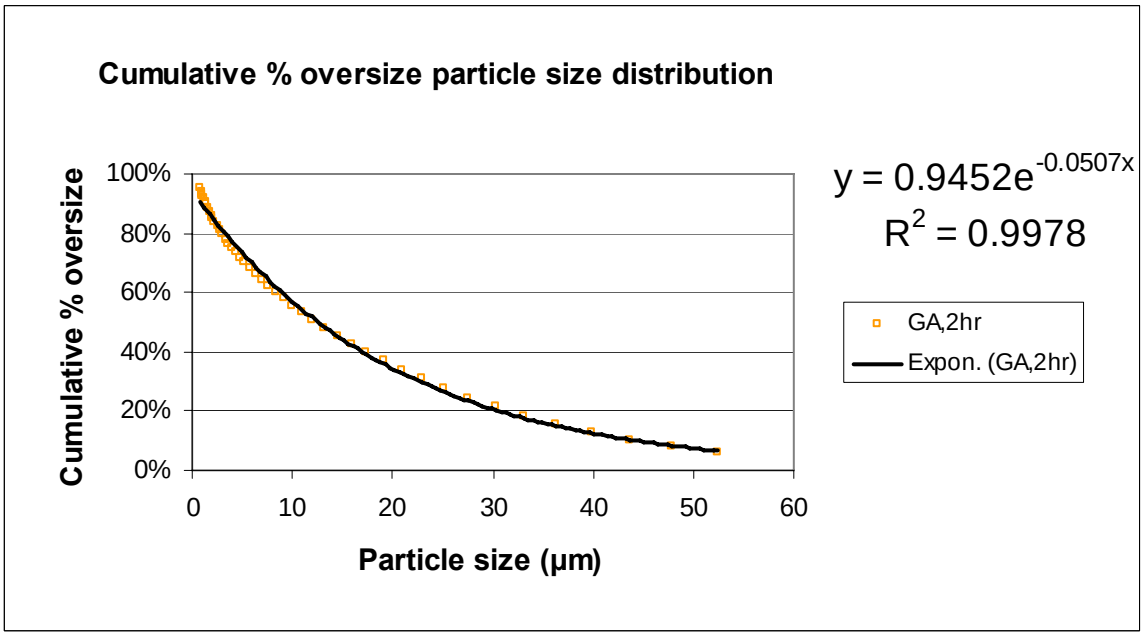
Cumulative % oversize particle size distribution
Cumulative % oversize
100%
80%
60%
40%
20%
0%
0
10
20
30
40
50
60
Particle size (µm)
y = 0.9452e-0.0507x
R2 = 0.9978
GA,2hr
Expon. (GA,2hr)

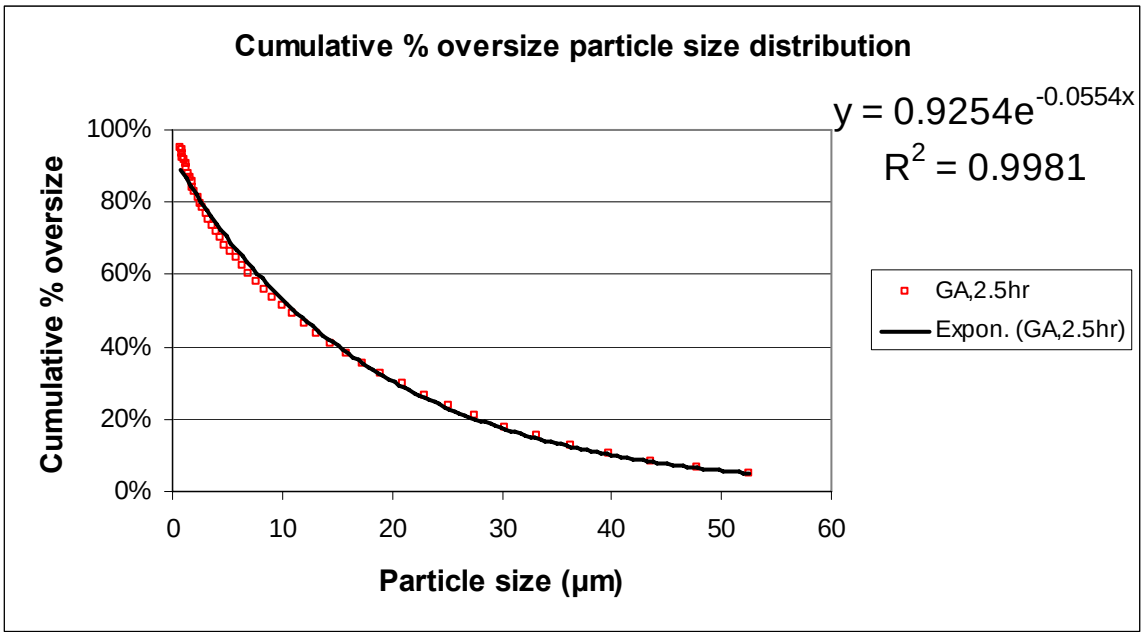
Cumulative % oversize particle size distribution
y = 0.9254e-0.0554x
R2 = 0.9981
Cumulative % oversize
100%
80%
60%
40%
20%
0%
0
10
20
30
40
50
60
Particle size (µm)
GA,2.5hr
Expon. (GA,2.5hr)

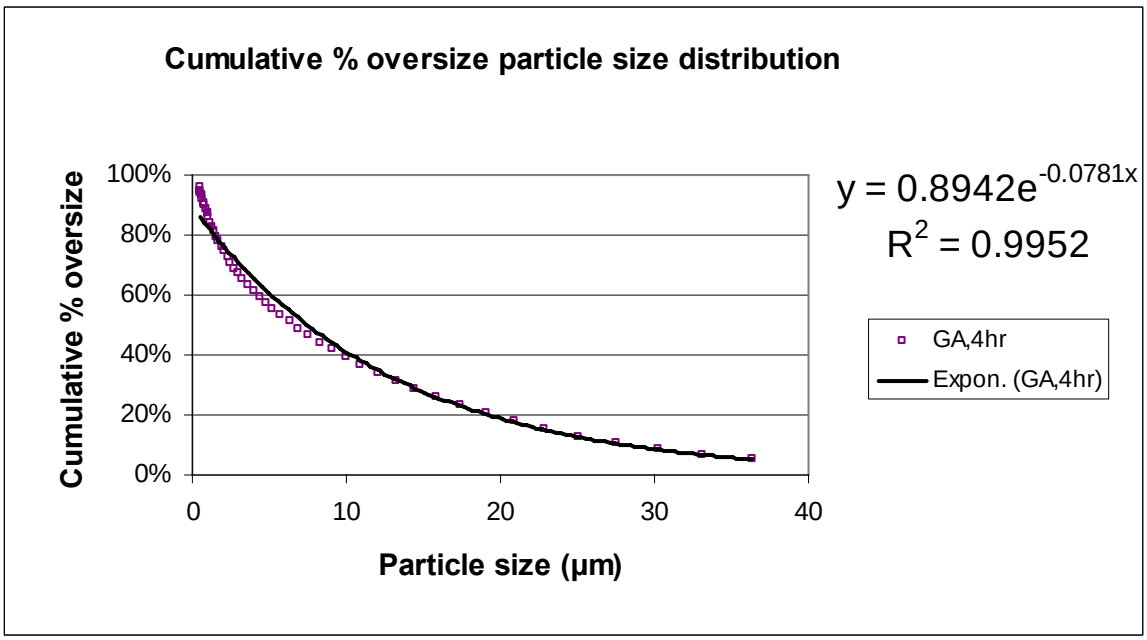
Cumulative % oversize particle size distribution
y = 0.8942e-0.0781x
R2 = 0.9952
Cumulative % oversize
100%
80%
60%
40%
20%
0%
0
10
20
30
40
Particle size (µm)
GA,4hr
Expon. (GA,4hr)

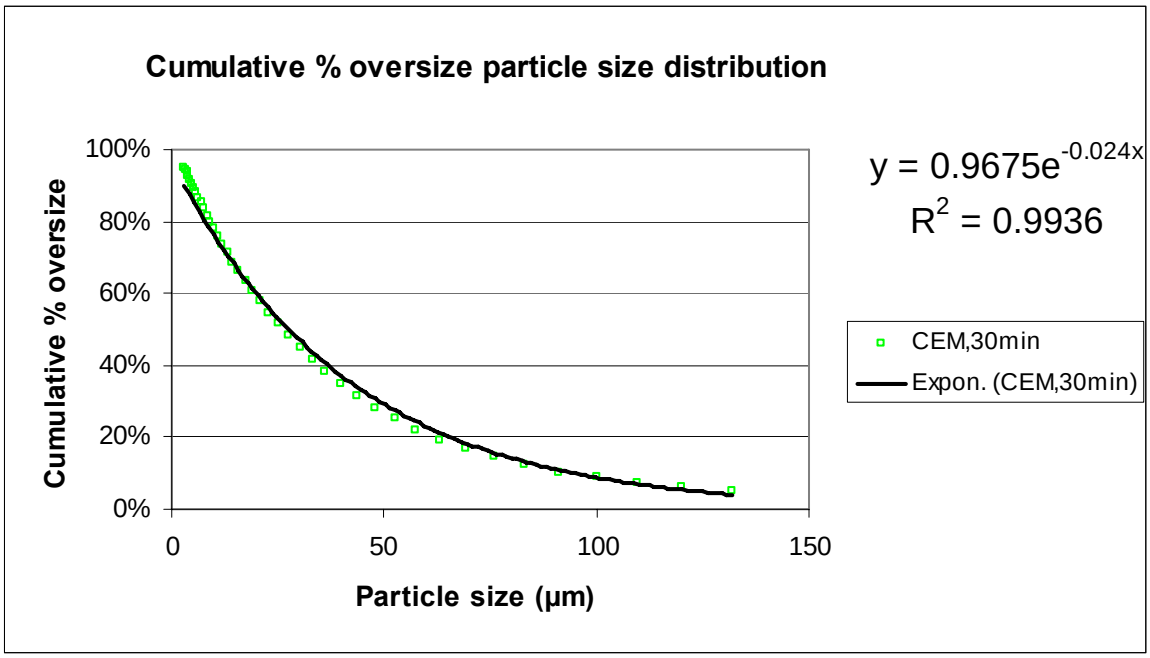
Cumulative % oversize particle size distribution
Cumulative % oversize
100%
80%
60%
40%
20%
0%
0
50
100
150
Particle size (µm)
y = 0.9675e-0.024x
R2 = 0.9936
CEM,30min
Expon. (CEM,30min)

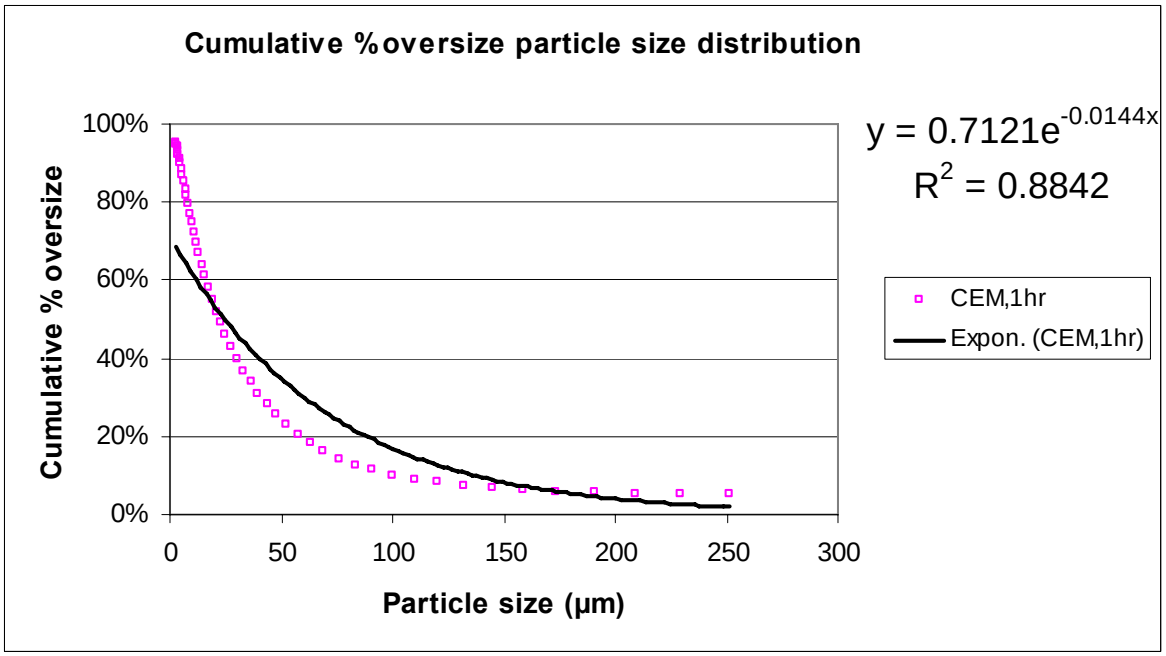
Cumulative %oversize particle size distribution
Cumulative % oversize
100%
80%
60%
40%
20%
0%
0
50
100
150
200
250
300
Particle size (µm)
y = 0.7121e-0.0144x
R2 = 0.8842
CEM,1hr
Expon. (CEM,1hr)

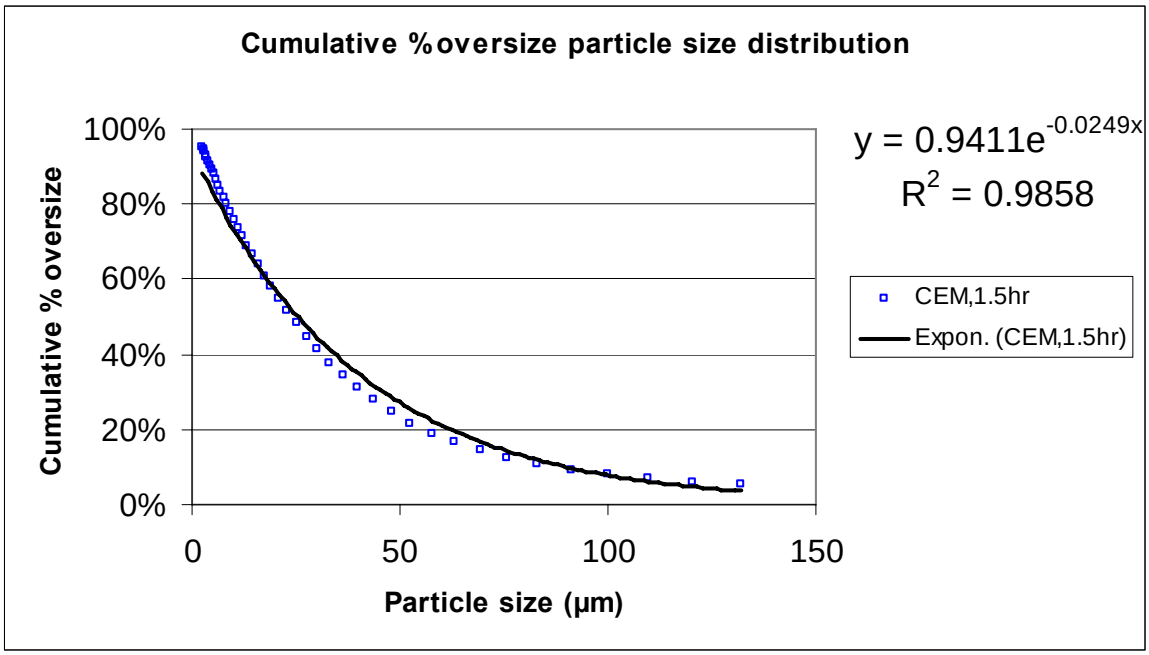
Cumulative %oversize particle size distribution
Cumulative % oversize
100%
80%
60%
40%
20%
0%
0
50
100
150
Particle size (µm)
y = 0.9411e-0.0249x
R2 = 0.9858
CEM,1.5hr
Expon. (CEM,1.5hr)

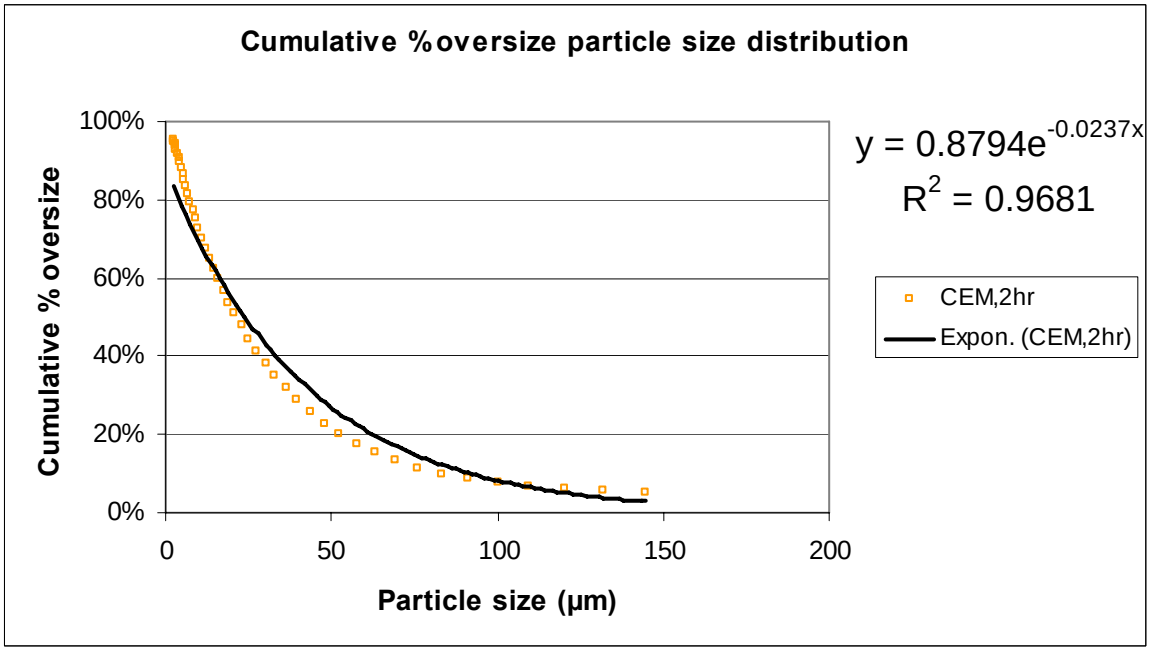
Cumulative %oversize particle size distribution
Cumulative % oversize
100%
80%
60%
40%
20%
0%
0
50
100
150
200
Particle size (µm)
y = 0.8794e-0.0237x
R2 = 0.9681
CEM,2hr
Expon. (CEM,2hr)

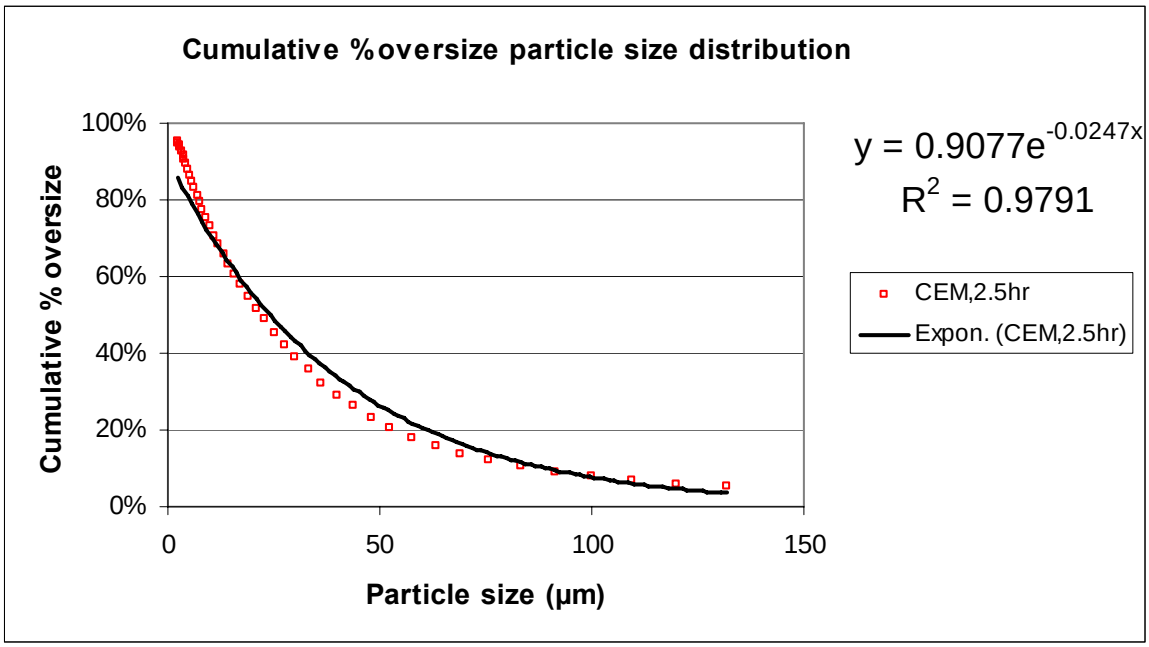
Cumulative %oversize particle size distribution
Cumulative % oversize
100%
80%
60%
40%
20%
0%
0
50
100
150
Particle size (µm)
y = 0.9077e-0.0247x
R2 = 0.9791
CEM,2.5hr
Expon. (CEM,2.5hr)

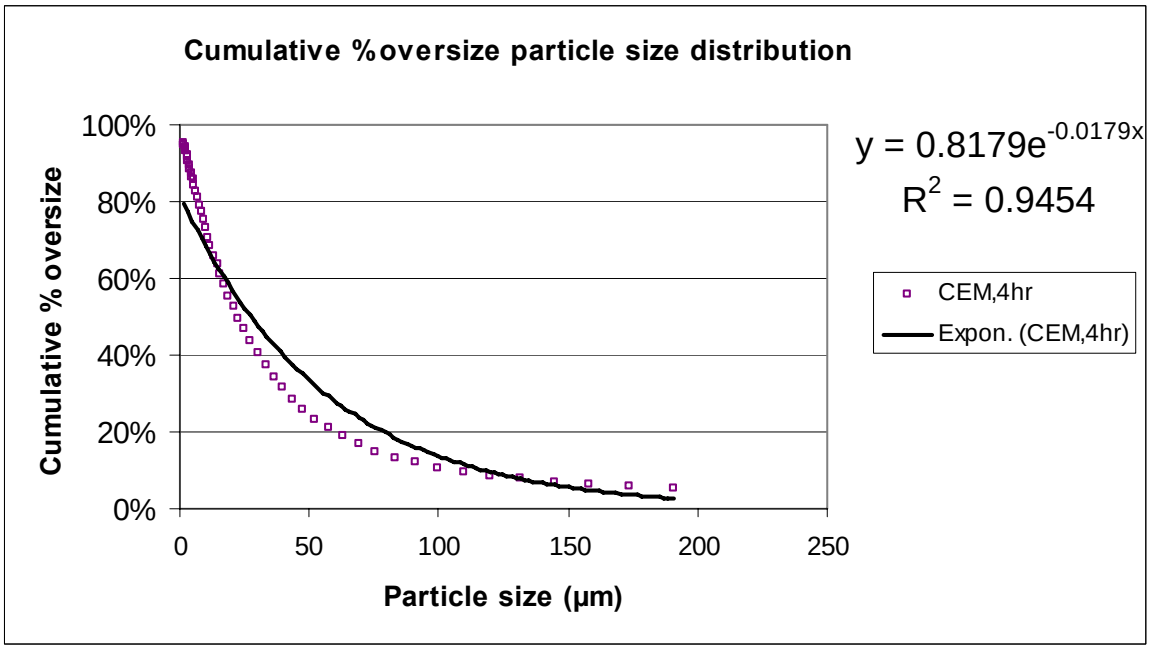
Cumulative %oversize particle size distribution
Cumulative % oversize
100%
80%
60%
40%
20%
0%
0
50
100
150
200
250
Particle size (µm)
y = 0.8179e-0.0179x
R2 = 0.9454
CEM,4hr
Expon. (CEM,4hr)

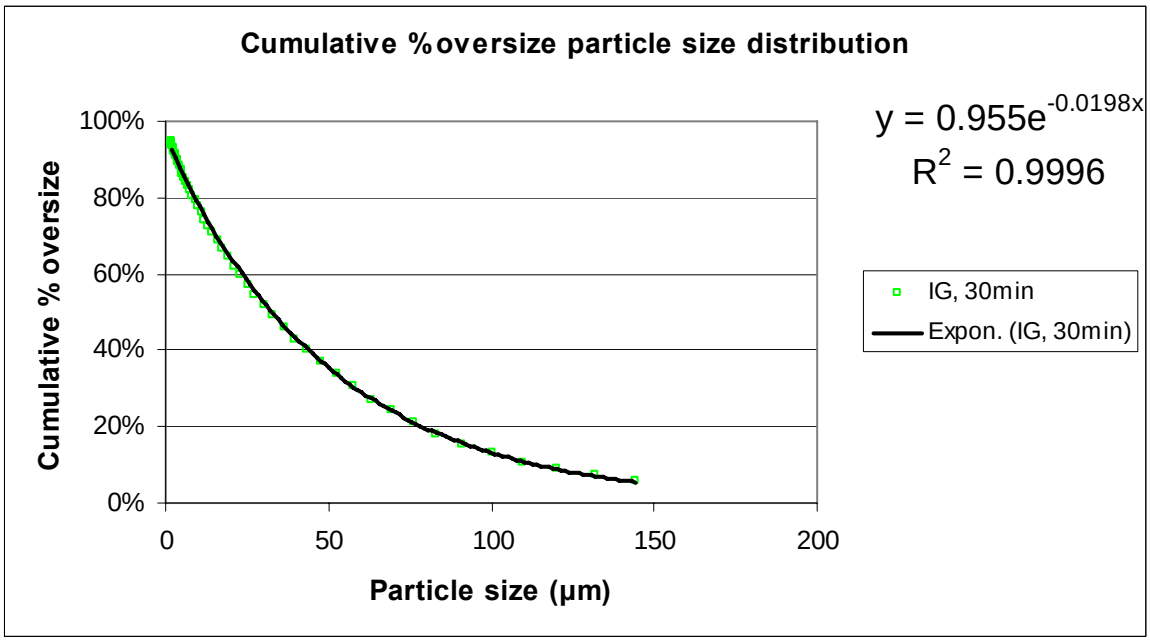
Cumulative %oversize particle size distribution
Cumulative % oversize
100%
80%
60%
40%
20%
0%
0
50
100
150
200
Particle size (µm)
y = 0.955e-0.0198x
R2 = 0.9996
IG, 30min
Expon. (IG, 30min)

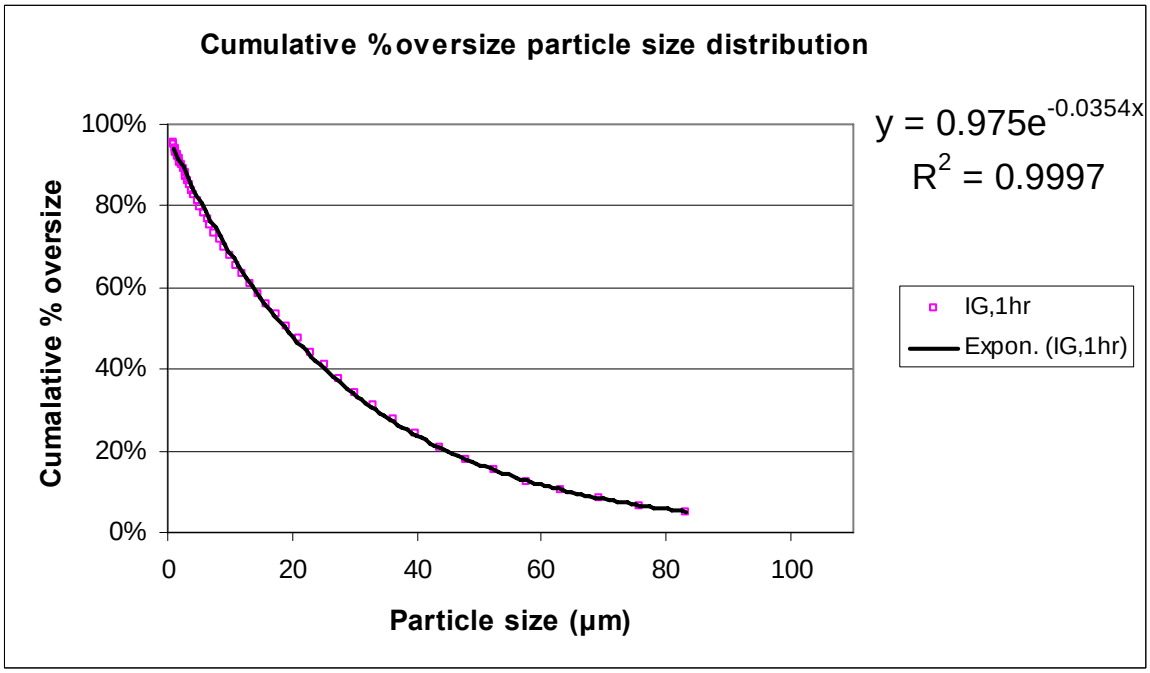
Cumulative %oversize particle size distribution
Cumalative % oversize
100%
80%
60%
40%
20%
0%
0
20
40
60
80
100
Particle size (µm)
y = 0.975e-0.0354x
R2 = 0.9997
IG,1hr
Expon. (IG,1hr)

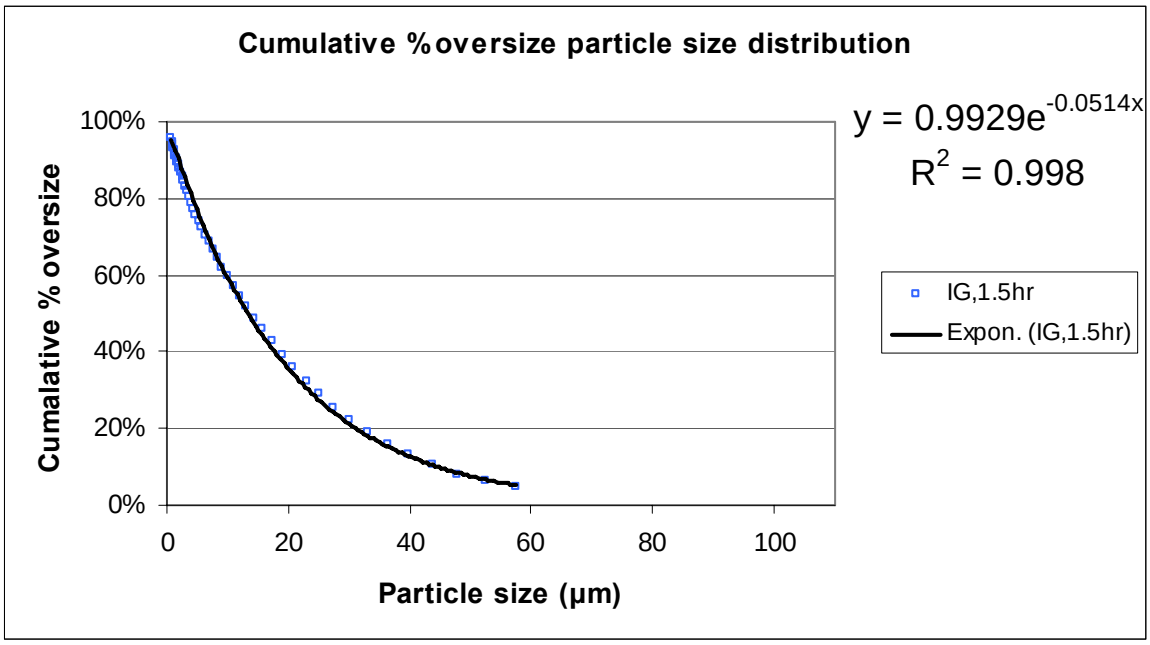
Cumulative %oversize particle size distribution
Cumalative % oversize
100%
80%
60%
40%
20%
0%
0
20
40
60
80
100
Particle size (µm)
y = 0.9929e-0.0514x
R2 = 0.998
IG,1.5hr
Expon. (IG,1.5hr)

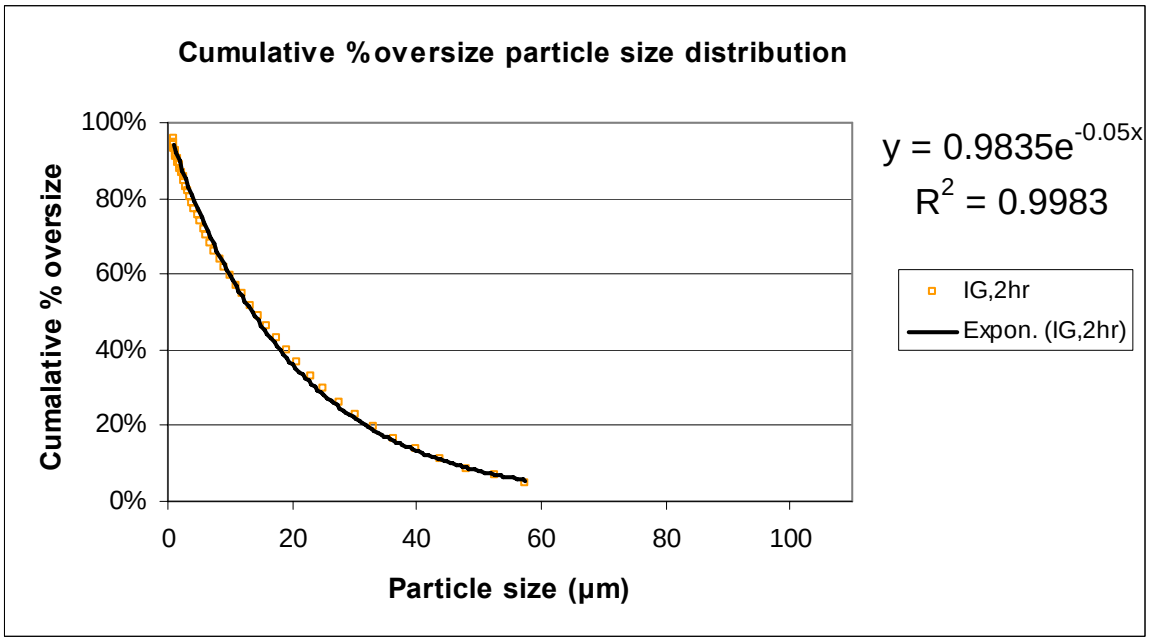
Cumulative %oversize particle size distribution
Cumalative % oversize
100%
80%
60%
40%
20%
0%
0
20
40
60
80
100
Particle size (µm)
y = 0.9835e-0.05x
R2 = 0.9983
IG,2hr
Expon. (IG,2hr)

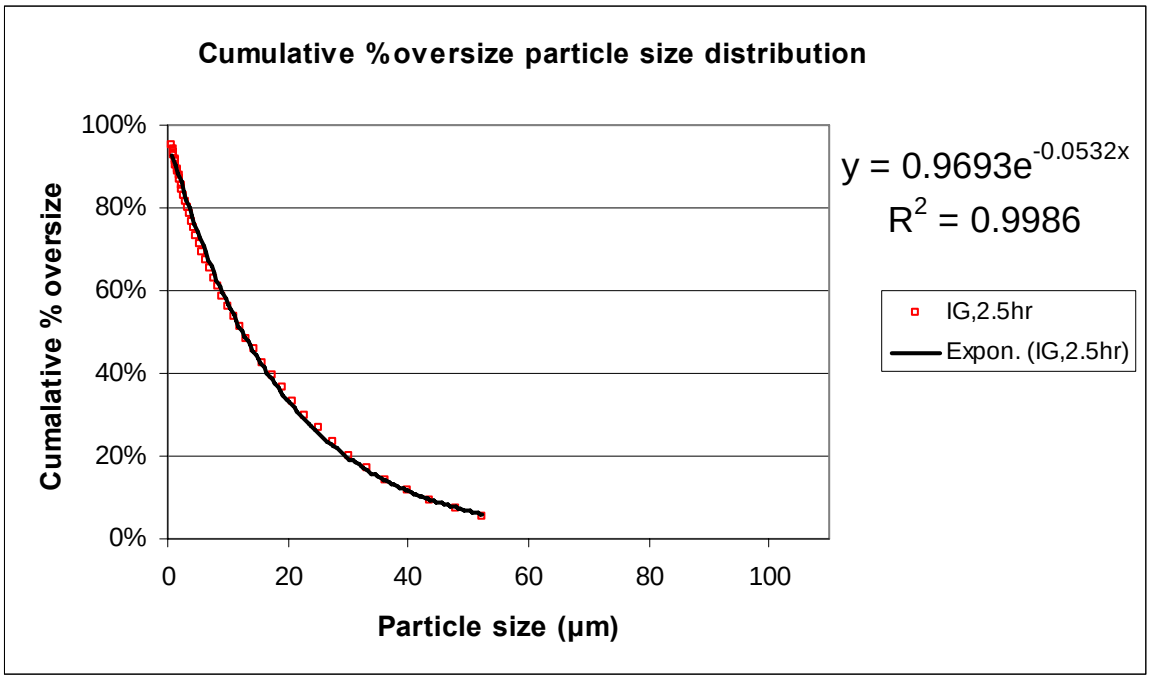
Cumulative %oversize particle size distribution
Cumalative % oversize
100%
80%
60%
40%
20%
0%
0
20
40
60
80
100
Particle size (µm)
y = 0.9693e-0.0532x
R2 = 0.9986
IG,2.5hr
Expon. (IG,2.5hr)

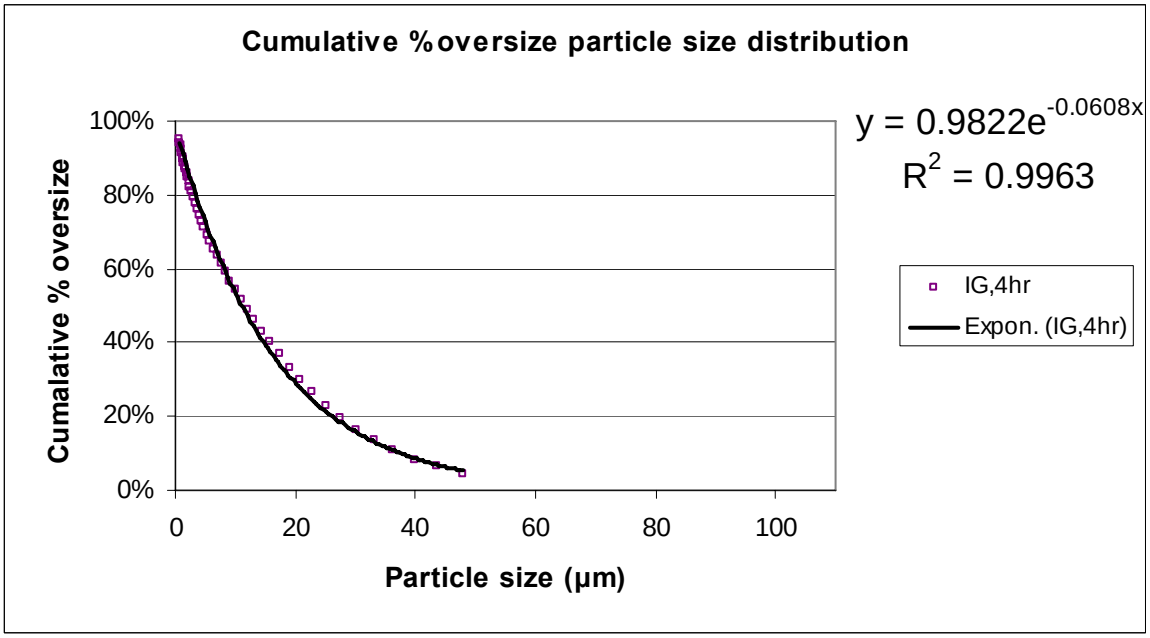
Cumulative %oversize particle size distribution
Cumalative % oversize
100%
80%
60%
40%
20%
0%
0
20
40
60
80
100
Particle size (µm)
y = 0.9822e-0.0608x
R2 = 0.9963
IG,4hr
Expon. (IG,4hr)

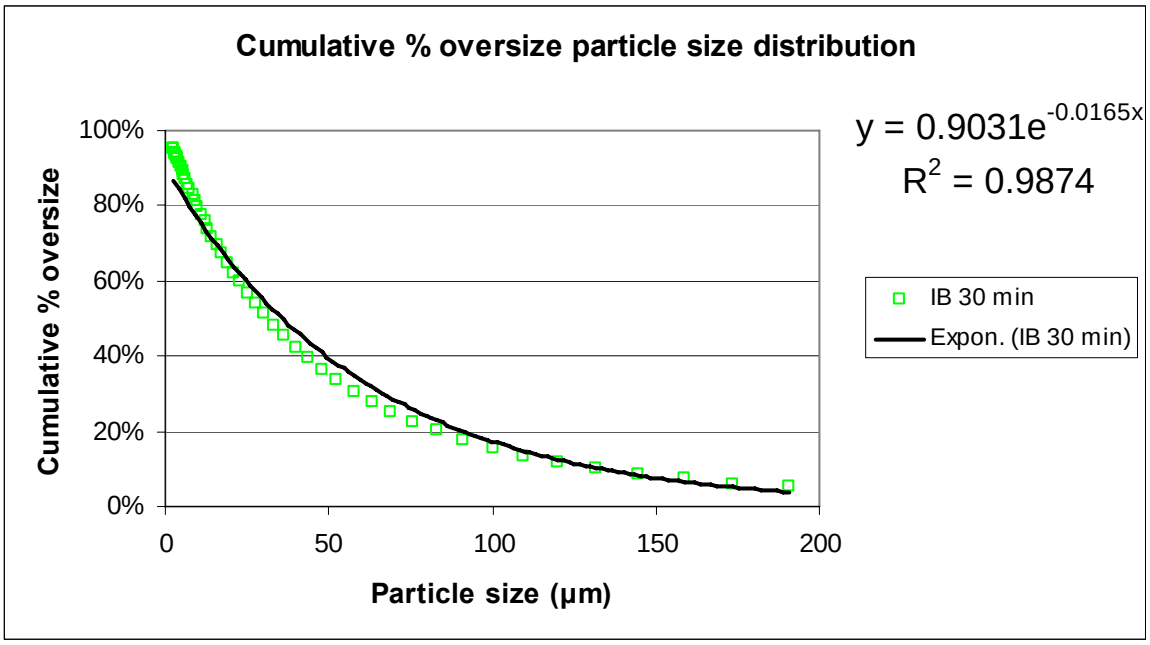
Cumulative % oversize particle size distribution
Cumulative % oversize
100%
80%
60%
40%
20%
0%
0
50
100
150
200
Particle size (µm)
y = 0.9031e-0.0165x
R2 = 0.9874
IB 30 min
Expon. (IB 30 min)

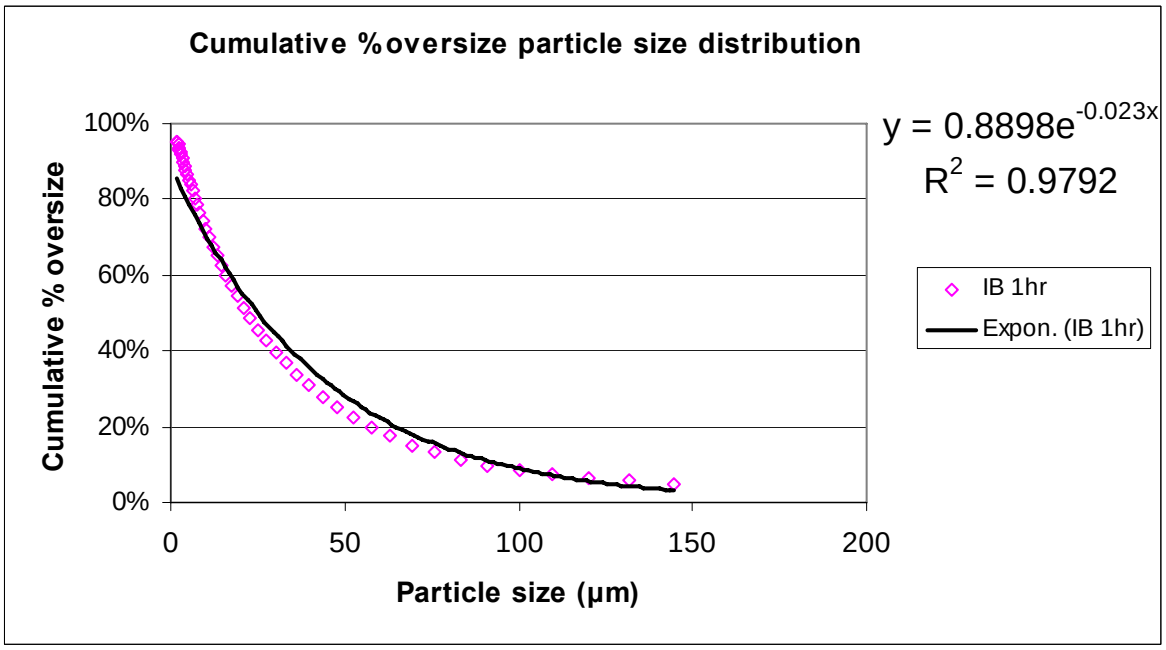
Cumulative %oversize particle size distribution
Cumulative % oversize
100%
80%
60%
40%
20%
0%
0
50
100
150
200
Particle size (µm)
y = 0.8898e-0.023x
R2 = 0.9792
IB 1hr
Expon. (IB 1hr)

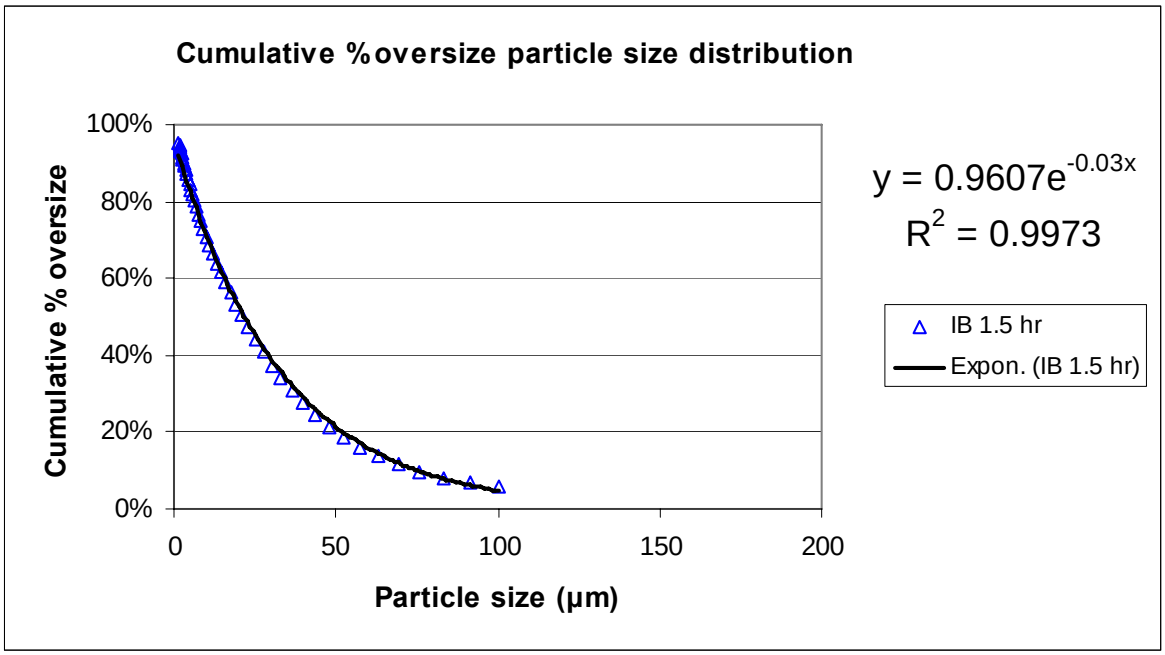
Cumulative %oversize particle size distribution
Cumulative % oversize
100%
80%
60%
40%
20%
0%
0
50
100
150
200
Particle size (µm)
y = 0.9607e-0.03x
R2 = 0.9973
IB 1.5 hr
Expon. (IB 1.5 hr)

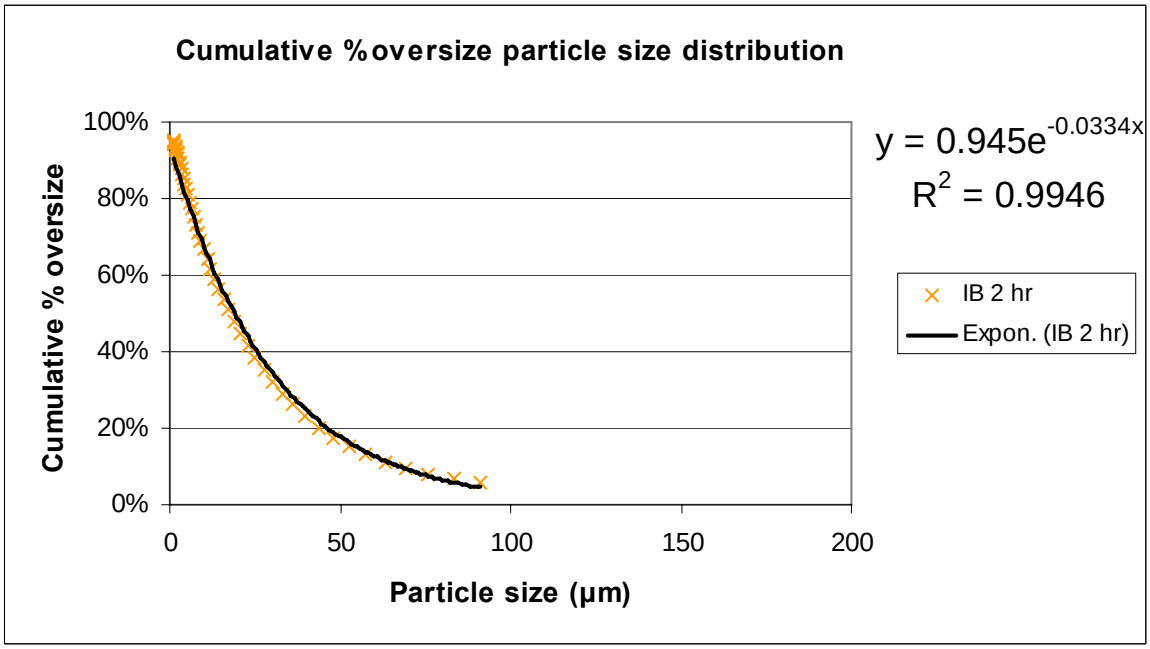
Cumulative %oversize particle size distribution
Cumulative % oversize
100%
80%
60%
40%
20%
0%
0
50
100
150
200
Particle size (µm)
y = 0.945e-0.0334x
R2 = 0.9946
IB 2 hr
Expon. (IB 2 hr)

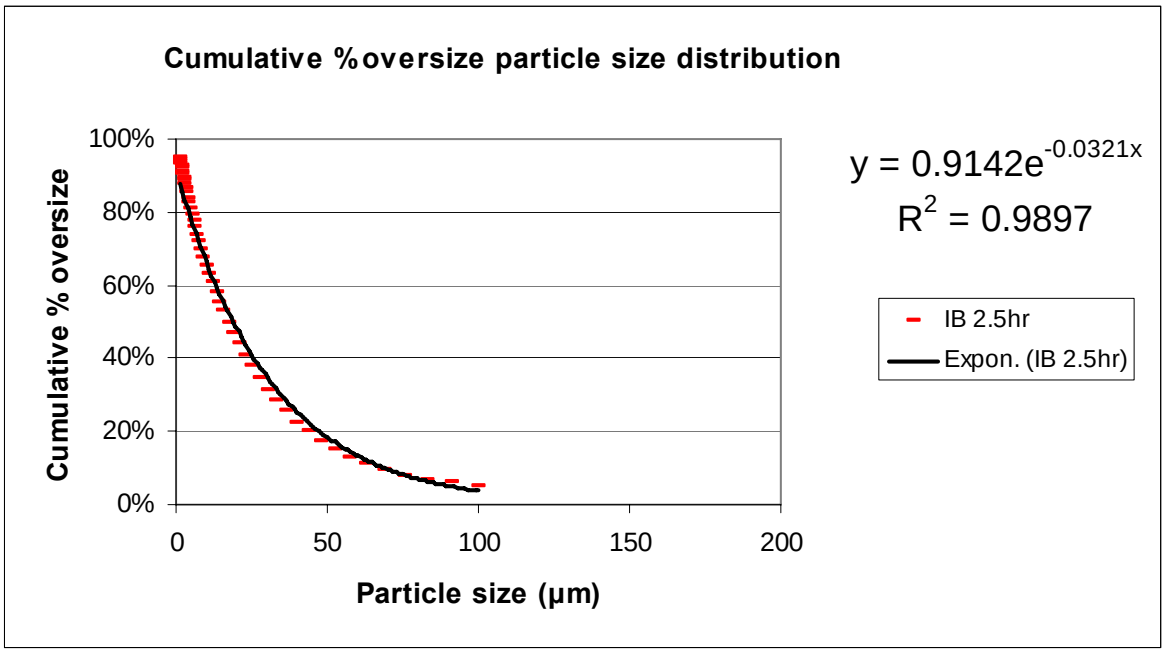
Cumulative %oversize particle size distribution
Cumulative % oversize
100%
80%
60%
40%
20%
0%
0
50
100
150
200
Particle size (µm)
y = 0.9142e-0.0321x
R2 = 0.9897
IB 2.5hr
Expon. (IB 2.5hr)

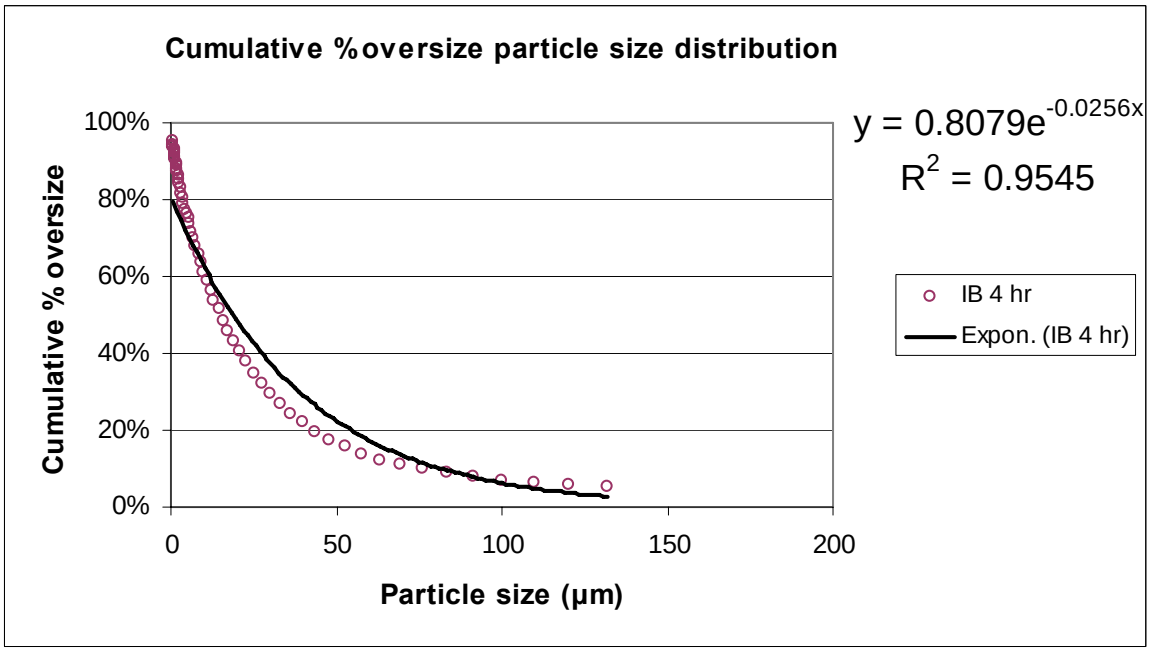
Cumulative %oversize particle size distribution
Cumulative % oversize
100%
80%
60%
40%
20%
0%
0
50
100
150
200
Particle size (µm)
y = 0.8079e-0.0256x
R2 = 0.9545
IB 4 hr
Expon. (IB 4 hr)

APPENDIX C

ROSIN-RAMMLER DISTRIBUTION GRAPHS

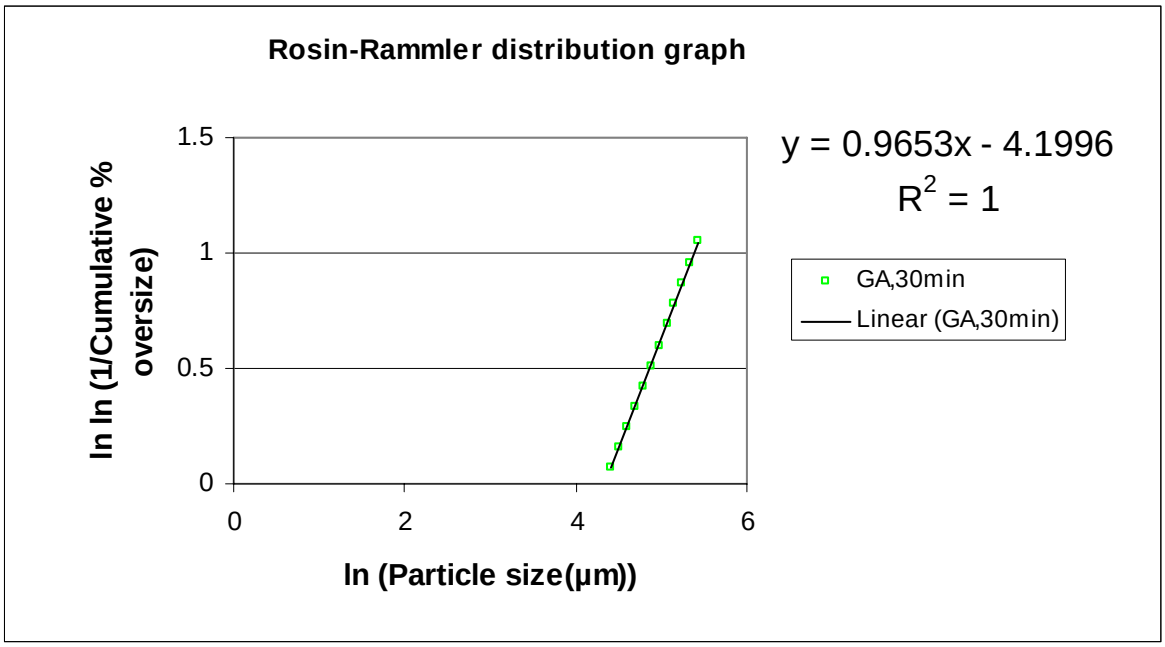
Rosin-Rammler distribution graph
ln ln (1/Cumulative % oversize)
1.5
1
0.5
0
0
2
4
6
ln (Particle size(µm))
y = 0.9653x - 4.1996
R2 = 1
GA,30min
Linear (GA,30min)

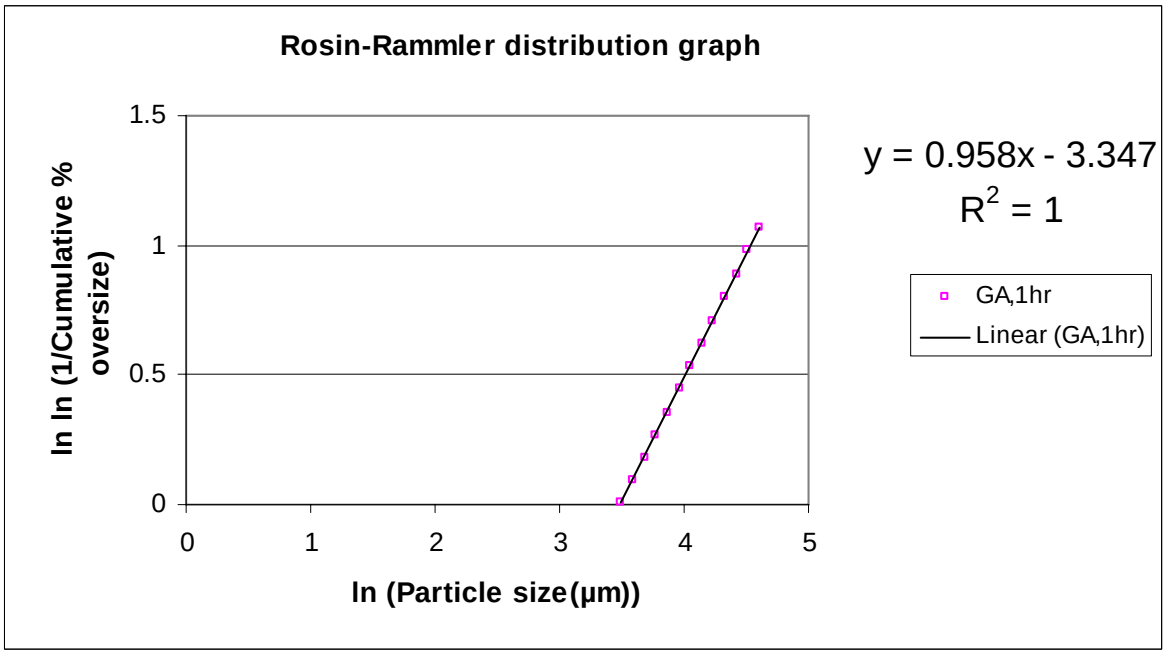
Rosin-Rammler distribution graph
ln ln (1/Cumulative % oversize)
1.5
1
0.5
0
0
1
2
3
4
5
ln (Particle size(µm))
y = 0.958x - 3.347
R2 = 1
GA,1hr
Linear (GA,1hr)

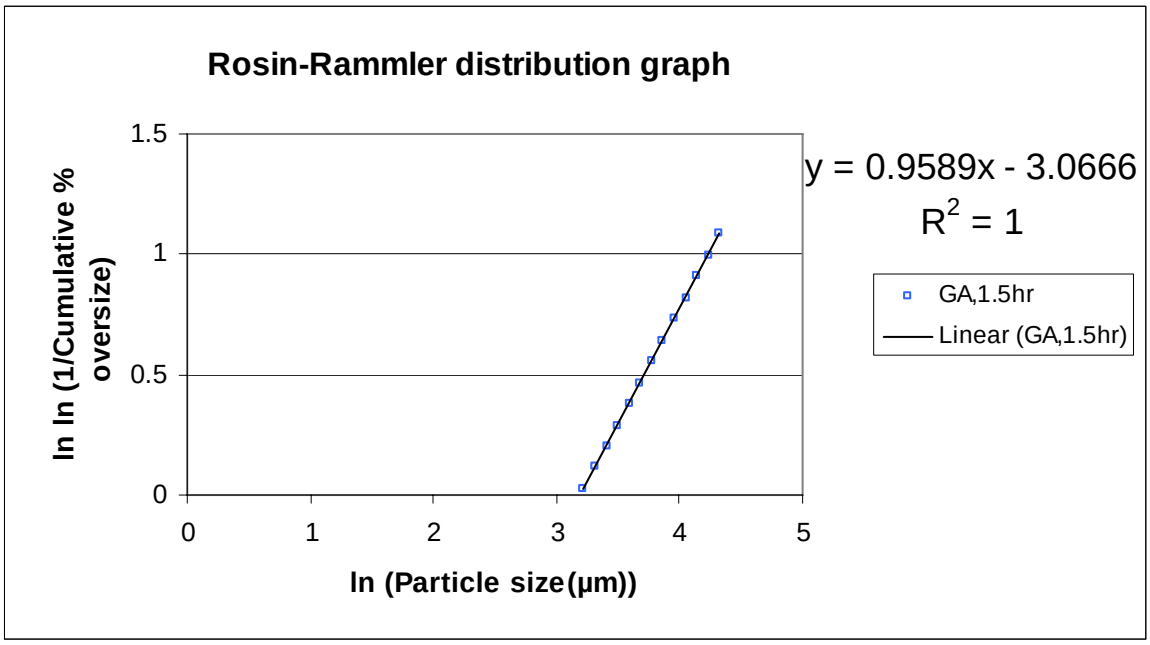
Rosin-Rammler distribution graph
ln ln (1/Cumulative % oversize)
1.5
1
0.5
0
0
1
2
3
4
5
ln (Particle size(µm))
y = 0.9589x - 3.0666
R2 = 1
GA,1.5hr
Linear (GA,1.5hr)

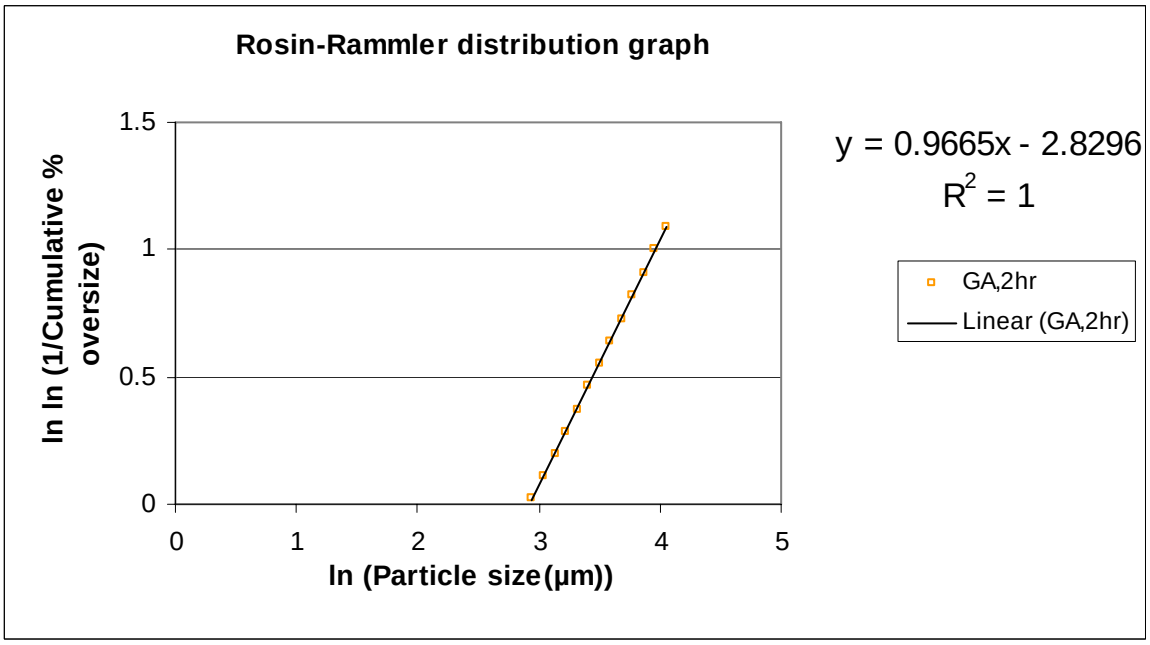
Rosin-Rammler distribution graph
ln ln (1/Cumulative % oversize)
1.5
1
0.5
0
0
1
2
3
4
5
ln (Particle size(µm))
y = 0.9665x - 2.8296
R2 = 1
GA,2hr
Linear (GA,2hr)

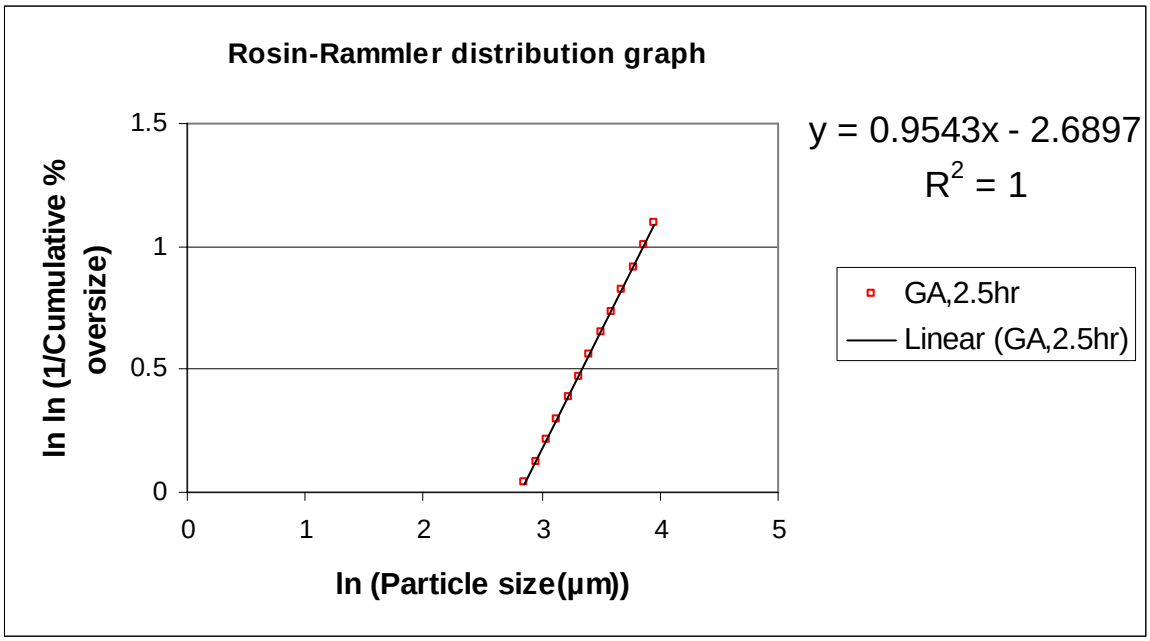
Rosin-Rammler distribution graph
ln ln (1/Cumulative % oversize)
1.5
1
0.5
0
0
1
2
3
4
5
ln (Particle size(µm))
y = 0.9543x - 2.6897
R2 = 1
GA,2.5hr
Linear (GA,2.5hr)

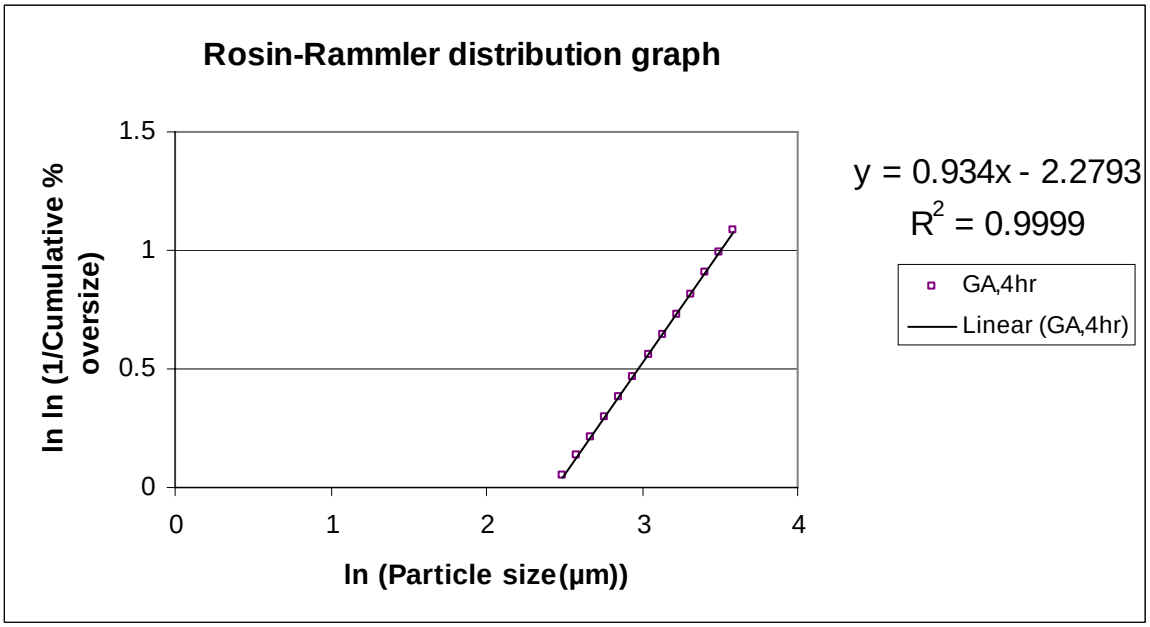
Rosin-Rammler distribution graph
ln ln (1/Cumulative % oversize)
1.5
1
0.5
0
0
1
2
3
4
ln (Particle size(µm))
y = 0.934x - 2.2793
R2 = 0.9999
GA,4hr
Linear (GA,4hr)

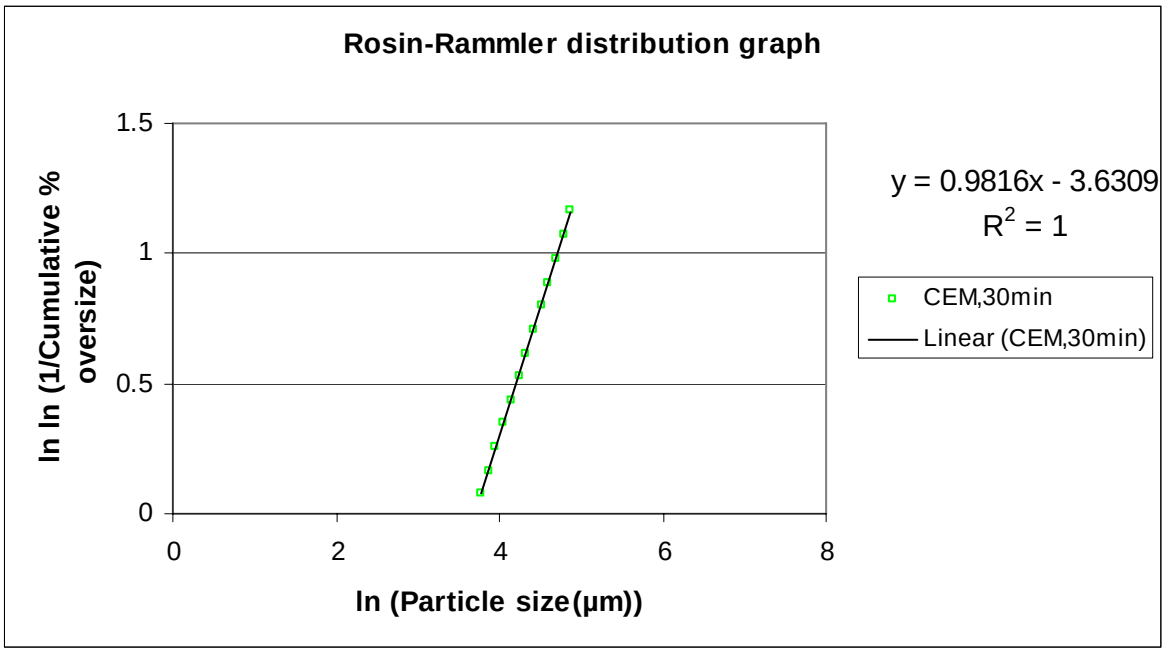
Rosin-Rammler distribution graph
ln ln (1/Cumulative % oversize)
1.5
1
0.5
0
0
2
4
6
8
ln (Particle size(µm))
y = 0.9816x - 3.6309
R2 = 1
CEM,30min
Linear (CEM,30min)

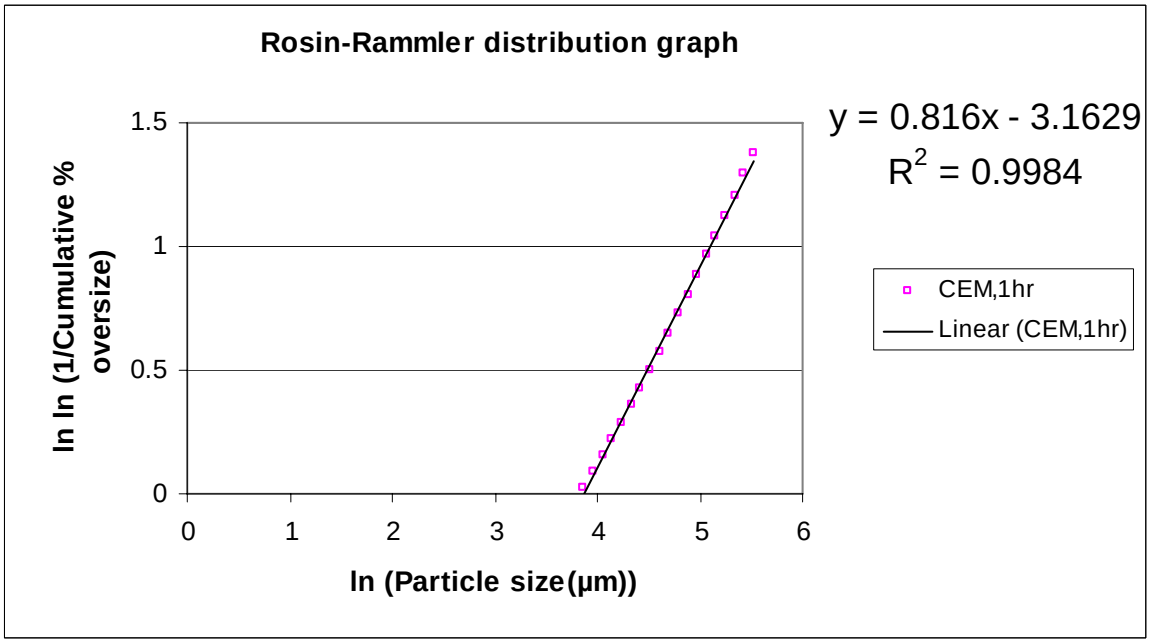
Rosin-Rammler distribution graph
ln ln (1/Cumulative % oversize)
1.5
1
0.5
0
0
1
2
3
4
5
6
ln (Particle size(µm))
y = 0.816x - 3.1629
R2 = 0.9984
CEM,1hr
Linear (CEM,1hr)

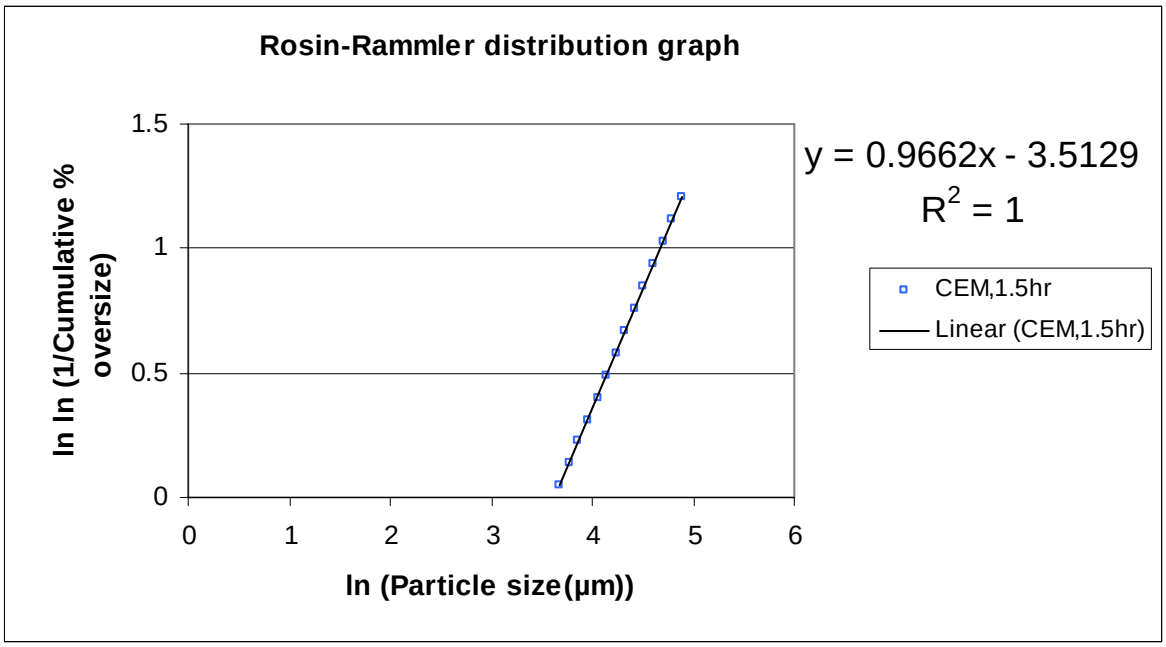
Rosin-Rammler distribution graph
ln ln (1/Cumulative % oversize)
1.5
1
0.5
0
0
1
2
3
4
5
6
ln (Particle size(µm))
y = 0.9662x - 3.5129
R2 = 1
CEM,1.5hr
Linear (CEM,1.5hr)

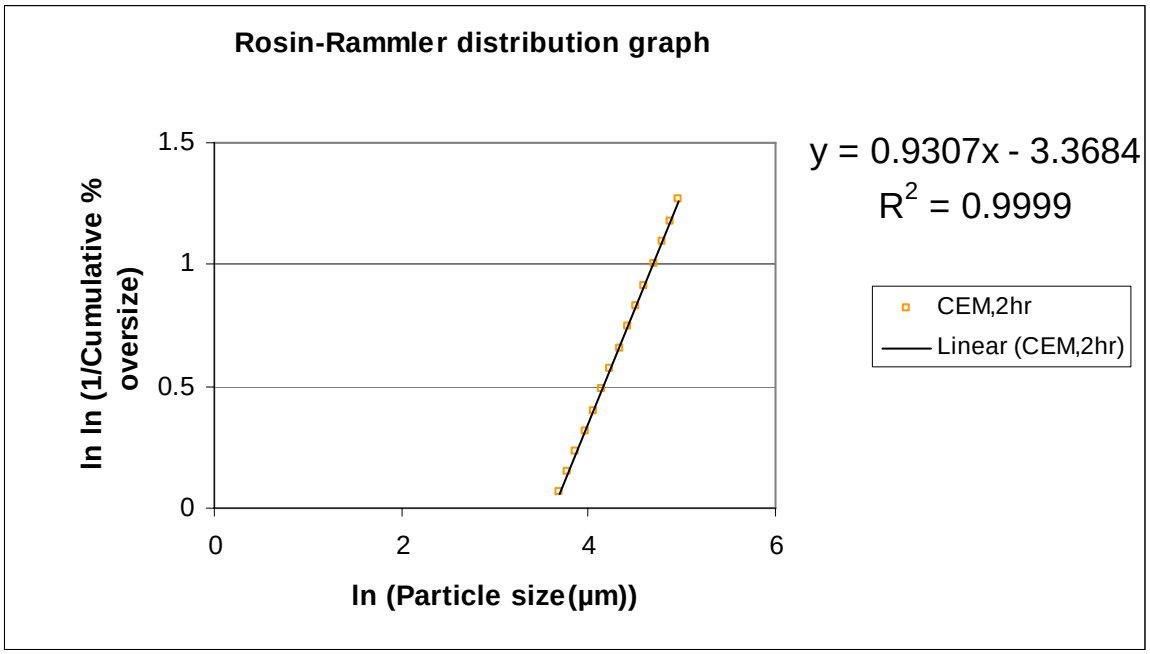
Rosin-Rammler distribution graph
ln ln (1/Cumulative % oversize)
1.5
1
0.5
0
0
2
4
6
ln (Particle size(µm))
y = 0.9307x - 3.3684
R2 = 0.9999
CEM,2hr
Linear (CEM,2hr)

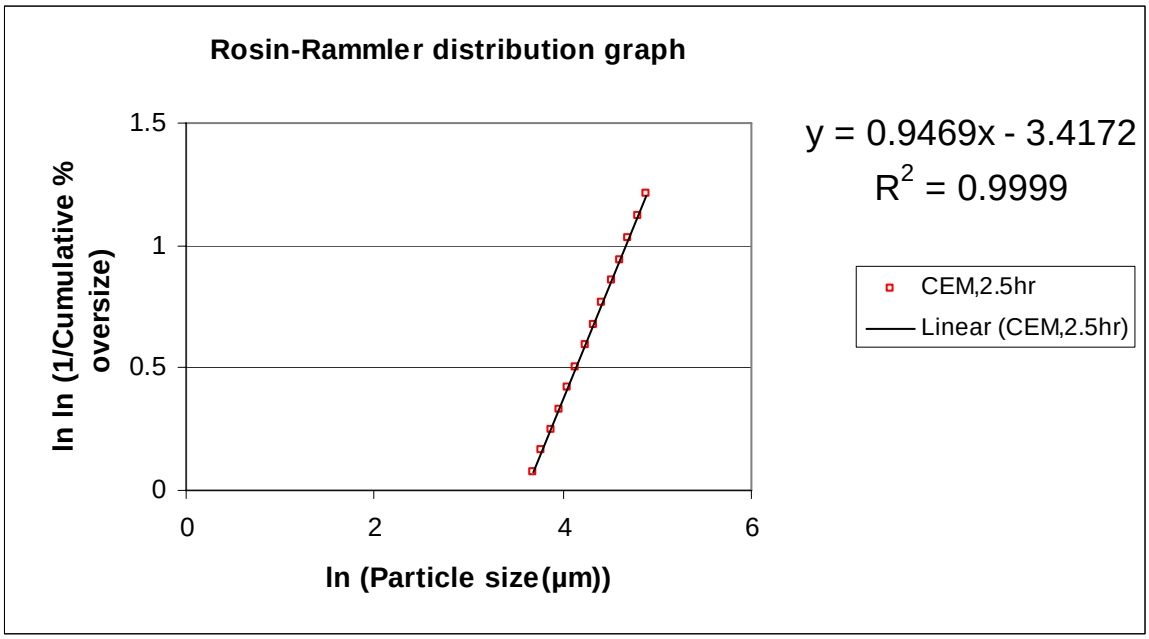
Rosin-Rammler distribution graph
ln ln (1/Cumulative % oversize)
1.5
1
0.5
0
0
2
4
6
ln (Particle size(µm))
y = 0.9469x - 3.4172
R2 = 0.9999
CEM,2.5hr
Linear (CEM,2.5hr)

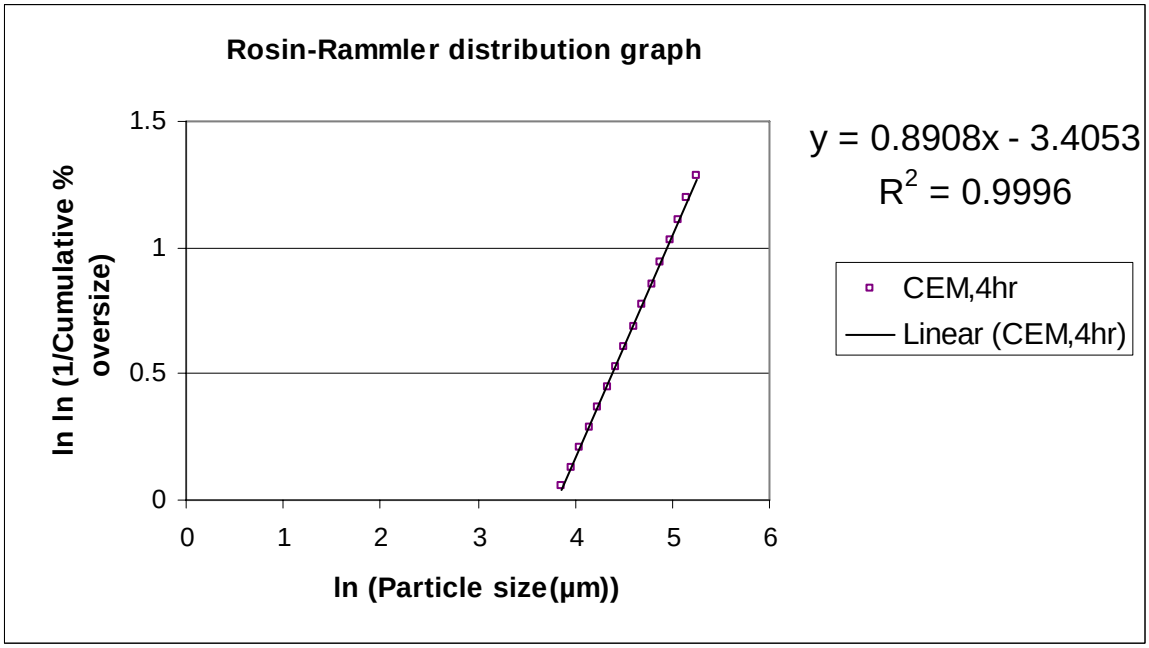
Rosin-Rammler distribution graph
ln ln (1/Cumulative % oversize)
1.5
1
0.5
0
0
1
2
3
4
5
6
ln (Particle size(µm))
y = 0.8908x - 3.4053
R2 = 0.9996
CEM,4hr
Linear (CEM,4hr)

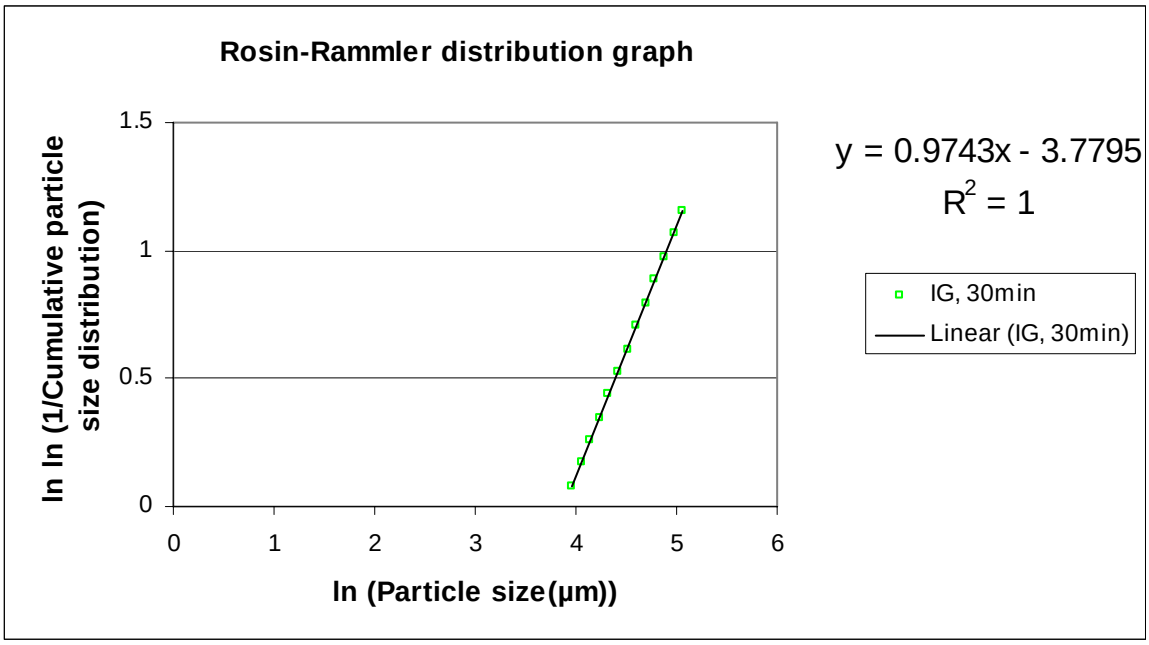
Rosin-Rammler distribution graph
ln ln (1/Cumulative particle size distribution)
1.5
1
0.5
0
0
1
2
3
4
5
6
ln (Particle size(µm))
y = 0.9743x - 3.7795
R2 = 1
IG, 30min
Linear (IG, 30min)

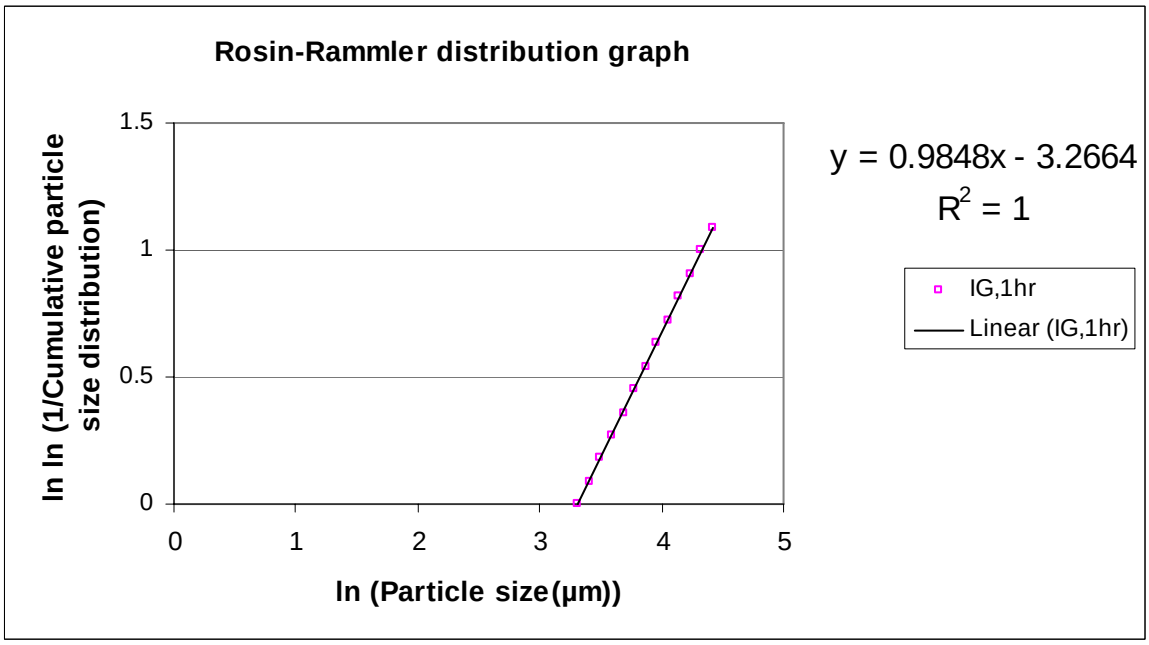
Rosin-Rammler distribution graph
ln ln (1/Cumulative particle size distribution)
1.5
1
0.5
0
0
1
2
3
4
5
ln (Particle size(µm))
y = 0.9848x - 3.2664
R2 = 1
IG,1hr
Linear (IG,1hr)

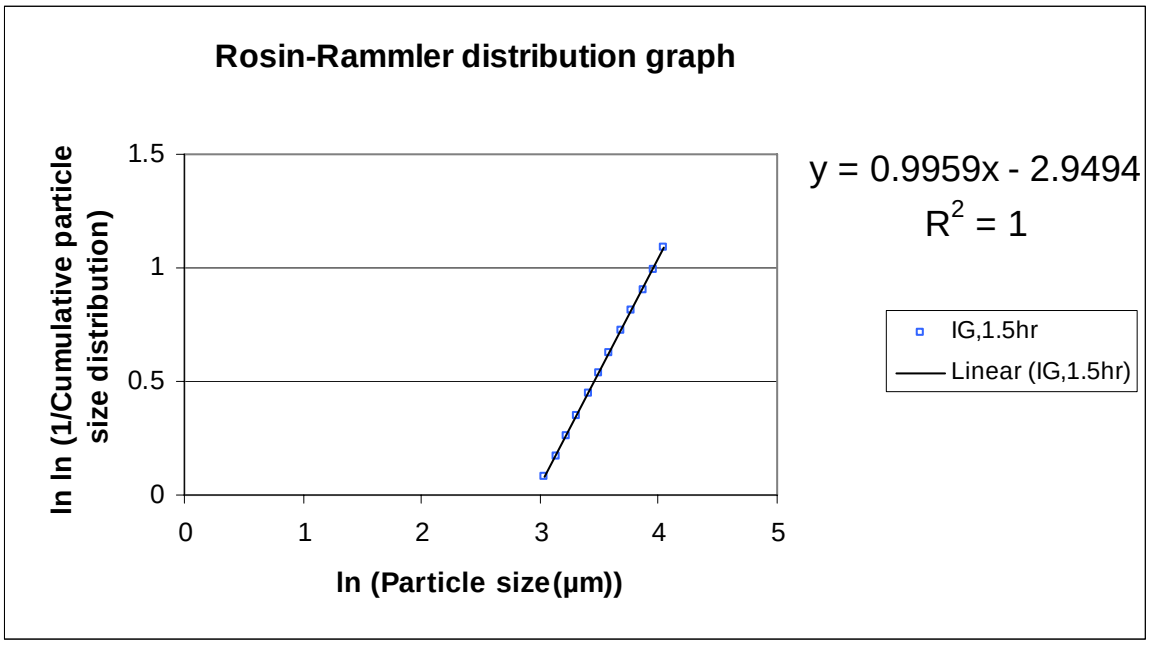
Rosin-Rammler distribution graph
ln ln (1/Cumulative particle size distribution)
ln (Particle size(µm))
y = 0.9959x - 2.9494
R2 = 1
IG,1.5hr
Linear (IG,1.5hr)

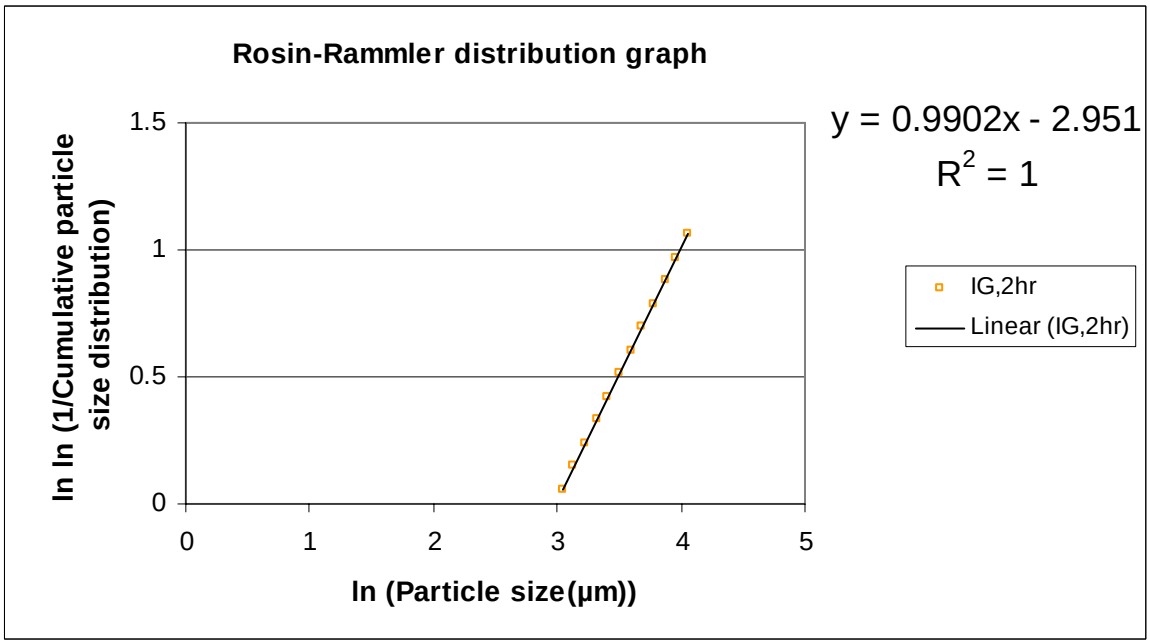
Rosin-Rammler distribution graph
ln ln (1/Cumulative particle size distribution)
ln (Particle size(µm))
y = 0.9902x - 2.951
R2 = 1
IG,2hr
Linear (IG,2hr)

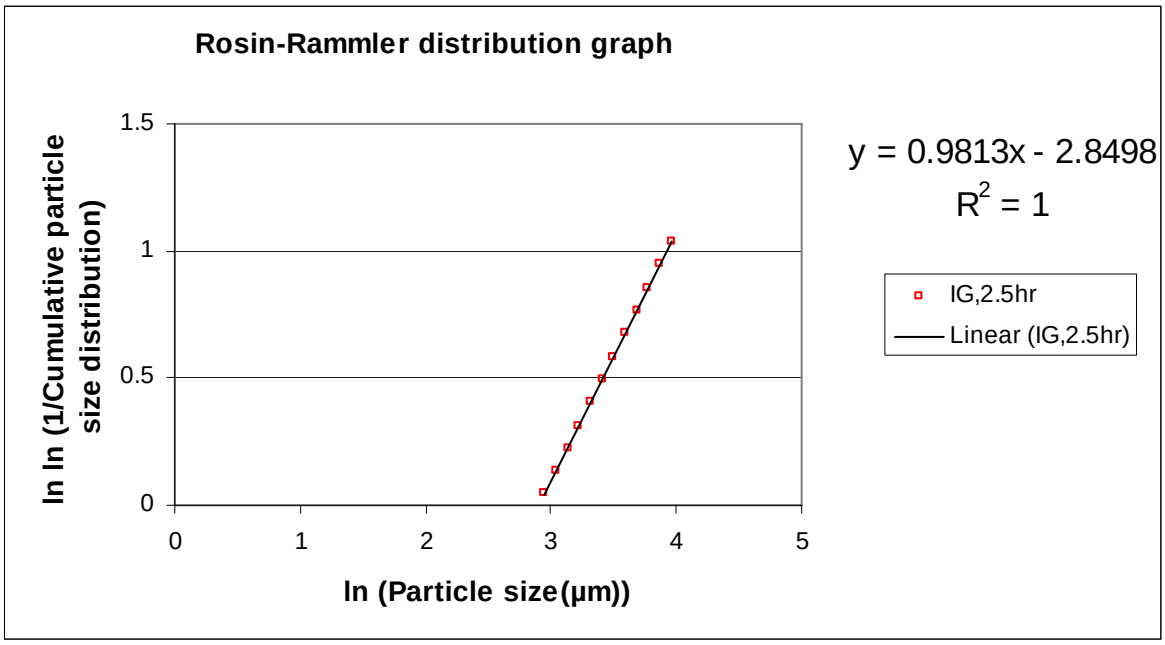
Rosin-Rammler distribution graph
ln ln (1/Cumulative particle size distribution)
1.5
1
0.5
0
0
1
2
3
4
5
ln (Particle size(µm))
y = 0.9813x - 2.8498
R2 = 1
IG,2.5hr
Linear (IG,2.5hr)

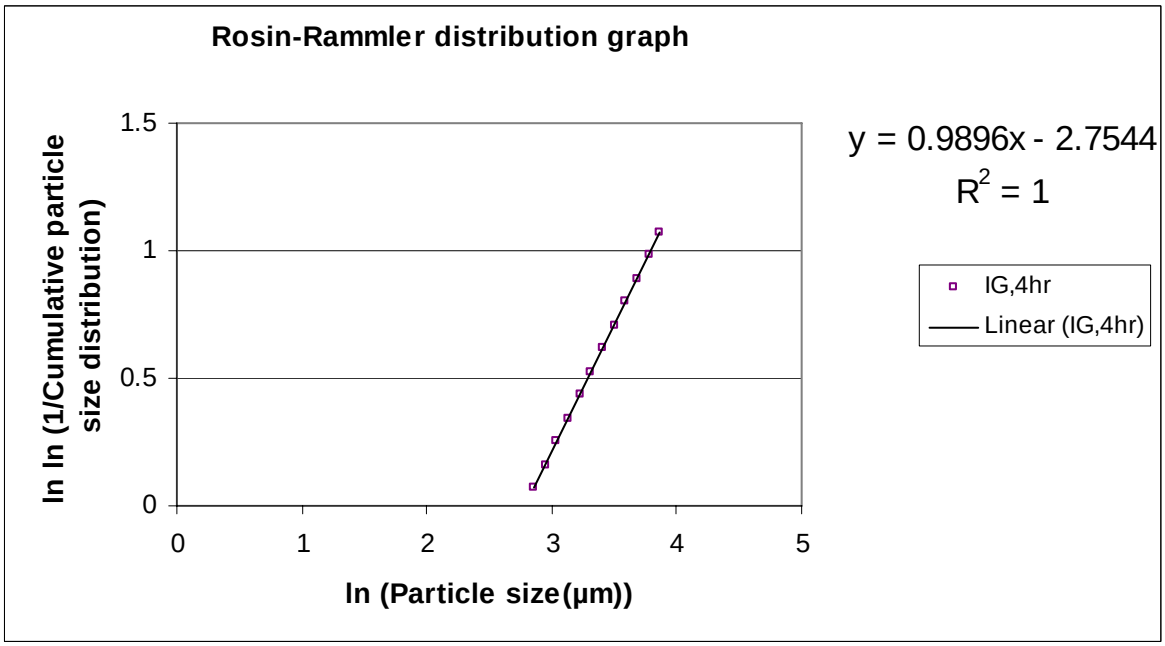
Rosin-Rammler distribution graph
ln ln (1/Cumulative particle size distribution)
1.5
1
0.5
0
0
1
2
3
4
5
ln (Particle size(µm))
y = 0.9896x - 2.7544
R2 = 1
IG,4hr
Linear (IG,4hr)

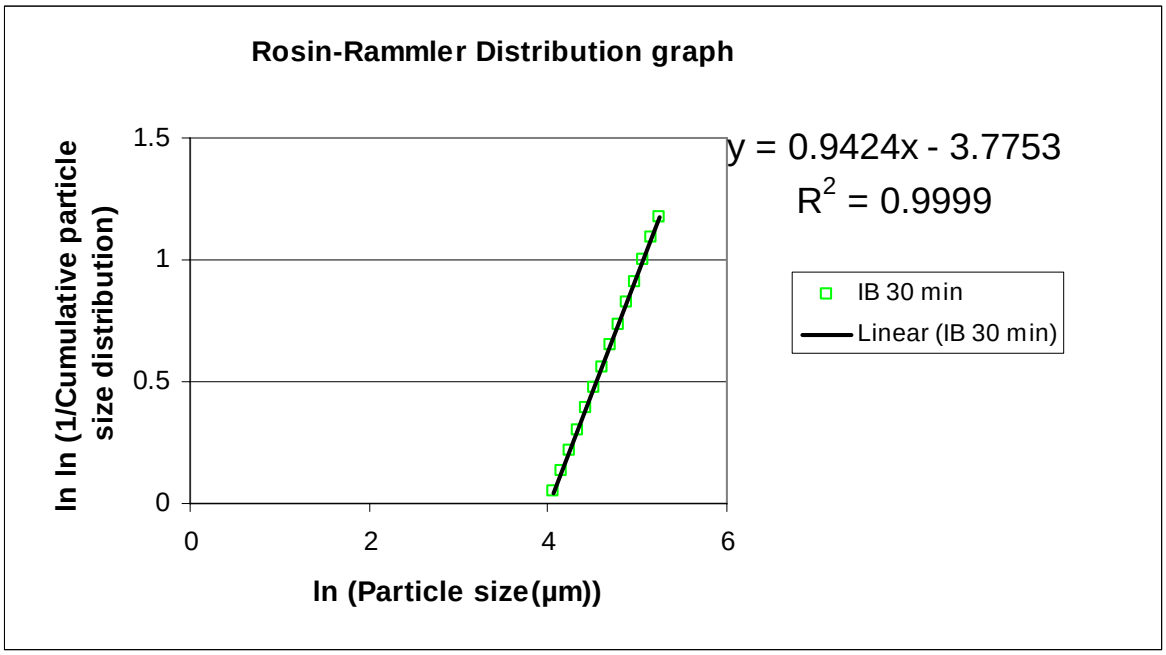
Rosin-Rammler Distribution graph
ln ln (1/Cumulative particle size distribution)
1.5
1
0.5
0
0
2
4
6
ln (Particle size(µm))
y = 0.9424x - 3.7753
R2 = 0.9999
IB 30 min
Linear (IB 30 min)

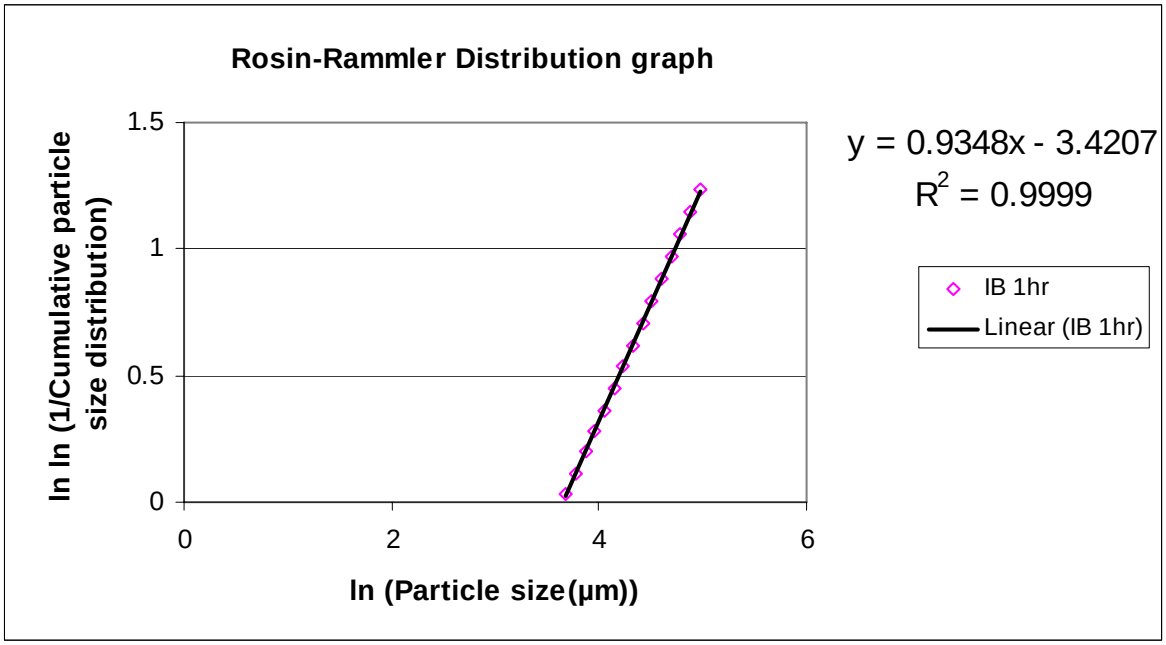
Rosin-Rammler Distribution graph
ln ln (1/Cumulative particle size distribution)
1.5
1
0.5
0
0
2
4
6
ln (Particle size(µm))
y = 0.9348x - 3.4207
R2 = 0.9999
IB 1hr
Linear (IB 1hr)

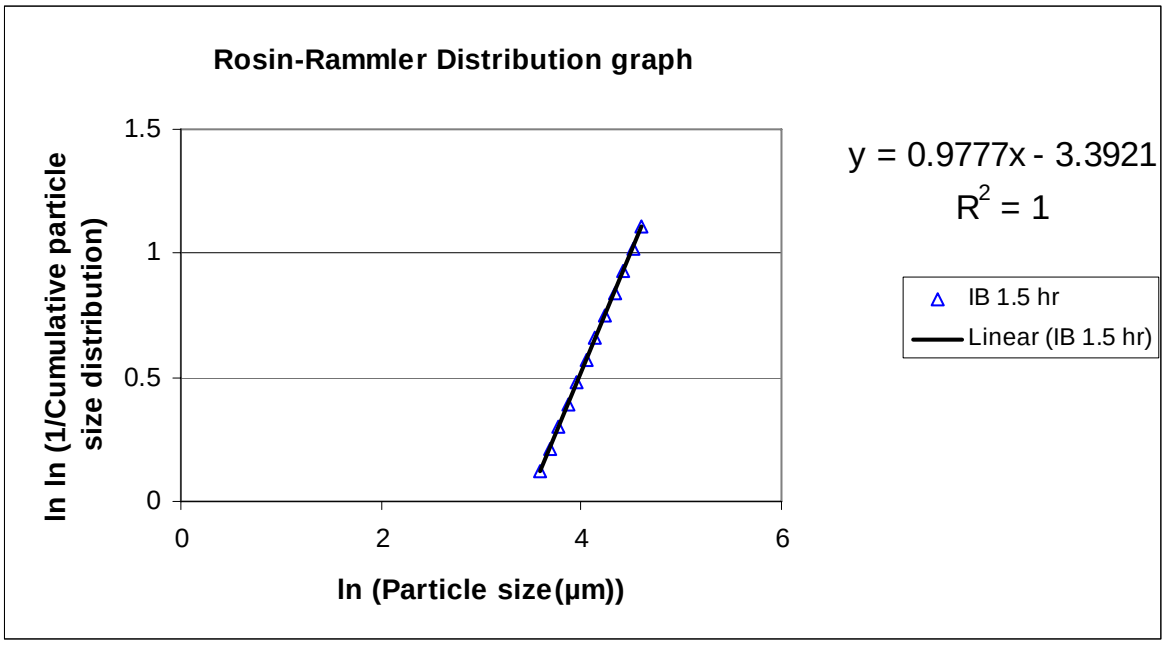
Rosin-Rammler Distribution graph
ln ln (1/Cumulative particle size distribution)
1.5
1
0.5
0
0
2
4
6
ln (Particle size(µm))
y = 0.9777x - 3.3921
R2 = 1
IB 1.5 hr
Linear (IB 1.5 hr)

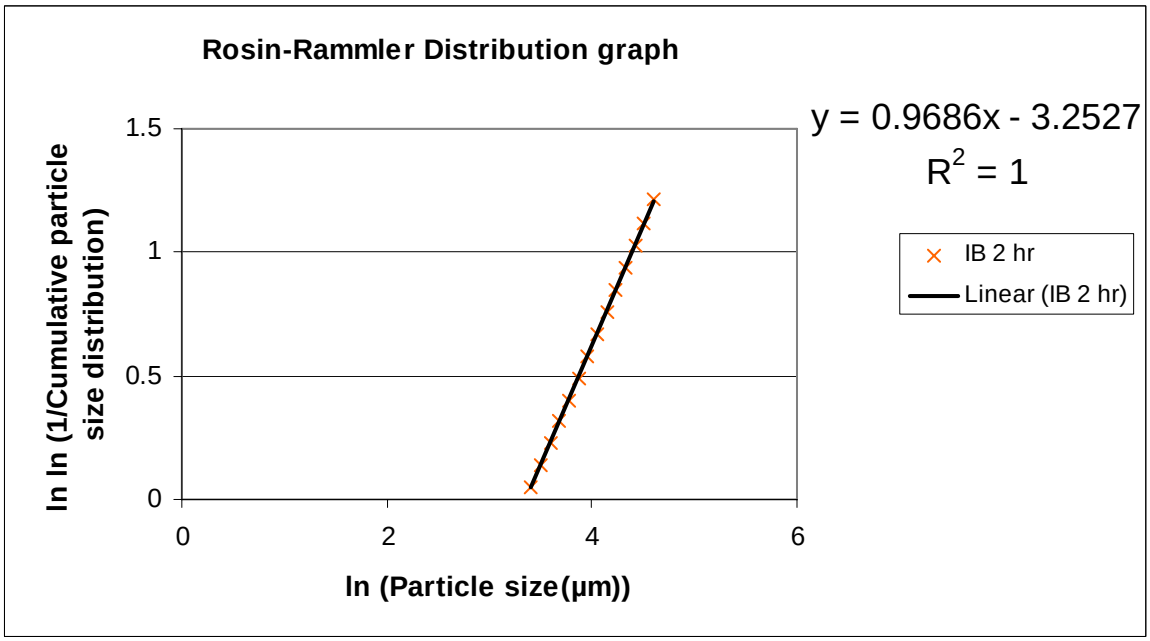
Rosin-Rammler Distribution graph
ln ln (1/Cumulative particle size distribution)
1.5
1
0.5
0
0
2
4
6
ln (Particle size(µm))
y = 0.9686x - 3.2527
R2 = 1
IB 2 hr
Linear (IB 2 hr)

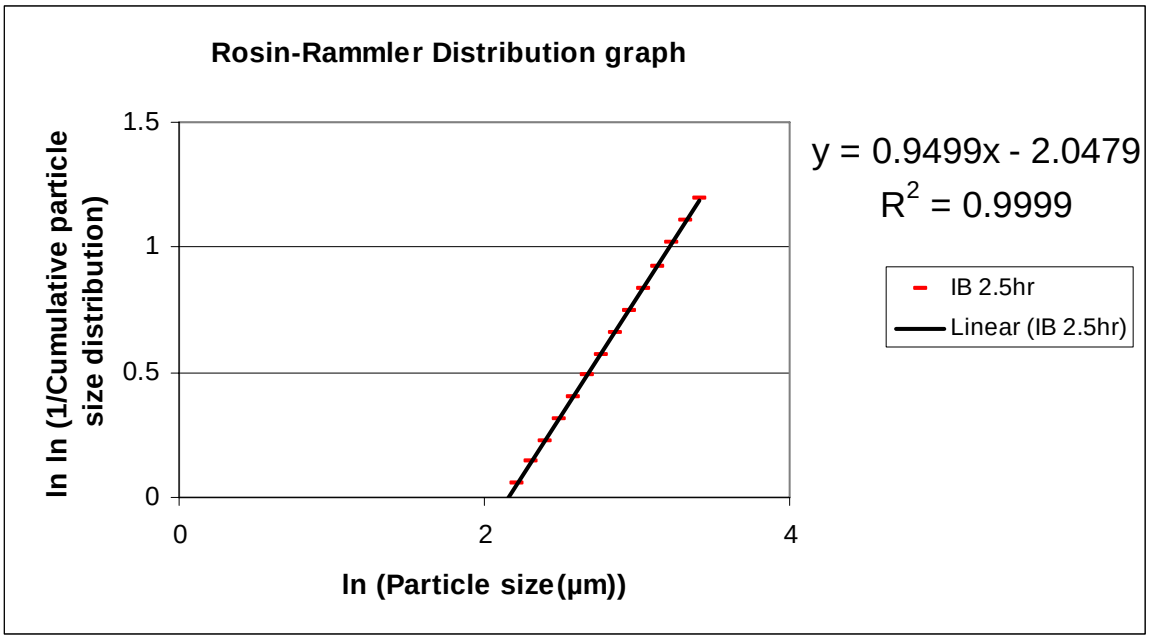
Rosin-Rammler Distribution graph
ln ln (1/Cumulative particle size distribution)
1.5
1
0.5
0
0
2
4
ln (Particle size(µm))
y = 0.9499x - 2.0479
R2 = 0.9999
IB 2.5hr
Linear (IB 2.5hr)

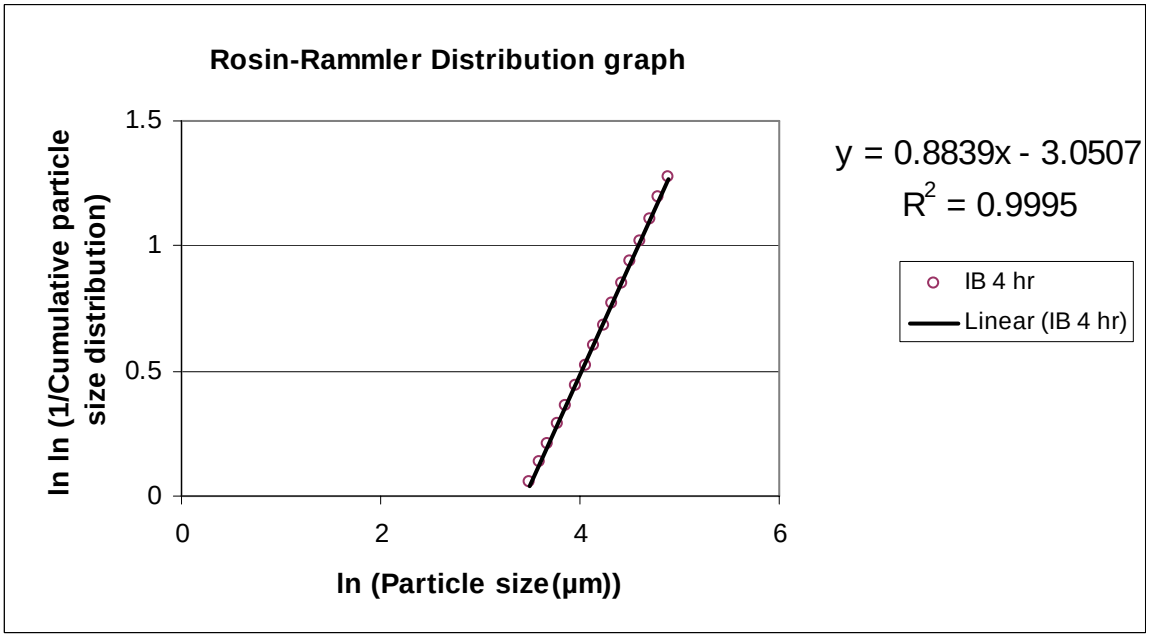
Rosin-Rammler Distribution graph
ln ln (1/Cumulative particle size distribution)
1.5
1
0.5
0
0
2
4
6
ln (Particle size(µm))
y = 0.8839x - 3.0507
R2 = 0.9995
IB 4 hr
Linear (IB 4 hr)

APPENDIX D

BLAINE SURFACE AREA CALCULATIONS

Cement	7.83gr		RD = 3.2
Sample	**time (sec)**	**cm^2/g**	**m^2/g**
30 min	125.1	3147	315
1 hour	138.9	3316	332
1.5 hours	175.3	3726	373
2 hours	217.1	4146	415
2.5 hours	228.5	4254	425
4 hours	227.6	4245	425

Gasification ash	6.65gr		RD =2.715
Sample	**time (sec)**	**cm^2/g**	**m^2/g**
30 min	68	2320	232
1 hour	173.8	3710	371
1.5 hours	253.8	4483	448
2 hours	355	5302	530
2.5 hours	437.7	5887	589
4 hours	668.5	7275	728

Intergrinding	7.28gr		RD = 2.976
Sample	**time (sec)**	**cm^2/g**	**m^2/g**
30 min	131.4	3226	323
1 hour	186.2	3840	384
1.5 hours	255.4	4497	450
2 hours	333	5135	513
2.5 hours	348	5249	525
4 hours	558.1	6648	665

APPENDIX E

MORTAR PRISMS STRENGTH SUMMARY FOR THE EFFECT OF GRINDING TIME ON THE PROPERTIES OF INTERBLENDED GASIFICATION ASH AND CEMENT

Summary Table

Interblending Gasification ash and Cement							
Compression (MPa)	**30 min**	**1 hour**	**1.5 hours**	**2 hours**	**2.5 hours**	**4 hours**	**Cement (2 hrs)**
2 days	10.1	11.9	11.2	20.1	18.4	17.6	17.6
7 days	19.5	24.1	23.5	34.3	29.7	31.3	31.5
28 days	30.8	32.1	33.1	45.1	45.4	43	44.9
Tension (MPa)	**30 min**	**1 hour**	**1.5 hours**	**2 hours**	**2.5 hours**	**4 hours**	**Cement (2 hours)**
2 days	3	3.5	3.3	4.9	4.5	4.8	3.8
7 days	5.2	5.8	5.5	7.3	6.7	7.4	7.3
28 days	7.3	7.7	8.2	8.9	8.8	8.9	8.2

APPENDIX F

MORTAR PRISMS STRENGTH SUMMARY FOR THE EFFECT OF GRINDING TIME ON THE PROPERTIES OF INTERGROUND GASIFICATION ASH AND CEMENT

Summary Table

Intergrinding Gasification Ash and Cement							
Compression (MPa)	**30 min**	**1 hour**	**1.5 hours**	**2 hours**	**2.5 hours**	**4 hours**	**Cement (2 hours)**
2 days	11.8	13.3	17	21.5	19.5	19.2	17.6
7 days	19.4	24.6	29.3	32.4	31.6	31.7	31.5
28 days	27.3	32.9	40.1	43.2	41.6	43.6	44.9
Tension (MPa)	**30 min**	**1 hour**	**1.5 hours**	**2 hours**	**2.5 hours**	**4 hours**	**Cement (2 hours)**
2 days	3	3.4	4.2	4.8	4.5	5.1	3.8
7 days	4.6	6	6.5	7.3	6.7	7.2	7.3
28 days	7	8	8.8	8.6	9	8.8	8.2

APPENDIX G

MORTAR PRISMS STRENGTH SUMMARY FOR THE EFFECT OF GYPSUM CONTENT ON THE PROPERTIES OF INTERGROUND GASIFICATION ASH AND CEMENT

Summary Table

Gypsum Content							
Compression (MPa)	**0%**	**0.50%**	**1%**	**1.50%**	**2%**	**2.50%**	**3%**
2 days	10.7	11.1	11.7	11.6	12	12.1	15.2
7 days	25.1	24.5	24.9	25.7	27.6	25.7	28.6
28 days	33.7	36.1	36.9	32.9	36.2	37.1	38.9
Tension (MPa)	**0%**	**0.50%**	**1%**	**1.50%**	**2%**	**2.50%**	**3%**
2 days	3.2	3.3	3.2	3.4	3.3	3.3	4.5
7 days	6	6	5.5	6.2	5.9	5.7	6.2
28 days	7.0	7.8	7.7	7.5	8.0	7.7	7.6

APPENDIX H

MORTAR PRISMS STRENGTH SUMARY FOR THE EFFECT OF REPLACEMENT LEVEL ON THE PROPERTIES OF INTERGROUND GASIFICATION ASH AND CEMENT

Summary Table

Replacement Level					
Compression (MPa)	**0%**	**10%**	**20%**	**35%**	**55%**
2 Days	32.1	34.4	26.1	18.3	6.5
7 Days	47.0	50.3	45.4	32.6	16.9
28 Days	56.9	57.9	53.2	43.3	28.9
Tension (MPa)	**0%**	**10%**	**20%**	**35%**	**55%**
2 Days	6.8	7.2	4.7	4.3	1.5
7 Days	8.8	9.2	9.1	7.2	4.4
28 Days	9.7	9.8	9.6	9.5	7.5

APPENDIX I

MORTAR PRISMS STRENGTH SUMMARY FOR THE COMPARISON BETWEEN MANUFACTURED AND COMMERCIAL CEMENT

Summary Table

Compression (MPa)	IB CEM+GYPSUM	IG CEM +GYPSUM	CEM I 42.5 R
2 Days	18.8	29.8	22.3
7 Days	34.5	49.4	36.2
28 Days	42.0	61.5	53.0
Tension (MPa)	**IB CEM+GYPSUM**	**IG CEM +GYPSUM**	**CEM I 42.5**
2 Days	4.2	5.9	5.0
7 Days	6.4	8.3	7.8
28 Days	8.3	10.0	9.9

APPENDIX J

CUBE STRENGTH SUMMARY

Cube Strength Summary Table

Summary	24 hour	7 days	28 days
IG (MPa)	6.33	22.64	31.5
IB FA (MPa)	6.31	15.93	26.7
IB GA (MPa)	7.59	19.29	28.0

APPENDIX K

SPECIFIC CREEP SUMMARY

Specific Creep Summary Table

Time (days)	IG GA (microstrain)	IB FA (microstrain)	IB GA (microstrain)
0	0.00	0.00	0.00
1	10.48	4.15	11.13
2	14.30	20.25	21.80
3	24.30	29.59	30.61
7	38.12	44.65	42.67
8	43.84	51.92	48.70
10	49.08	57.63	53.80
13	58.61	68.02	64.47
15	67.19	77.88	72.82
17	71.48	83.59	75.60
41	97.69	97.09	89.98
48	116.27	113.70	115.49
53	120.08	120.97	116.42
64	129.61	124.09	119.20
120	148.20	137.07	136.83
127	155.82	142.78	141.00
132	159.16	145.89	143.78
146	163.92	153.68	150.28
167	171.07	160.95	158.16
269	188.23	175.49	173.00
309	201.09	169.78	184.60

APPENDIX L

POROSITY SUMMARY

Summary Table

Mix	Porosity
IG	15.1%
IB FA	15.9%
IB GA	15.4%

APPENDIX M

PERMEABILITY CALCULATIONS

Summary Table

Mix	IG			IB FA			IB GA		
Pressure bar	2	2	2	2	2	2	2	2	2
Diameter (m)	0.06935	0.0694	0.06935	0.0693	0.0694	0.06935	0.0694	0.06945	0.06935
Area (m^2)	0.003777312	0.00378276	0.0037773	0.003771867	0.003783	0.003777	0.00378276	0.003788	0.003777
Time average (s)	4.85	10.93	8.29	12.83	10.81	11.15	11.53	8.29	9.79
Reading(m^3/s)	1.88262E-05	8.3735E-06	1.1E-05	7.10137E-06	8.42E-06	7.78E-06	7.85095E-06	1.08E-05	9.38E-06
Thickness of disc (m)	0.02	0.02	0.02	0.02	0.02	0.02	0.02	0.02	0.02
e	2.02E-16	2.02E-16	2.02E-16	2.02E-16	2.02E-16	2.02E-16	2.02E-16	2.02E-16	2.02E-16
Permeability (m/s)	1.621E-20	7.213E-21	9.461E-21	6.125E-21	7.21E-21	6.37E-21	6.688E-21	9.07E-21	8.14E-21
Permeabilty average (m/s)	1.096E-20			6.569E-21			7.967E-21		
OPI	19.96			20.18			20.098		